Supporting Information

Transition Metal-Free Direct Hydrogenation of Esters *via* a Frustrated Lewis Pair

Joshua S. Sapsford,[†] Dániel Csókás,[‡] Roland Turnell-Ritson,[†] Liam A. Parkin,[†] Andrew D. Crawford,[†] Imre Pápai,*[,‡] Andrew E. Ashley*[,†]

† Molecular Sciences Research Hub, Imperial College, London W12 0BZ, U.K.

‡ Institute of Organic Chemistry, Research Center for Natural Sciences, Budapest H-1117, Hungary

* Imre Pápai − Institute of Organic Chemistry, Research Center for Natural Sciences, Budapest H-1117, Hungary; orcid.org/0000-0002-4978-0365; Email: papai.imre@ttk.mta.hu

* Andrew E. Ashley − Molecular Sciences Research Hub, Imperial College, London W12 0BZ, U.K.; orcid.org/0000-0002- 5575-7866; Email: a.ashley@imperial.ac.uk

1. Contents

2. Experimental details

2.1. General experimental details

All reactions were conducted under a N_2 atmosphere, unless stated otherwise. All manipulations were carried out either in an MBraun Labmaster DP glovebox or by using standard Schlenk line techniques. All solvents, reagents and substrates were degassed, dried before use and stored under a N_2 atmosphere. 1,2-dichlorobenzene (DCB) was purchased and stored over 4 Å molecular sieves. Pentane was dried using an Innovative Technology Pure Solv™ SPS-400 system and stored over K. Et_2O was distilled from Na/fluorenone and stored over K. $CHCl_3$ and $CDCl_3$ were dried over 4 Å molecular sieves prior to use. C_6D_6 was dried over a K mirror. Acetone was stirred over B_2O_5 and distilled before use. 2,4,6-Collidine (col), 2,6-lutidine (lut) and liquid substrates and were degassed, distilled and dried over 4Å molecular sieves prior to use. Solid substrates were dried under vacuum before use. $LiAlH_4$ was purchased and recrystallised from Et_2O prior to use. $HNTf_2$ was purchased and sublimed prior to use. 2 M HCl in Et_2O was purchased and used without further purification. *i*Pr_4Sn was prepared according to the procedure published previously.[1] H_2 was purchased from BOC (research grade) and dried by passage through a Matheson Tri-Gas WeldassureTM Purifier drying column.

NMR spectra were recorded on Bruker AV-400 or DRX-400 spectrometers. ^{1}H and ^{13}C NMR spectra were referenced internally to proteo solvent signals; ^{19}F and ^{119}Sn NMR spectra were referenced externally to $CFCl_3$ and $SnMe_4$ respectively. Chemical shifts are reported in ppm. $^{119}Sn\{^{1}H\}$ NMR are provided only if there are peaks visible at any stage of a reaction. For all reactions reported, conversions were calculated by the relative ratios between the integrals of the reagents and product peaks. PhMe was added as an internal standard to NMR-scale hydrogenations of HCOOEt and HCOOMe, where the particularly volatile Me_2O was a product, which was used to accurately calculate the amount of starting ester. It should be noted in these reactions that the amount of Me_2O is likely underestimated, due to the compound partitioning into the headspace volume of the NMR tube; only the concentration of the solution-phase species could be determined.

Mass spectral data were collected and processed by Dr Lisa Haigh (Imperial College London) and elemental analyses were conducted by Elemental Microanalysis Ltd.

Single crystal X-ray diffraction data were collected with an Oxford Diffraction Xcalibur unit; crystals were mounted on a nylon MicroLoop™ using perfluoropolyether oil and measured in a stream of N_2 at 172.95(10) K. Using Olex2,[2] all structures were solved using the Superflip charge flipping package.[3] All data were subsequently refined with the ShelXL[4] refinement package using Least Squares minimisation.

2.2. Synthesis & characterisation of compounds

2.2.1. Synthesis of *i*Pr$_3$SnNTf$_2$ (1-NTf$_2$)

*i*Pr$_4$Sn (2.31 g, 7.95 mmol) and HNTf$_2$ (2.13 g, 7.58 mmol) were combined in CHCl$_3$ (20 mL) and stirred at 60 °C for 8 days (attempts to improve the reaction rate by increasing the temperature led to impurities which were impossible to remove during subsequent purification). The solution was concentrated *in vacuo*, resulting in a viscous liquid. Pentane (30 mL) was carefully layered onto this solution, which was then cooled to −40 °C and left for 2 weeks. White block crystals formed, and the supernatant was homogeneous. The crystals were isolated *via* filtration at −40 °C, washed with pentane (3 x 20 mL) at 0 °C and dried *in vacuo* to yield *i*Pr$_3$SnNTf$_2$ as a white crystalline solid. After two further crystallisations following the same procedure, the total yield of *i*Pr$_3$SnNTf$_2$ was 3.83 g, 7.25 mmol, 96%.

^{1}H NMR (CDCl$_3$, 400 MHz) δ 1.45 ($^3J_{117Sn\text{-}1H}$ = 87.4 Hz, $^3J_{119Sn\text{-}1H}$ = 91.4 Hz, 18*H*, SnCH(C*H*$_3$)$_2$), 2.10 (septet, $^3J_{1H\text{-}1H}$ = 7.6 Hz, 3*H*, Sn(C*H*)$_3$).

^{13}C{^{1}H} NMR (CDCl$_3$, 101 MHz) δ 20.8 (s, $^2J_{117/119Sn\text{-}13C}$ = 18.3 Hz, Sn(CH(*C*H$_3$)$_2$), 29.8 (s, $^1J_{117Sn\text{-}13C}$ = 297.2 Hz, $^1J_{119Sn\text{-}13C}$ = 311.2 Hz, Sn*C*H), 119.2 (q, $^1J_{19F\text{-}13C}$ = 321.1 Hz, *C*F$_3$).

^{19}F NMR (CDCl$_3$, 377 MHz) δ −77.3 (s).

^{119}Sn{^{1}H} NMR (CDCl$_3$, 149 MHz) δ 213.9 (br s).

Elemental analysis found (calc.) C$_{11}$H$_{21}$F$_6$NO$_4$S$_2$Sn: C 24.89 (25.02), H 3.95 (4.01) N 2.68 (2.65).

MS ES+ (PhMe) *m*/*z* = 290 [*i*Pr$_3$SnN(H)Tf$_2$+].

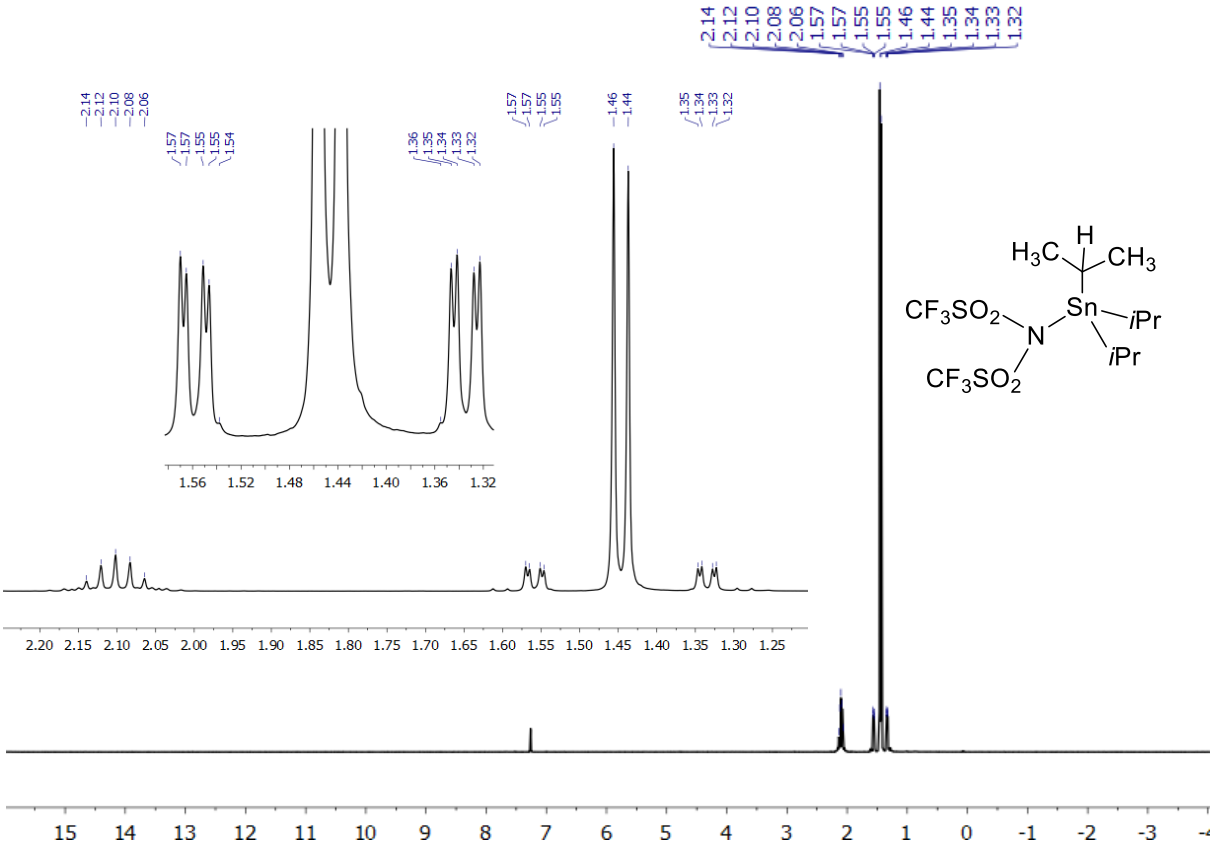

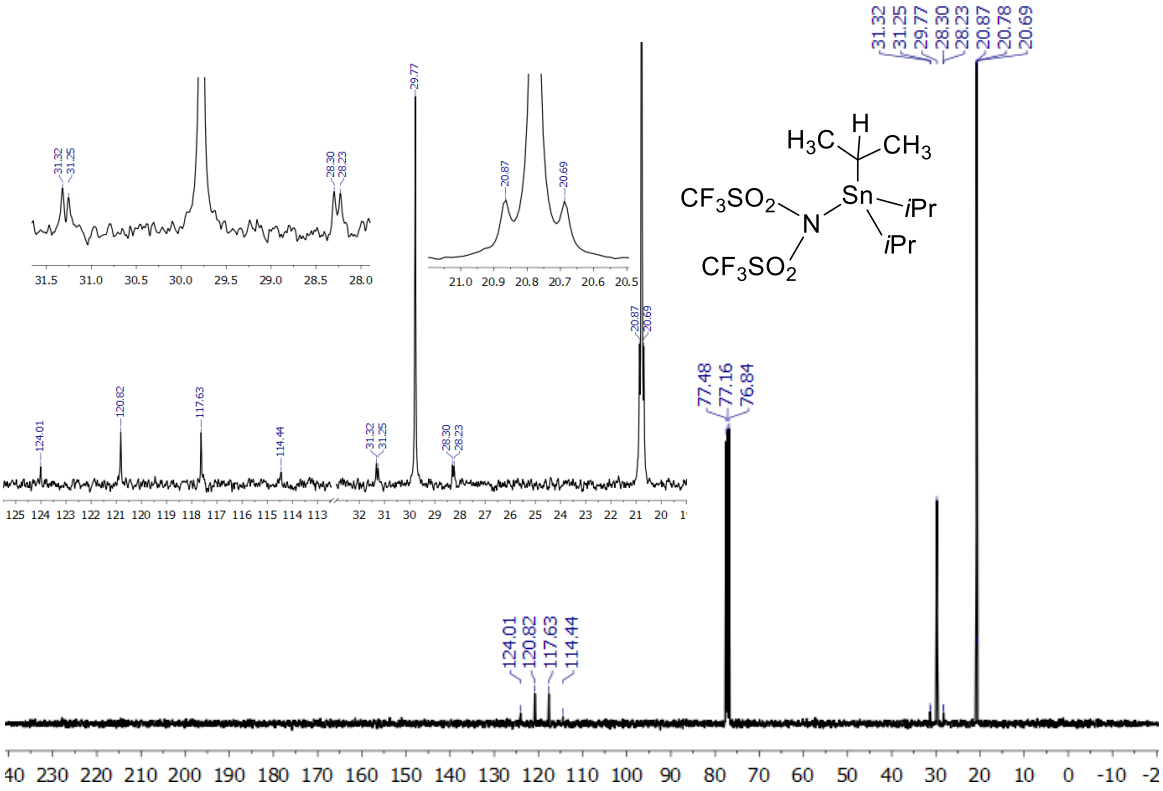

δ (^{13}C) / ppm

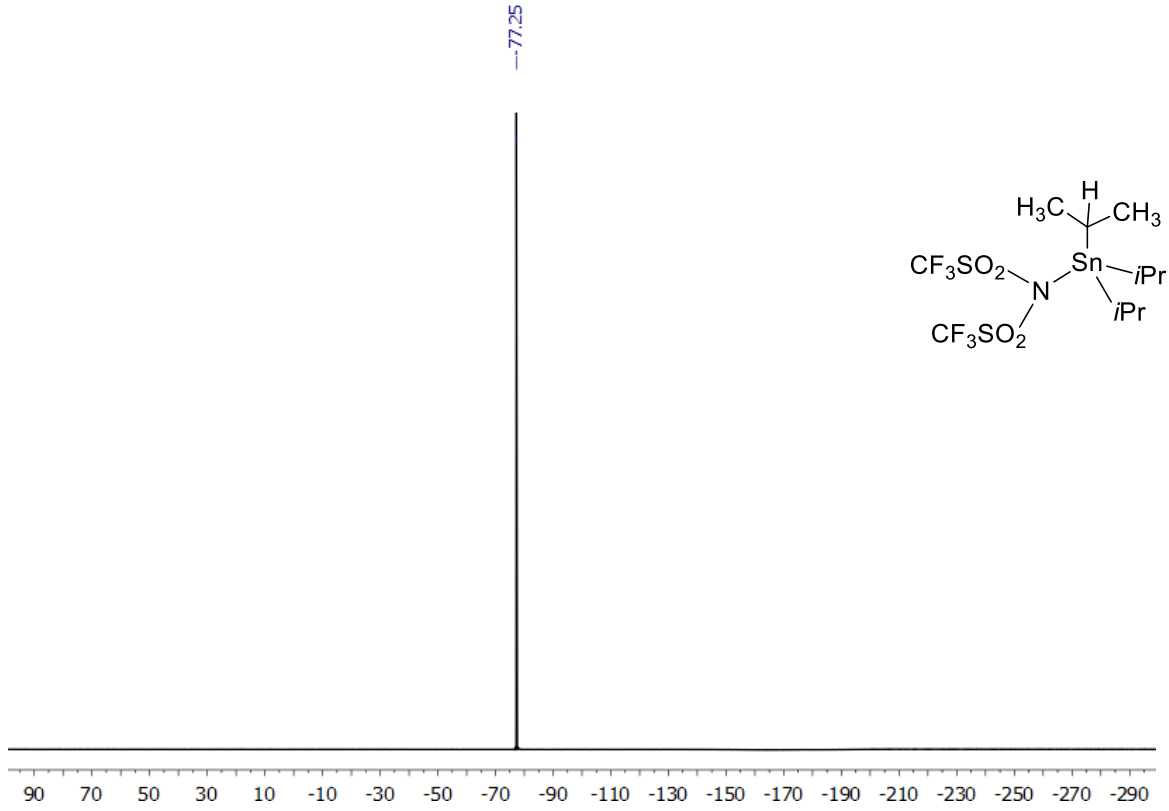

δ (^{19}F) / ppm

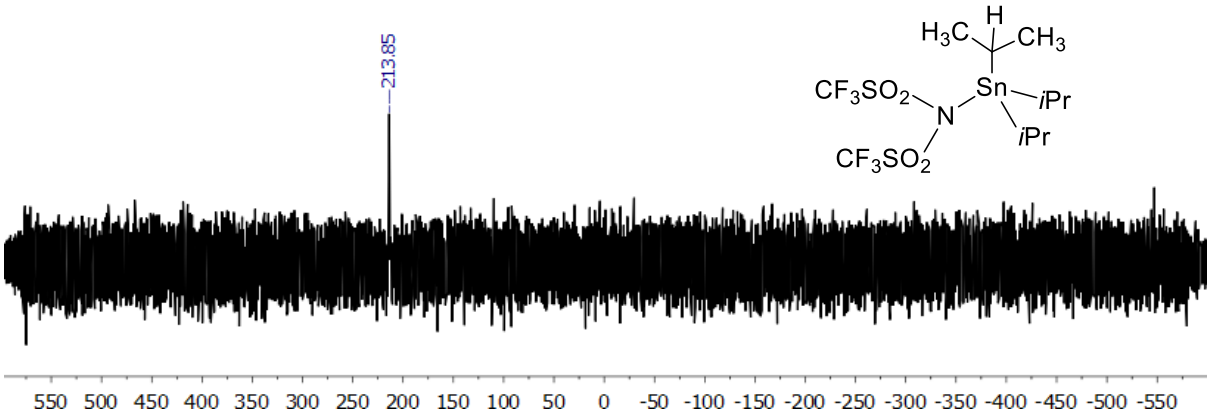

Figure S1 ^{1}H, $^{13}C\{^{1}H\}$, ^{19}F and $^{119}Sn\{^{1}H\}$ NMR spectra of **1**-NTf_2 in $CDCl_3$. Inset provides an expanded view of the alkyl region in the ^{1}H NMR spectrum.

2.2.2. Synthesis of *i*Pr$_3$SnH (1-H)

A procedure for the synthesis of **1**-H was reported in a previous procedure,[1] but a more convenient route *via* reduction of *i*Pr$_3$SnCl is provided below.

*i*Pr$_4$Sn (1.00 g, 3.44 mmol) and a solution of 2 M HCl in Et$_2$O (8.0 mL) were combined in CHCl$_3$ (20 mL) and stirred at RT for 12 h. The volatiles were removed *in vacuo* to furnish crude *i*Pr$_3$SnCl (^{119}Sn{^{1}H} NMR (CDCl$_3$): δ = 109.3 ppm) as a colourless oil (850 mg) that was *ca*. 90% pure by ^{1}H NMR spectroscopy (the impurities are proposed to be *i*Pr$_2$SnCl$_2$ and *i*Pr$_4$Sn), which was found to be sufficiently pure for the synthesis of **1**-H.

To a stirred solution of crude *i*Pr$_3$SnCl (500 mg) in Et$_2$O (15 mL) at −78 °C was added LiAlH$_4$ (77.0 mg, 2.029 mmol) in Et$_2$O (15 mL) dropwise. The solution was warmed to RT and stirred for a further 3 h, whereupon a white precipitate formed. The solvent was removed *in vacuo* and the product extracted into pentane (3 x 10 mL). The solvent was removed *in vacuo* to yield a colourless liquid, which was distilled (RT, 5 x 10−2 mbar) to isolate **1**-H (150 mg, 0.603 mmol). The NMR spectral data match those previously reported.[1]

^{1}H NMR (400 MHz, C$_6$D$_6$) δ 1.20-1.51 (m, 21*H*), 5.32 (s, $^1J_{117Sn\text{-}1H}$ = 1409 Hz, $^1J_{119Sn\text{-}1H}$ = 1476 Hz).

^{119}Sn{^{1}H} NMR (149 MHz, C$_6$D$_6$) δ –49.2.

2.2.3. Synthesis of lutidinium triflimide (lut-H·NTf$_2$)

Lutidine (30.1 µL, 0.258 mmol) and HNTf$_2$ (72.5 mg, 0.258 mmol) were combined and stirred for 1 h at RT to afford the title compound as a viscous oil (98.2 mg, 0.253 mmol, 98%). The NMR spectral data are consistent with those previously reported.[5]

^{1}H NMR (CDCl$_3$, 400 MHz) δ 2.84 (s, 6*H*, Me), 7.54 (d, $^3J_{1H\text{-}1H}$ = 8.2 Hz, 2*H*, Ar), 8.21 (t, $^3J_{1H\text{-}1H}$ = 8.2 Hz, 1*H*, Ar), 13.40 (s, 1*H*, lut-*H*$^+$).

^{19}F NMR (CDCl$_3$, 377 MHz) δ −78.9 (s).

3. H_2 activation with auxiliary bases

3.1. General procedure for H_2 activation experiments

1-NTf_2 and a LB (col/lut) were combined in 1,2-dichlorobenzene in an NMR tube fitted with a J. Youngs tap with a capillary insert containing C_6D_6. The solution was freeze-pump-thaw degassed and cooled to −196 °C whereupon H_2 (1 bar) was admitted. The tube was sealed and warmed to RT (the pressure of H_2 is *ca*. 4 bar). The solution was occasionally agitated, and the reaction monitored by NMR spectroscopy.

There is a subtle change in the **1**-NTf_2 ^{1}H NMR alkyl resonances was observed upon addition of either LB, suggesting there is an interaction between the species (see Section 12.2 for a computational treatment of this association). H_2 activation with both LBs proceeds at a modest rate. The long and variable T_1 of the **1**-*H* resonance makes quantitative integration of this peak unreliable, Qualitatively, the rate of reaction of the **1**-NTf_2/col pair at 4 bar H_2 is comparable that of **1**-OTf/col at 10 bar H_2. Further, more extreme broadening of the **1**-NTf_2 alkyl peaks and upfield movement of the methine resonance in the ^{1}H NMR spectrum is observed after H_2 cleavage, which may suggest that the **1**-H product is associating with remaining **1**-NTf_2. Comparable adducts between Gp 14 R_3E-H and their potent $[R_3E]^+$ Lewis acids are known e.g. $[Et_3Si\text{-}H\cdot SiEt_3]^+$.[6]

3.2. NMR spectra of H_2 activation by 1-NTf_2/lut

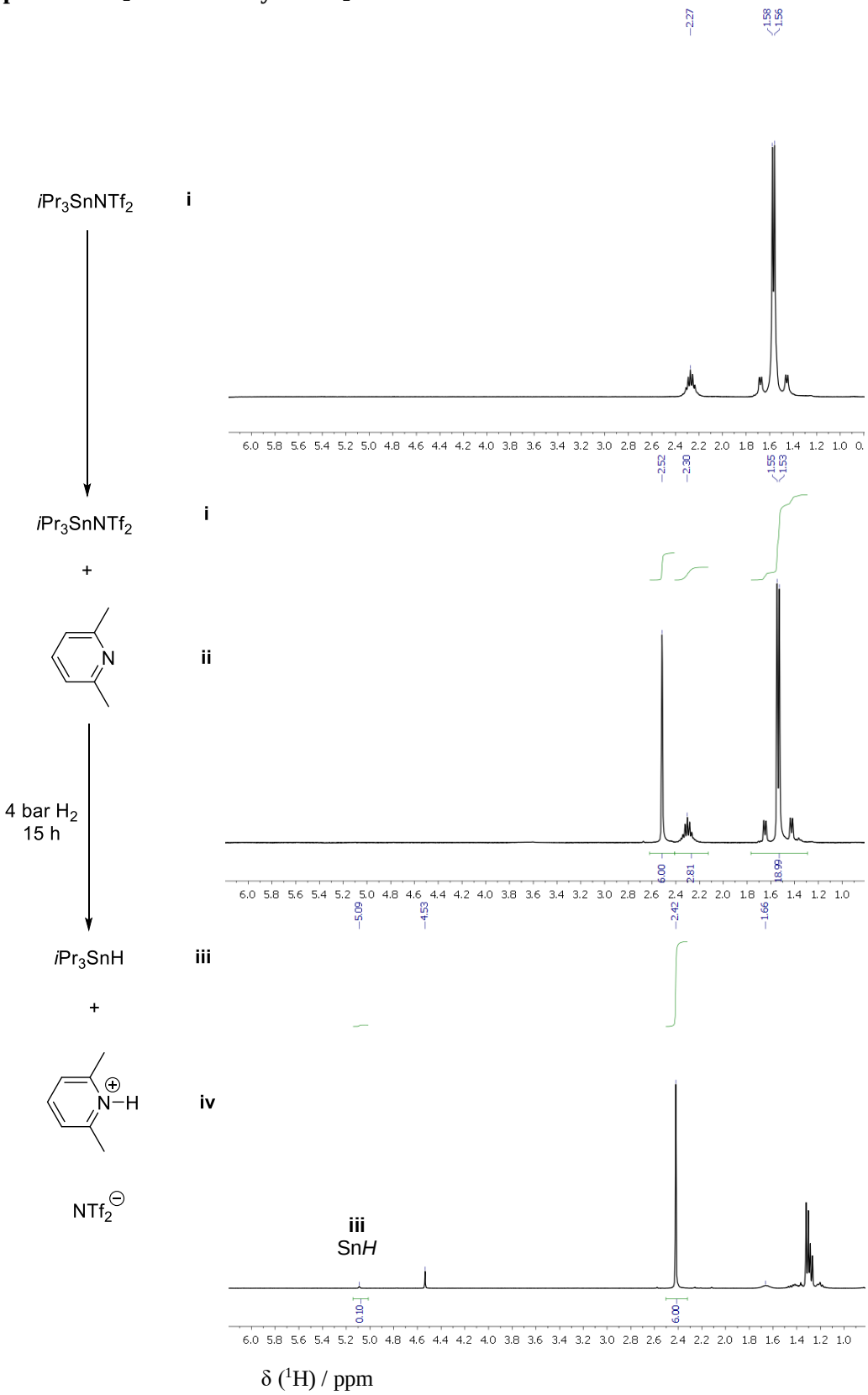

Figure S2 ^{1}H NMR spectra of (a) **1**-NTf_2 in DCB; (b) after the addition of lut; (c) after admission of H_2 and left 15 h at RT.

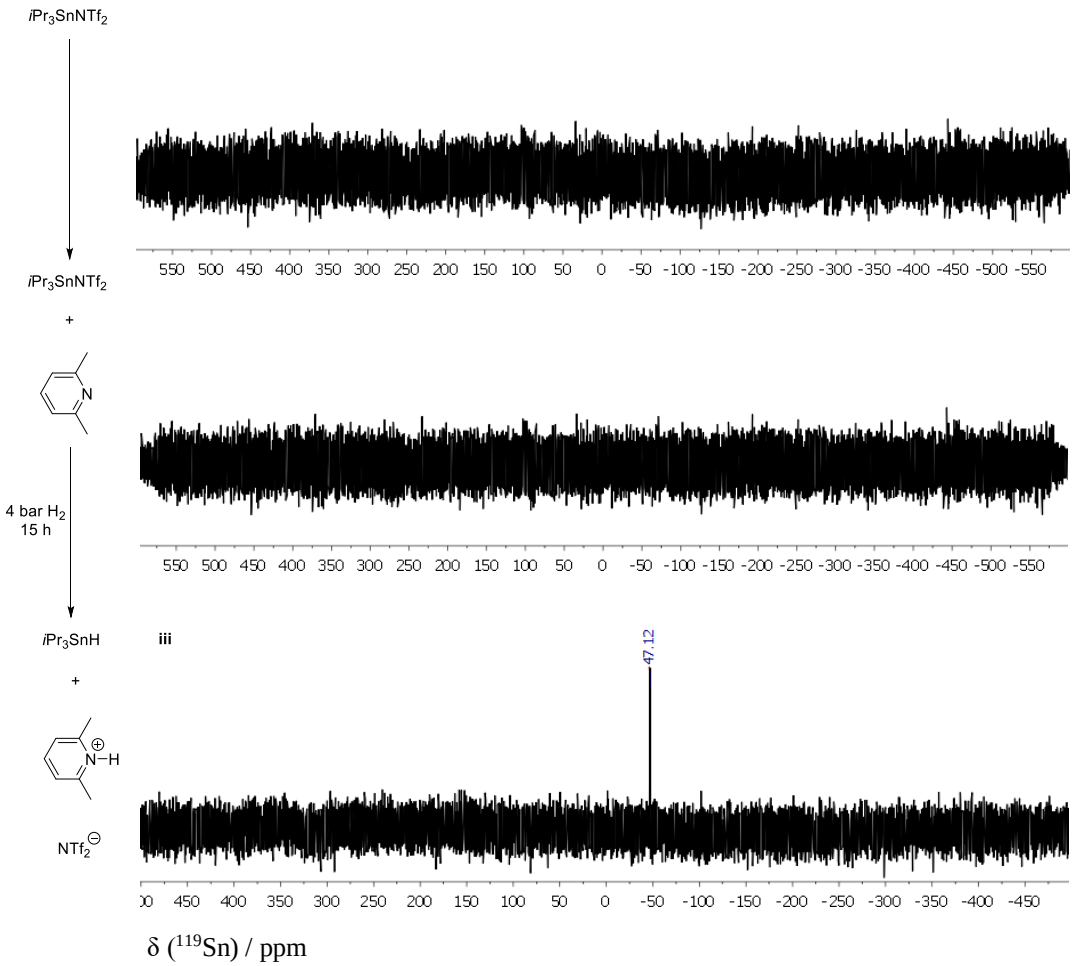

Figure S3 $^{119}Sn\{^{1}H\}$ NMR spectra of (a) **1**-NTf_2 in DCB; (b) after the addition of lut; (c) after admission of H_2 and left 15 h at RT.

3.3. NMR spectra of H_2 activation by 1-NTf_2/col

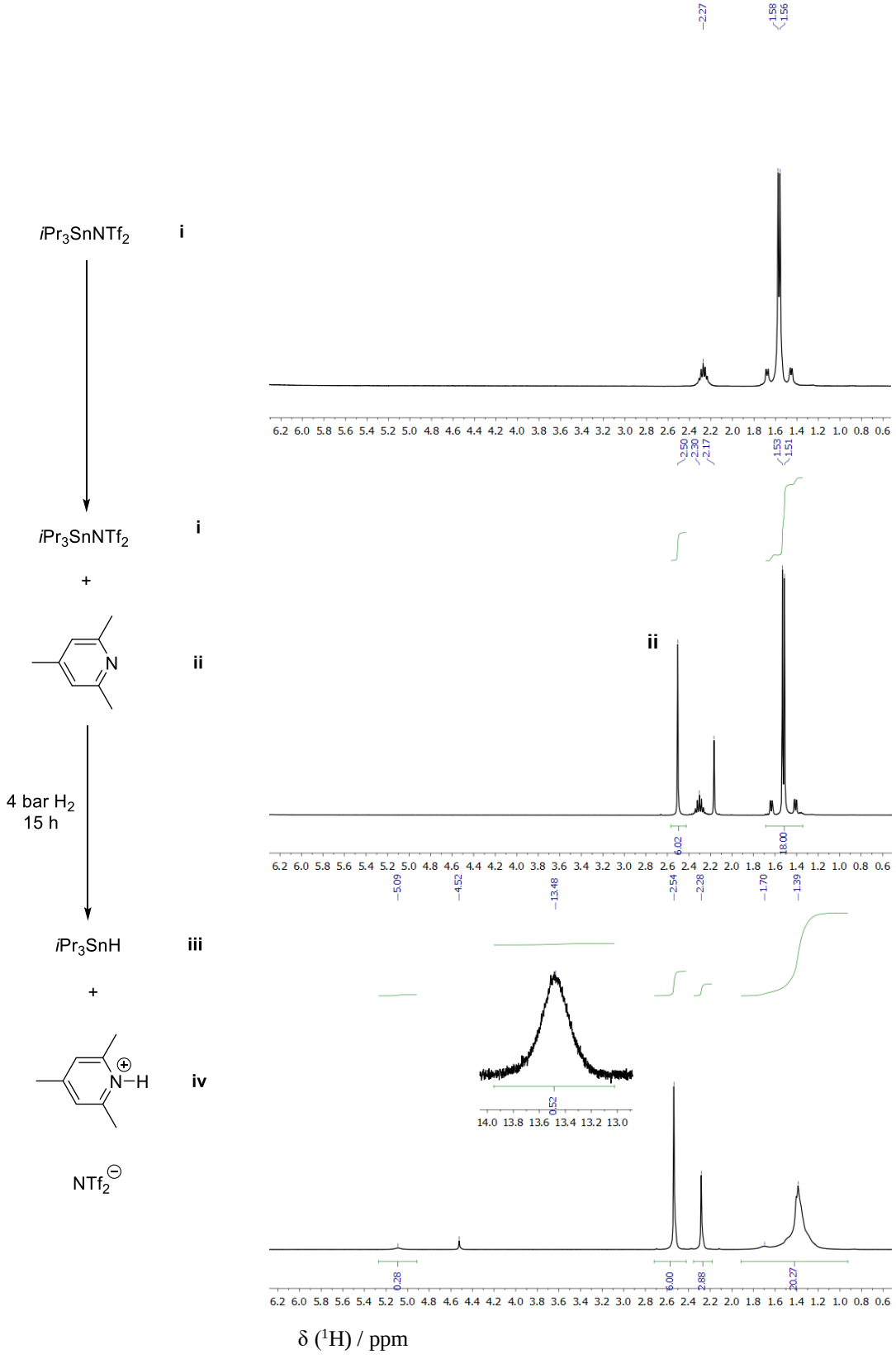

Figure S4 ^{1}H NMR spectra of (a) **1**-NTf_2 in DCB; (b) after the addition of col; (c) after admission of H_2 and left 15 h at RT. Inset provide an expanded view of the col–H^+ resonance. The relative integral of the col–H^+ and col *o*-CH_3 resonances corresponds to a 52% conversion of the reactants to **1**–H and col–H^+.

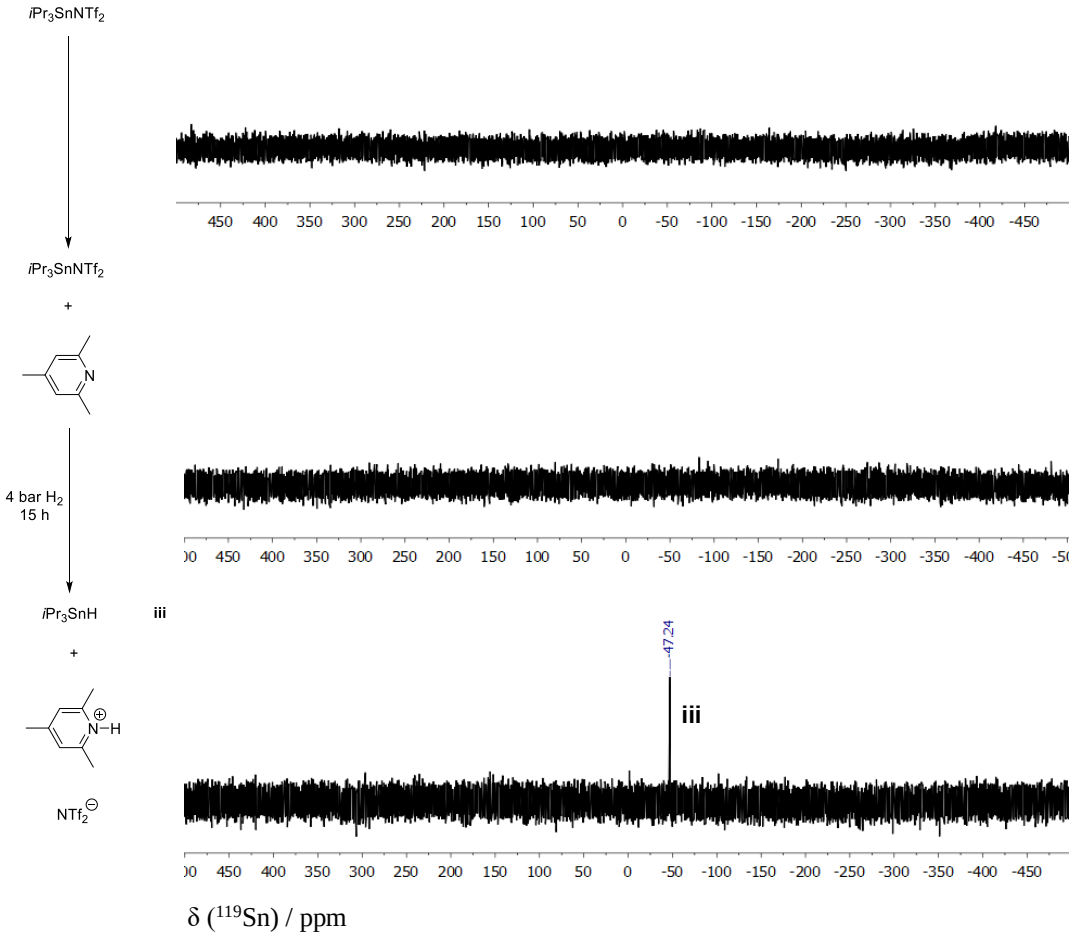

Figure S5 $^{119}Sn\{^{1}H\}$ NMR spectra of (a) **1**-NTf_2 in DCB; (b) after the addition of col; (c) after admission of H_2 and left 15 h at RT.

4. Imine hydrogenations

4.1. Procedure for catalytic hydrogenations of imines

To a DCB (0.5 mL) solution of imine (0.20 mmol) [and, for N–Ar imines, 2,6-lutidine (2.6 µL, 0.02 mmol)] was added **1**-NTf_2 (10.6 mg, 0.02 mmol), in an NMR tube fitted with a J Young's tap containing a capillary insert of C_6D_6. The solution was freeze-pump-thaw degassed and H_2 (1 bar) was admitted to the evacuated tube at −196 °C (*ca*. 4 bar at RT). The reaction mixture was heated at 120 °C and monitored periodically by ^1H NMR spectroscopy.

The NMR spectra were acquired at the beginning and end of the reactions.

Table S1 Results of imine hydrogenation catalyzed by 1-NTf_2.

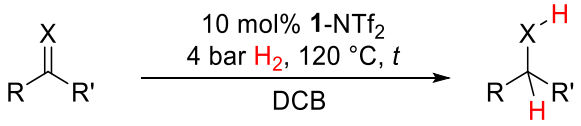

	X	R	R'	LB[a]	*t* (h)	Conversion (%)[b]
1	N*t*Bu	Ph	H	-	12	93
2	N*t*Bu	4-Br-Ph	H	-	12	96
3	NPh	Ph	H	lut	16	>99
4	NPh	Ph	Me	lut	12	98

[a] 10 mol% LB was added, if required. [b] Conversions measured by NMR spectroscopy *in situ* by the ratio of the integrals of peaks assigned to the product amine and reactant imine.

4.2. NMR spectra for catalytic hydrogenations of imines

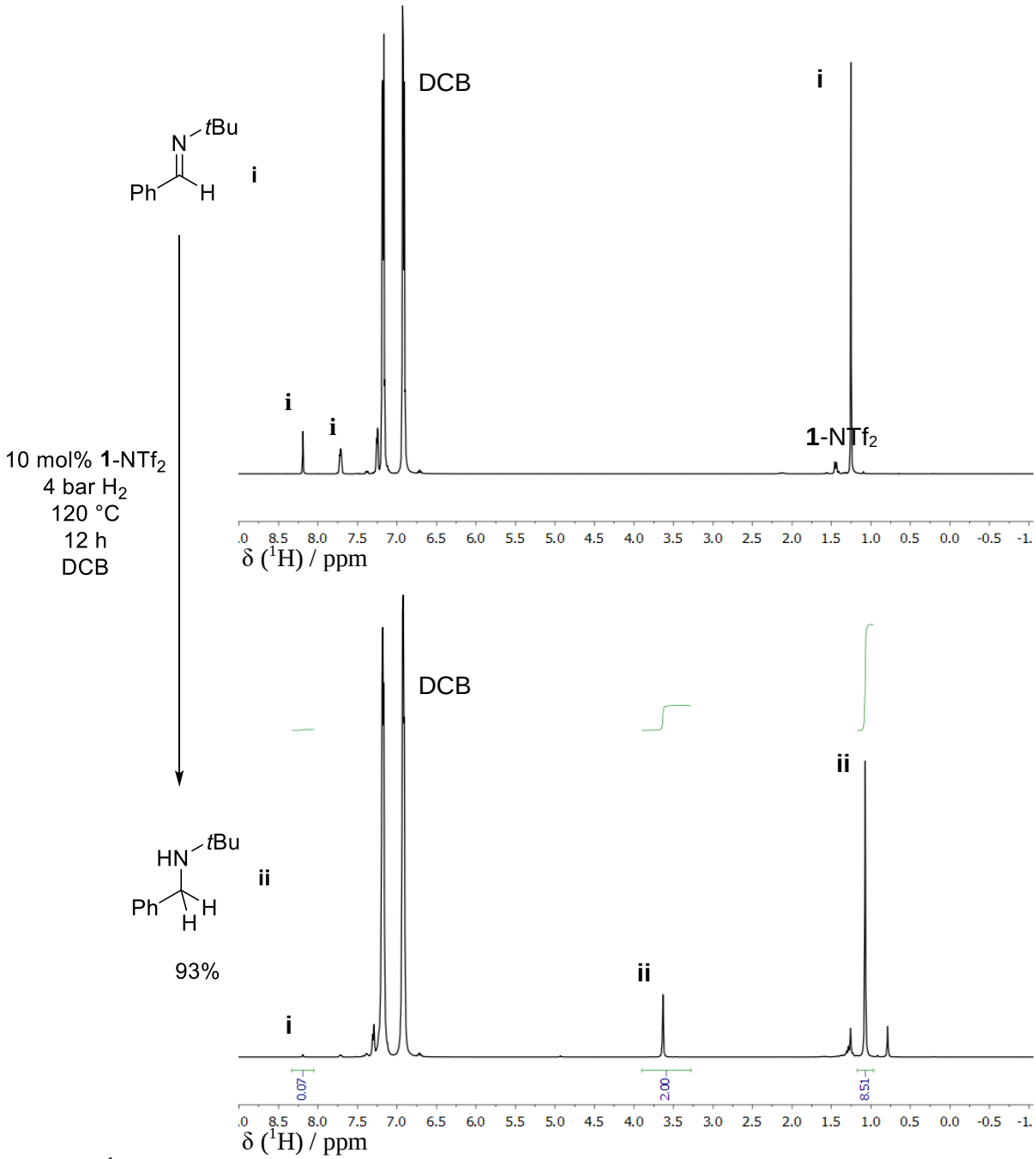

Figure S6 ^{1}H NMR spectra supporting the hydrogenation of PhC(H)=N*t*Bu. NMR spectral data of the product match literature values.[7]

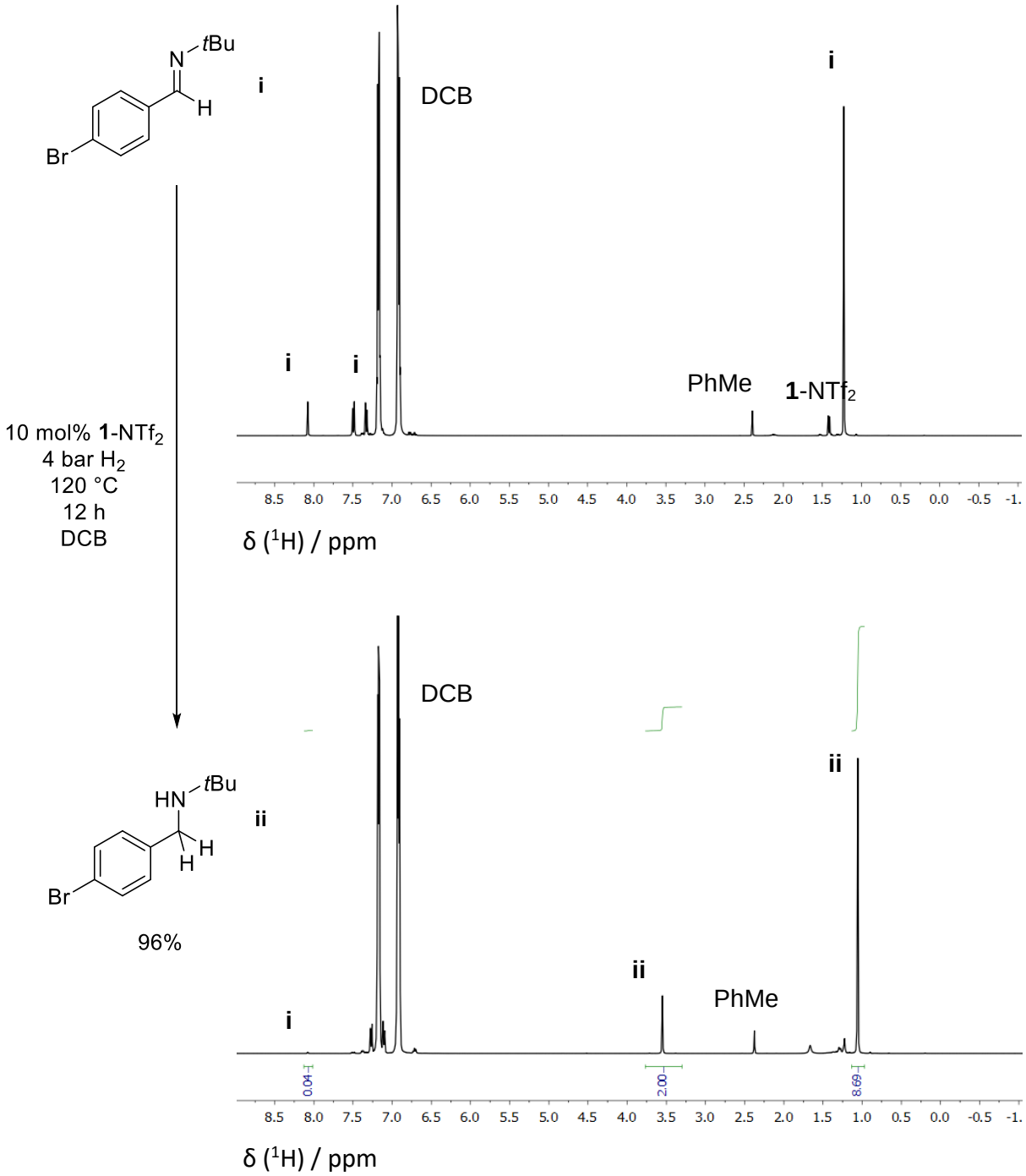

Figure S7 ^{1}H NMR spectra supporting the hydrogenation of (4-Br)C_6H_4C(H)=N*t*Bu. NMR spectral data of the product match literature values.[1]

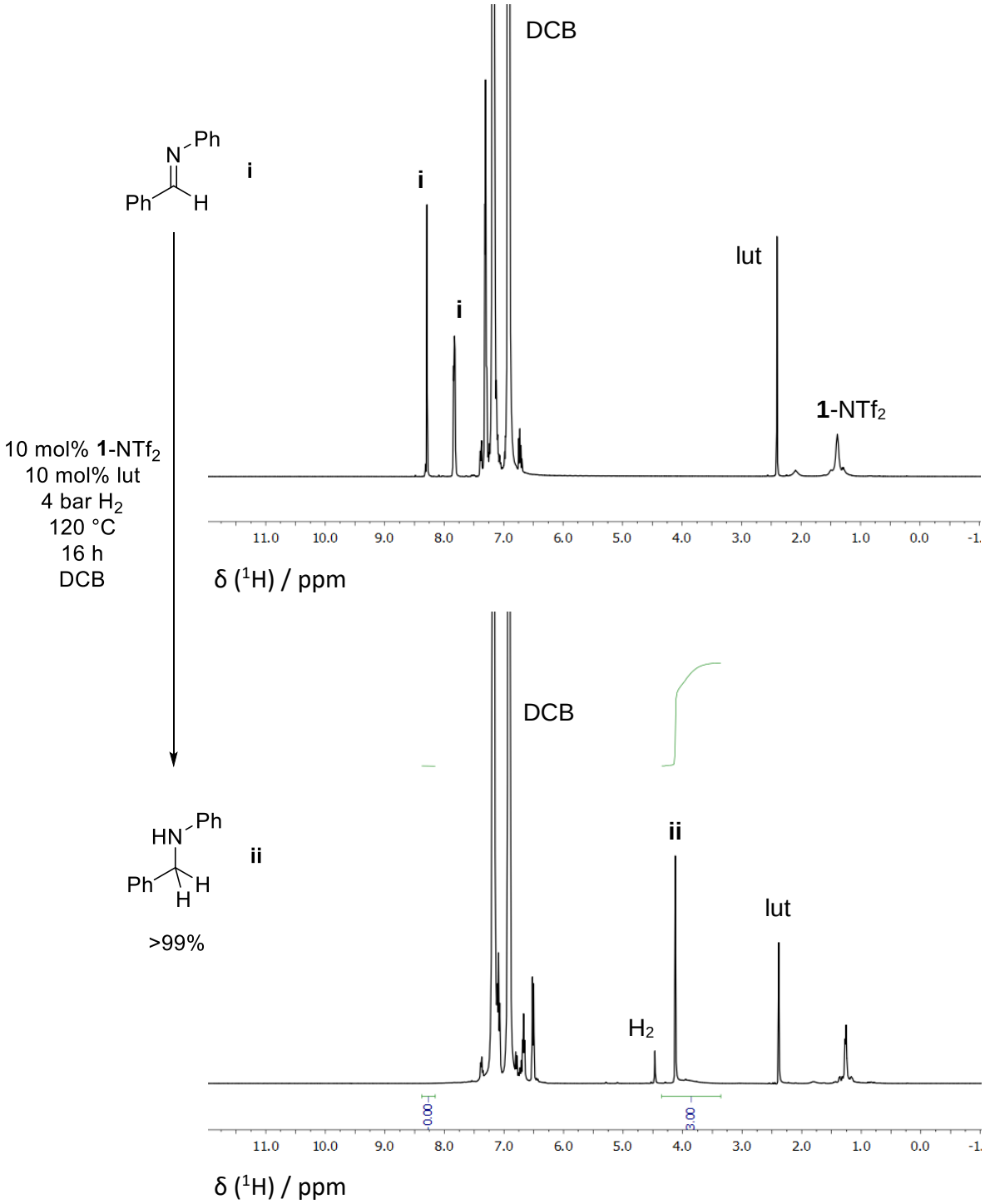

Figure S8 ^{1}H NMR spectra supporting the hydrogenation of PhC(H)=NPh. NMR spectral data of the product match literature values.[1]

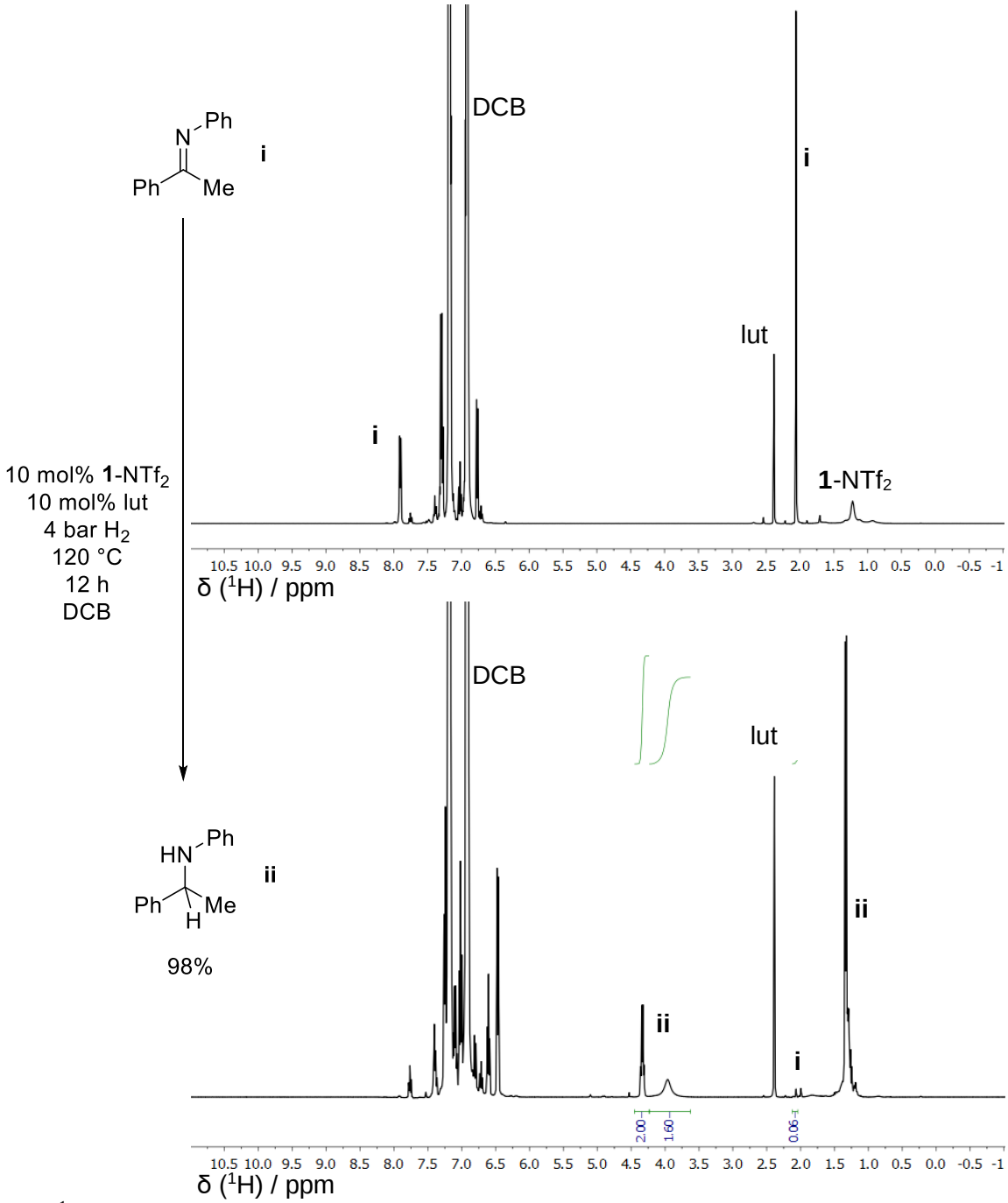

Figure S9 ^{1}H NMR spectra supporting the hydrogenation of PhC(Me)=NPh. NMR spectral data of the product match literature values.[8]

5. Carbonyl hydrogenations

5.1. Procedure for catalytic hydrogenations of acetone

To a solution of acetone (0.20 mmol) and a LB (0.02 mmol) in DCB (0.5 mL) was added **1**-NTf_2 (10.6 mg, 0.02 mmol) in a Wilmad high pressure NMR tube fitted with a PV-ANV PTFE valve. H_2 was admitted up to an internal pressure of 10 bar at RT. The reaction mixture was heated and monitored periodically by ^{1}H NMR spectroscopy.

The reaction run using 4 bar H_2 was prepared according to the procedure for imine hydrogenations provided in Supporting Information Section 4.

For reactions prepared on the 'open bench' undried DCB was used and the solution was freeze-pump-thaw degassed prior to the admission of 10 bar H_2 at RT.

Attempts to heat the 'open bench' reactions at higher temperatures (i.e. 180°C) did not result in superior conversions.

The NMR spectra were acquired at the beginning and end of the reactions.

Table S2 Results of acetone hydrogenation catalyzed by 1-NTf_2/LB pairs (lut = 2,6-lutidine, col = 2,4,6-collidine).

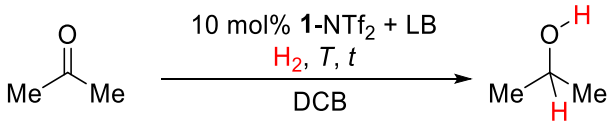

	LB	H_2 *P* (bar)	*T* (°C)	*t* (h)	Conversion (%)[a]
1	col	4	180	90	78
2	col	10	120	32	74
3	lut	10	120	44	49
4[b]	col	10	120	44	58
5[b]	lut	10	120	44	22

[a] Conversions measured by NMR spectroscopy *in situ* by the ratio of the integrals of peaks assigned to the product amine and reactant imine. [b] Reaction prepared on the open bench using undried commercial grade solvent before pressurization.

5.2. NMR spectra for catalytic hydrogenations of acetone

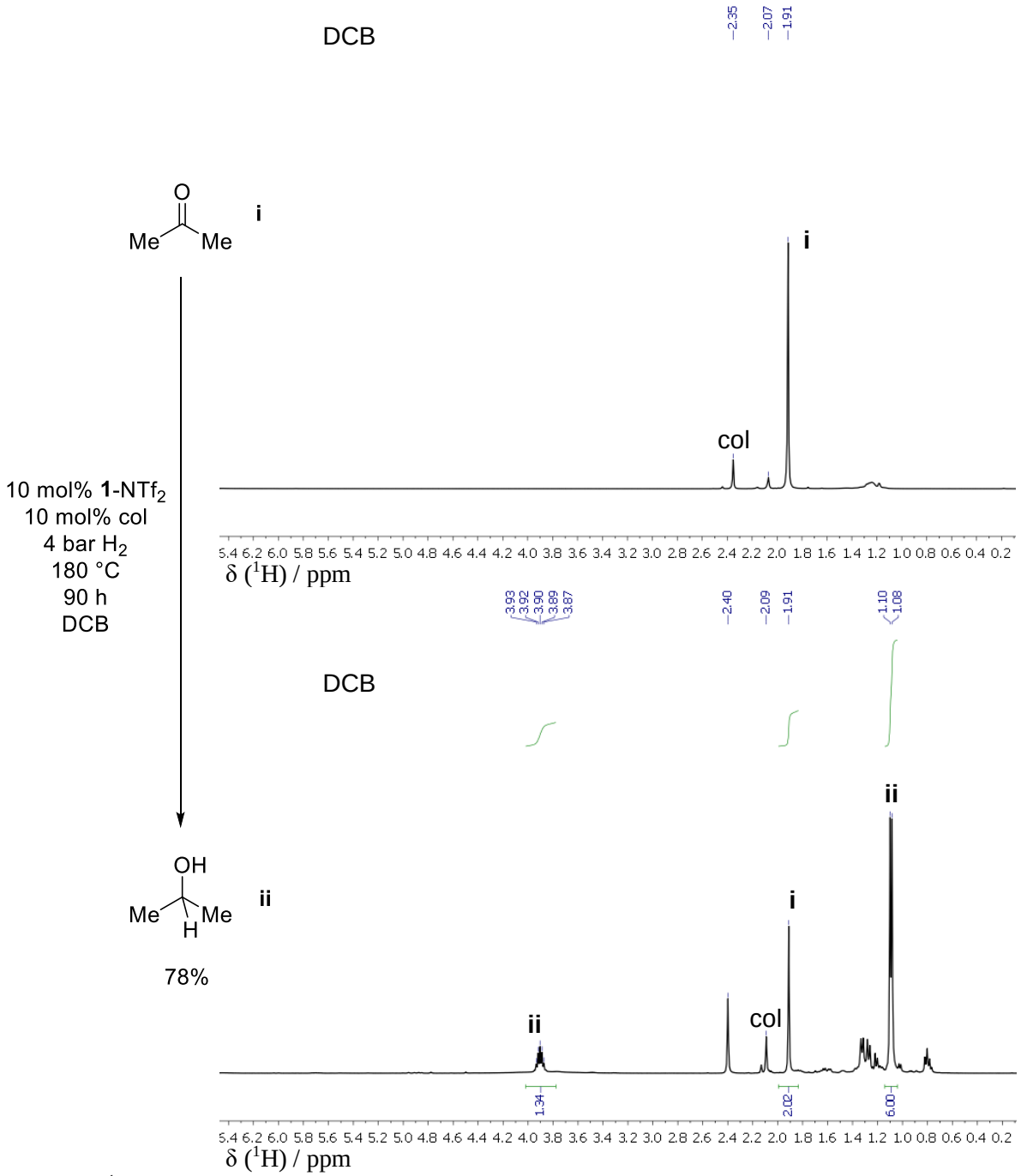

Figure S10 ^{1}H NMR spectra for the hydrogenation of Me_2CO by **1**-NTf_2/col using 4 bar H_2. NMR spectral data of the product match literature values.[9]

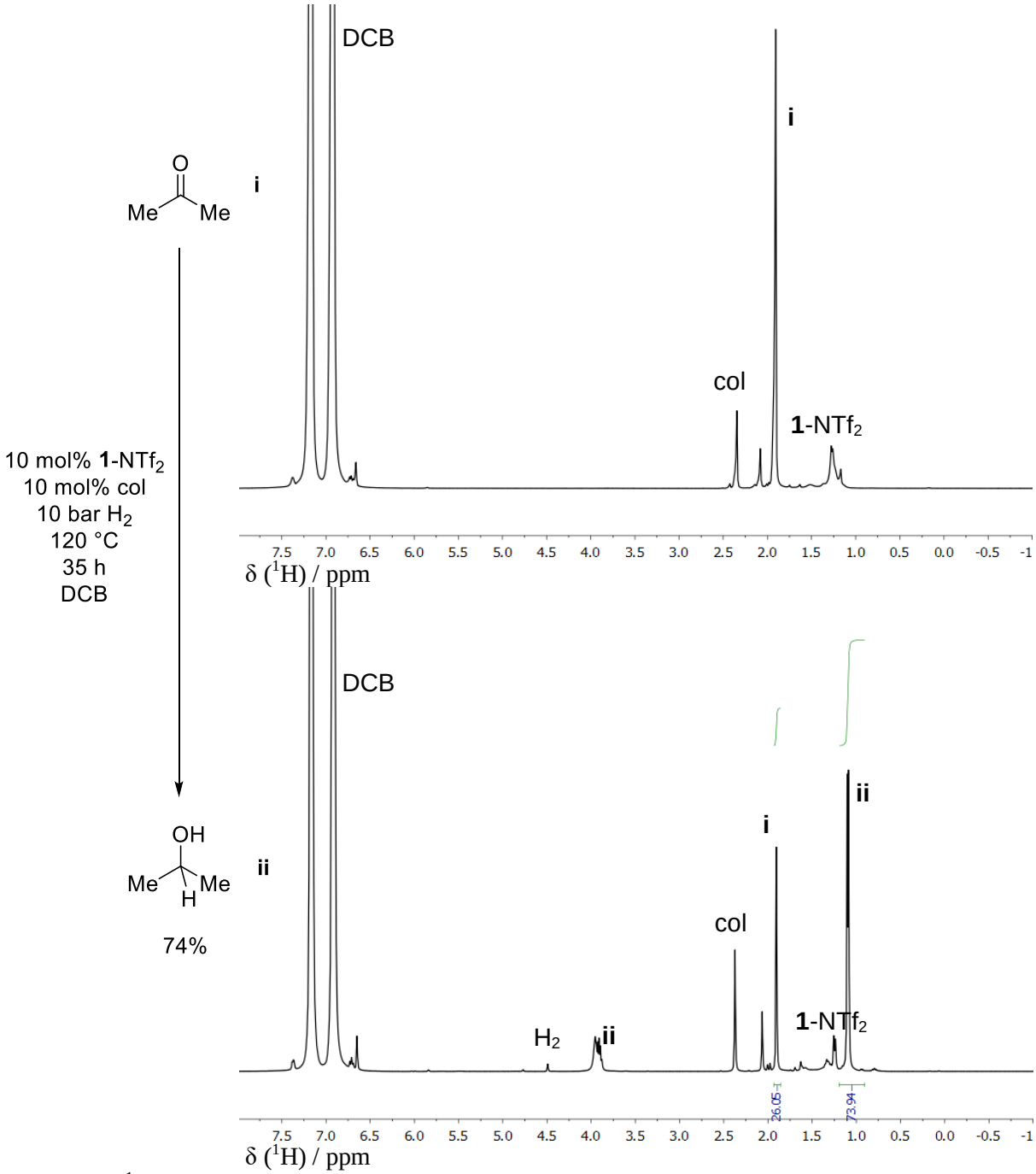

Figure S11 ^{1}H NMR spectra for the hydrogenation of Me_2CO by **1**-NTf_2/col (10 bar). NMR spectral data of the product match literature values.[9]

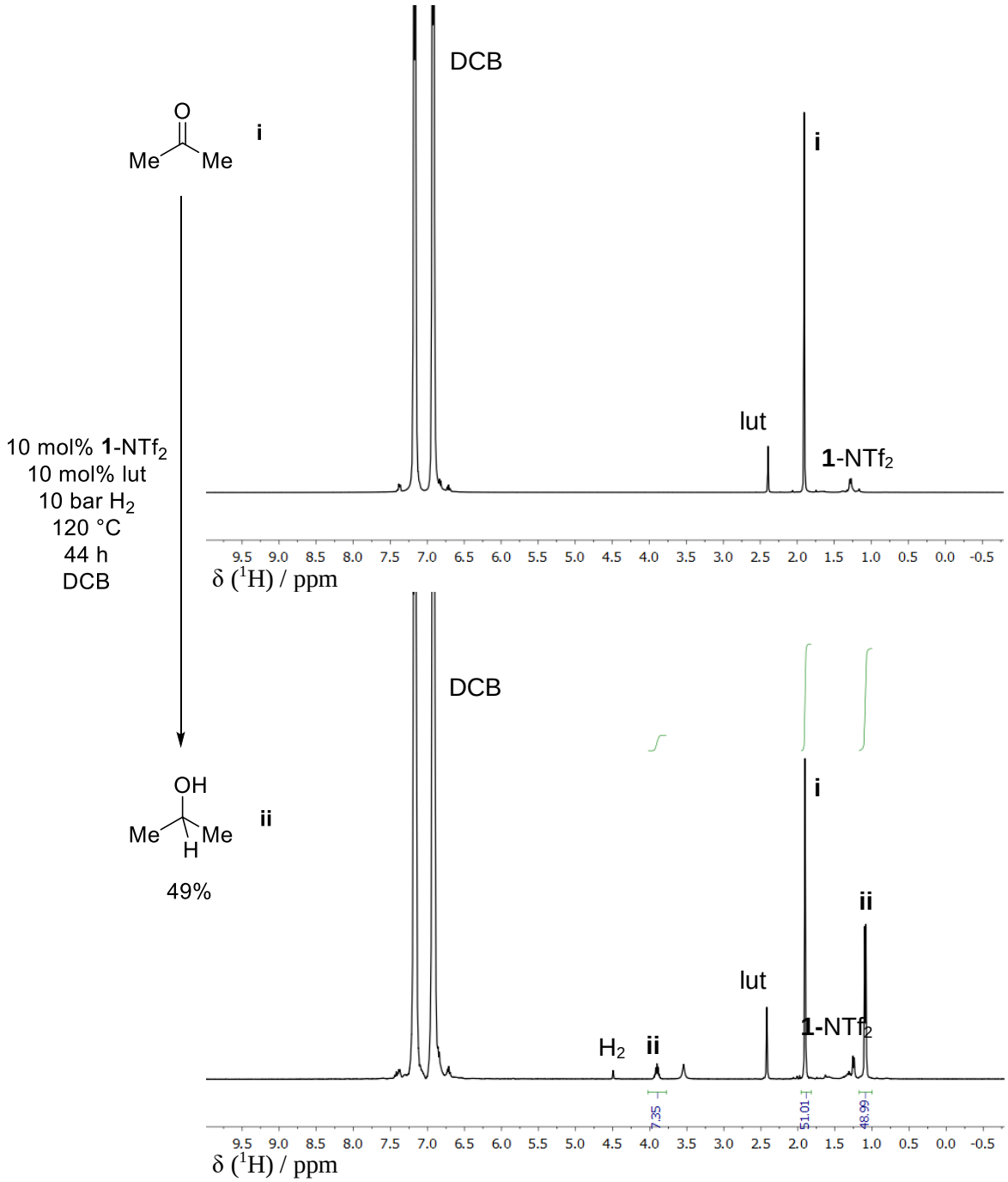

Figure S12 ^{1}H NMR spectra for the hydrogenation of Me_2CO by **1**-NTf_2/lut (10 bar). NMR spectral data of the product match literature values.[9]

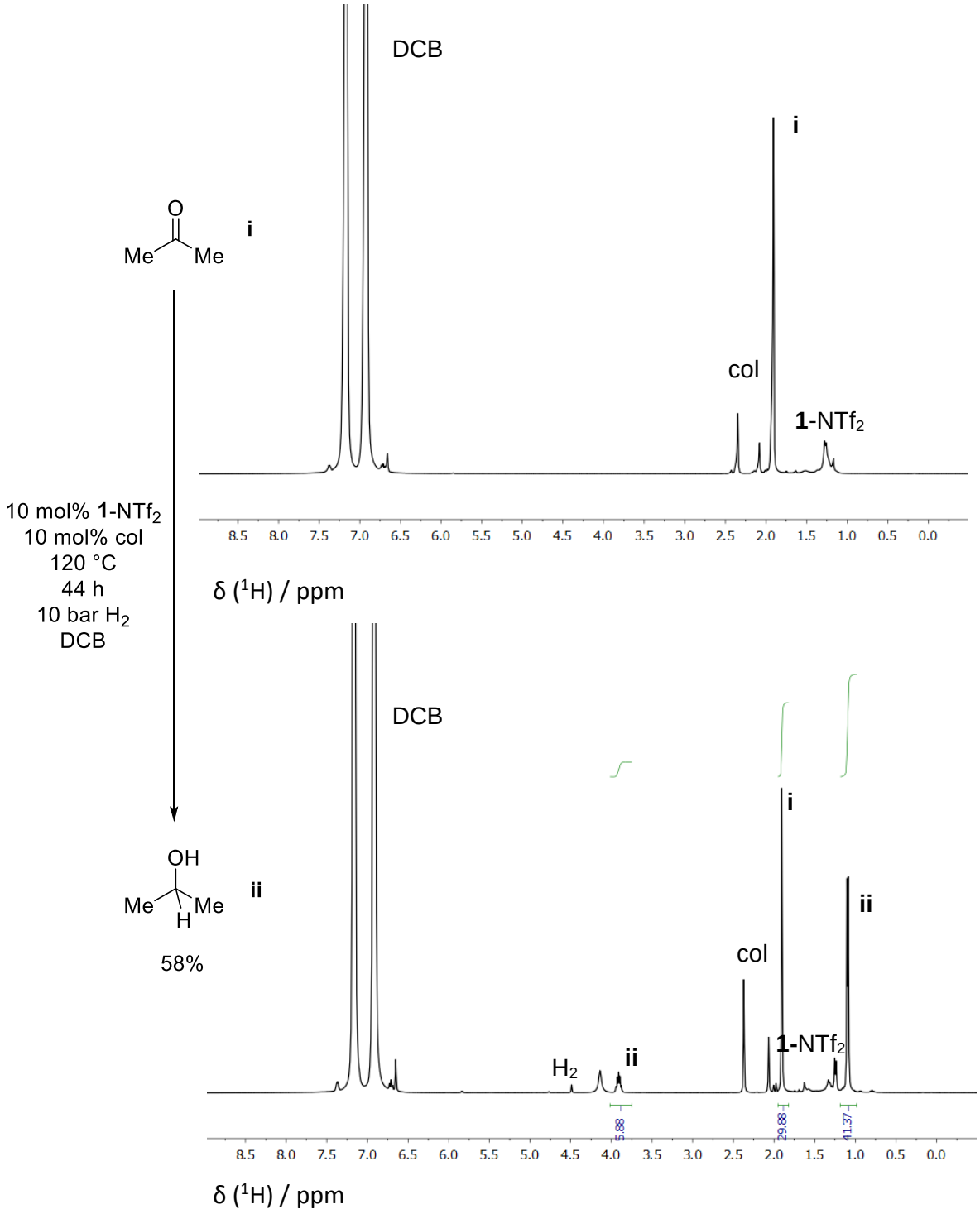

Figure S13 ^{1}H NMR spectra for the open bench hydrogenation of Me_2CO by **1**-NTf_2/col (10 bar). NMR spectral data of the product match literature values.[9]

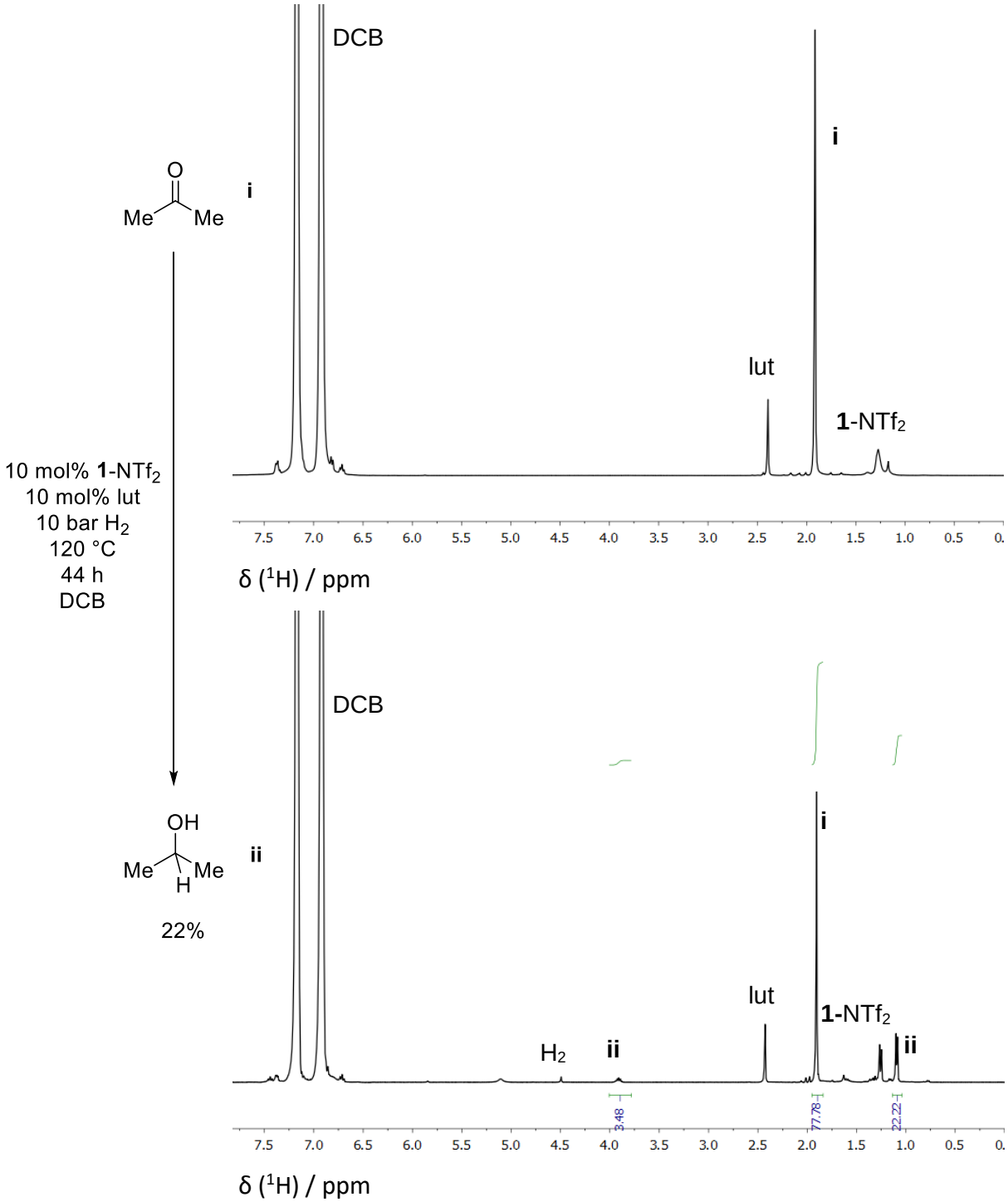

Figure S14 ^{1}H NMR spectra supporting the open bench hydrogenation of Me_2CO by **1**-NTf_2/lut (10 bar). NMR spectral data of the product match literature values.[9]

6. Ester hydrogenations

6.1. Procedure for catalytic hydrogenations of esters

To a solution of ester (0.20 mmol), 2,6-lutidine (2.4 µL, 0.020 mmol) in DCB (0.5 mL) was added *i*Pr_3SnNTf_2 (10.6 mg, 0.020 mmol) in a Wilmad high pressure NMR tube fitted with a PV-ANV PTFE valve. H_2 was admitted up to an internal pressure of 10 bar at RT. The reaction mixture was heated at and monitored periodically by NMR spectroscopy.

The NMR spectra were acquired at the beginning and end of the reactions.

6.2. Optimisation of the reaction conditions for ester hydrogenations

Hydrogenations of CF_3COOEt or MeCOOEt conducted at 180 °C with **1**-NTf_2/lut/H_2 in DCB resulted in some conversion to alcohol products yet catalysis halted within a few hours, concomitant with appreciable darkening of the solution, indicative of decomposition. Conversely analogous reactions at 120°C gave inferior conversions and the reactions were very slow, although the sample remained colourless. Consequently, 150 °C was adopted as a compromise temperature for ester hydrogenations, to access desirable rates under conditions where no sample decomposition was evident.

The production of EtOH clearly inhibits **1**-NTf_2 during the hydrogenation of MeCOOEt, which is proposed to be *via* deprotonation of [**1**-O(H)Et]$^+$ by lut (see computational section), to form **1**-OEt. In support of this hypothesis, using col as a stronger LB resulted in poorer conversions. We hypothesised that using a weaker LB than lut may suppress this deprotonation pathway, yet the trialled weaker LBs did not lead to improvements:

1,4-dioxane was used as a solvent instead of DCB (and acted as the LB), inspired by the success in utilising this strategy for carbonyl hydrogenations catalysed by $B(C_6F_5)_3$.[10,11] Although very limited ester hydrogenation was observed, degradation of **1**-NTf_2 was evident, presumably due to the high acidity of the conjugate acid of 1,4-dioxane. A similar outcome was observed when EtOH, 2-methyl-6-chloropyridine or 2,6-dichloropyridine were used as the LB (10 mol% in DCB) which suggests that a base of intermediate basicity is required to suppress protonative dealkylation of [**1**]$^+$, while also permitting adequate H_2 heterolysis for reduction. When 2-picoline was used, which is a structurally related pyridine but lacking the steric bulk of lutidine/collidine and with a lower basicity, formation of an adduct was seen (ca. 0.5 ppm downfield shift for the *i*Pr resonances in the ^{1}H NMR spectrum); no H_2 cleavage at RT or 150°C is observed, which can be rationalised by the formation of a classical Lewis pair that also does not have the requisite cumulative Lewis acidity/basicity to engage in H_2 heterolysis in conjunction with **1**-NTf_2, and $MeCO_2Et$ was unsurprisingly not hydrogenated using this Lewis base.

The following LBs did not seem to effect H_2 activation in conjunction with **1**-NTf_2, as no hydrogenation of MeCOOEt was observed: Ph_3P, trimesitylphosphine, 2,6-dimethylaniline, 2,4,6-tris-*tert*-butylaniline. Neither evidence for adduct formation nor an appreciable interaction between the LA and LB akin to that for lut/col + **1**-NTf_2, could be observed by ^{119}Sn{^{1}H} or ^{31}P{^{1}H} NMR spectroscopy. It is possible that these LBs are unable to form encounter complexes with **1**-NTf_2, either due to steric or electronic factors, that can activate H_2 at a productive rate.

6.3. Ester substrate scope for hydrogenations mediated by 1-NTf_2

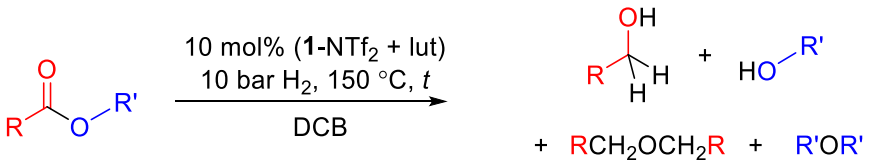

Table S3 Results of ester hydrogenation catalyzed by 1-NTf_2/lut.

Entry	R	R'	*t* (h)	Ester conversion, %	Ether formed (%)	TON (H_2)[f]
1	CF_3	Et	72	80[a,b]	Et_2O (6.4)[d]	16
2	CF_3	*n*Bu	61	10[a,b]	*n*Bu_2O (1.3)[d]	2.2
3	H	Et	40	37[c]	Me_2O (2.9)[d]	7.4
4	H	Me	40	38[c]	Me_2O (2.7)[e]	7.6
5	Me	Et	35	4[a]	Et_2O (0.15)[e]	0.8
6	*i*Pr	Et	40	0	0	0
7	CF_3	Ph	48	9[a]	0	1.8
8	CF_3	*i*Pr	48	7[a]	0	1.4
9[g]	CF_3	C_6F_5	48	3[a]	0	0.6
10[g]	CF_3	CH_2CF_3	0	0	0	0

[a]Conversions measured using *in situ* ^{1}H NMR spectroscopy, calculated as the ratio of peak integrals assigned to alcohol and ether products vs reactant ester. [b]CF_3CH_2O-ethers were not formed. [c]Conversions measured by ^{1}H NMR spectroscopy *in situ* by the ratio of the integrals of ester and product peaks vs PhMe internal standard, due to the volatility of Me_2O. [d]Calculated as % of ether product from initial ester, on the basis that one mole of ester produces 0.5 mol of ether. [e]Calculated as % of ether product from initial ester, on the basis that one mole of ester produces one mol of ether. [f]TON defined as number of H_2 molecules cleaved per **1**-NTf_2. [g]These substrates reacted with **1**-NTf_2/lut during the hydrogenation.

For reactions producing MeOH and Me_2O (which is formed via MeOH condensation), the values obtained from ^{1}H NMR integration are lower than that expected from ester conversion (which are calculated via relative integration against the internal PhMe standard), and is due to the volatility of Me_2O which partitions predominantly in the NMR tube headspace.

Disappointingly, expanding the substrate scope from CF_3OOEt to esters with different R' groups was unsuccessful. Even the change from Et to *n*Bu prevented successful catalysis (TON ≥ 2), effectively achieving only a single turnover, which was attributed to the inhibitory effect of the alkyl alcohol products. It was anticipated that ester 7 would produce PhOH, a poorly nucleophilic alcohol due to resonance of the O lone pair and the Ph ring, however this was not successful. Attempting hydrogenation of ester 8 to produce *i*PrOH, the same product as from successful catalytic hydrogenation of acetone, was also unsuccessful, presumably because *i*PrOH inhibits **1**-NTf_2 for the reduction step, but not H_2 cleavage. Esters 9 and 10 reacted with the **1**-NTf_2/lut pair, as evidenced by a rapid decrease in the intensity of the ^{1}H NMR resonances for the *i*Pr groups associated with **1**-NTf_2; this was disappointing given that ester 9, $CF_3COOCH_2CF_3$, was stoichiometrically hydrostannated at an exceptional rate (see Section 8.2, Figures S36-S38).

Clearly, the success of catalysis is extremely sensitive to the functionality of the ester and its corresponding alcohol products. Nevertheless, it should be noted that even the stoichiometric direct hydrogenations of esters (i.e. using H_2 as the terminal reductant) is remarkable for systems that do not feature a transition metal.

6.4. NMR spectra of ester hydrogenations

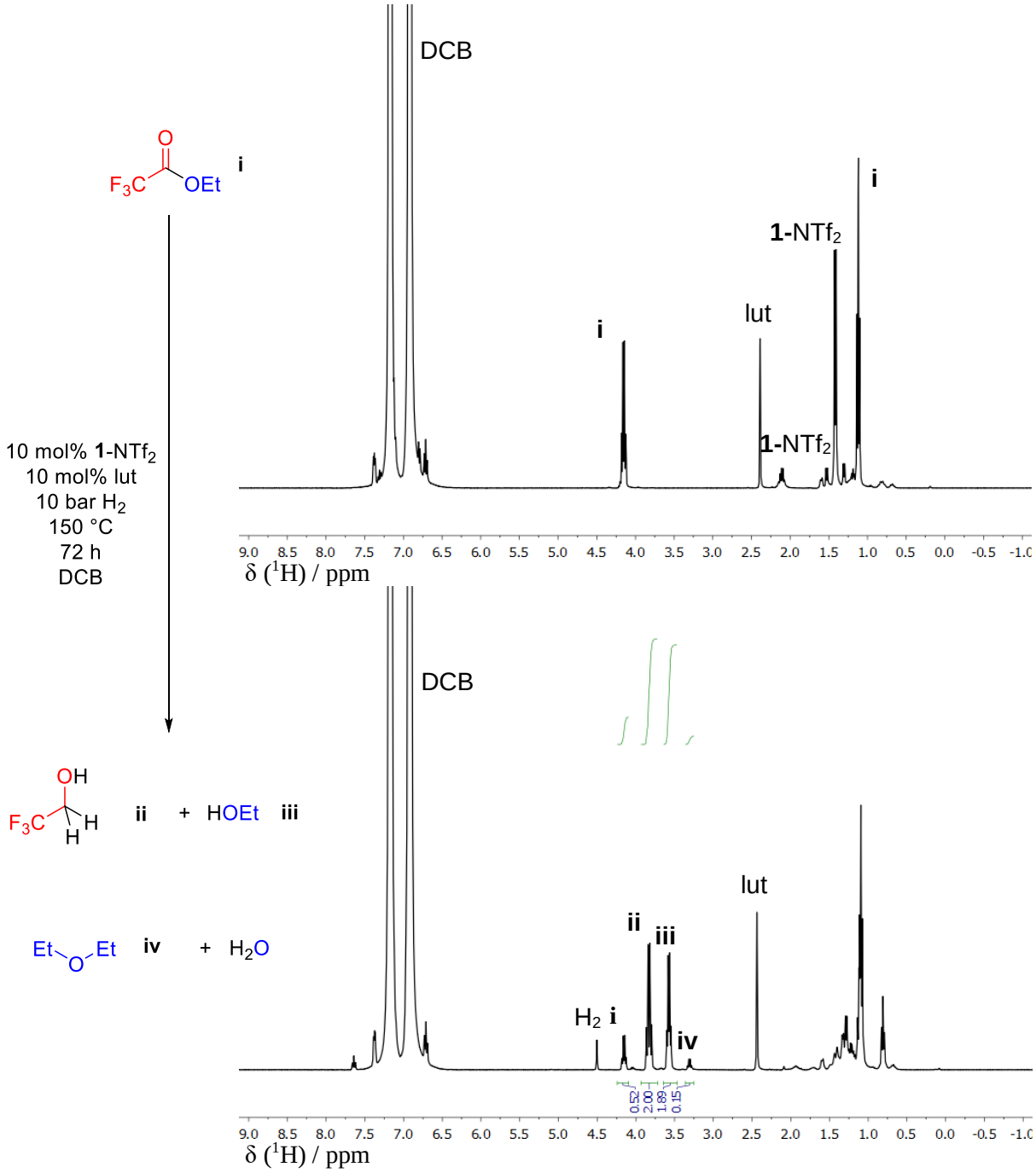

Figure S15 ^{1}H NMR spectra supporting the hydrogenation of CF_3COOEt with **1**-NTf_2/lut. All species were assigned based on the shifts of authentic samples in DCB.

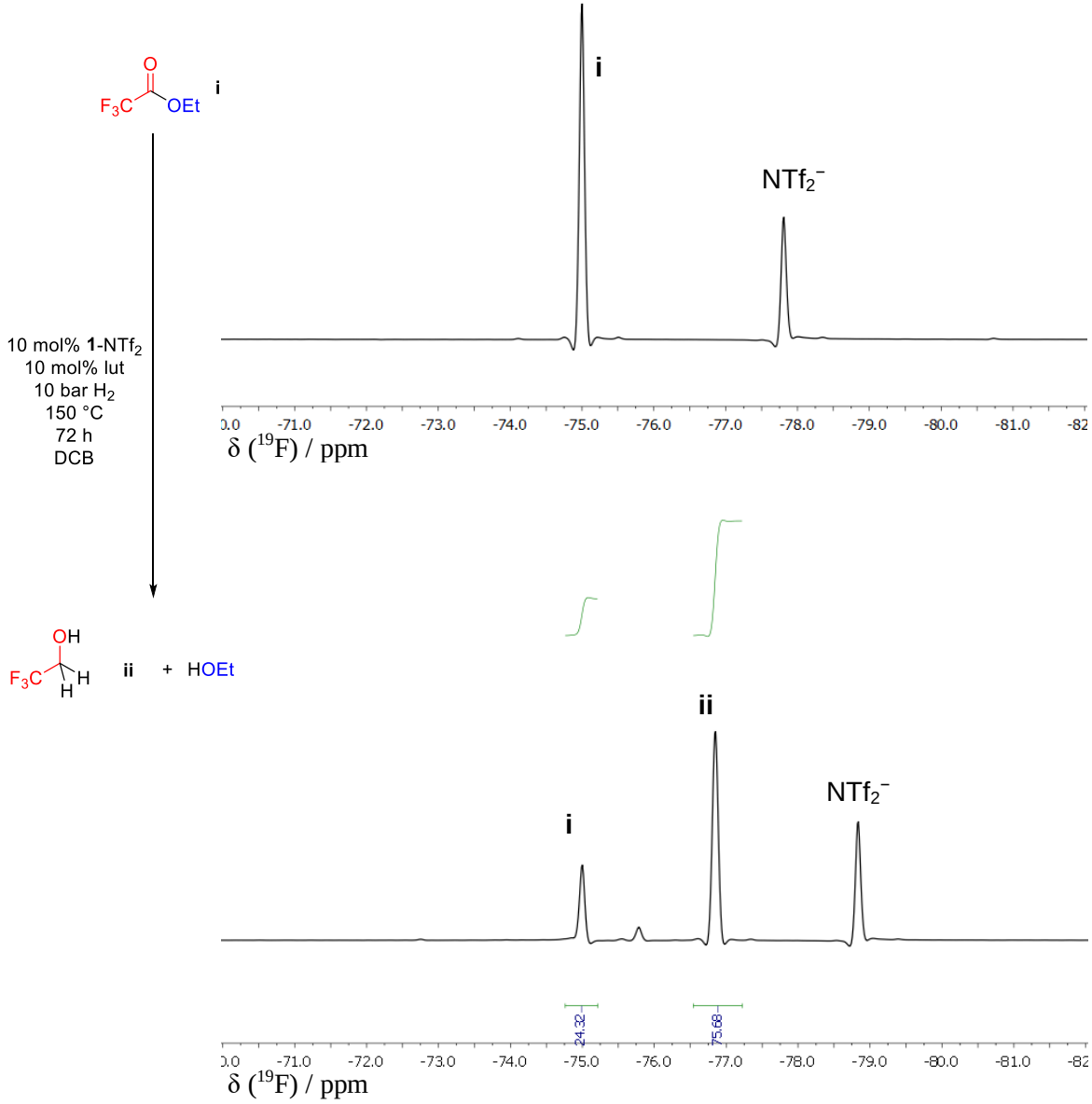

Figure S16 $^{19}F\{^{1}H\}$ NMR spectra supporting the hydrogenation of CF_3COOEt with **1**-NTf_2/lut. All species were assigned based on the shifts of authentic samples in DCB.

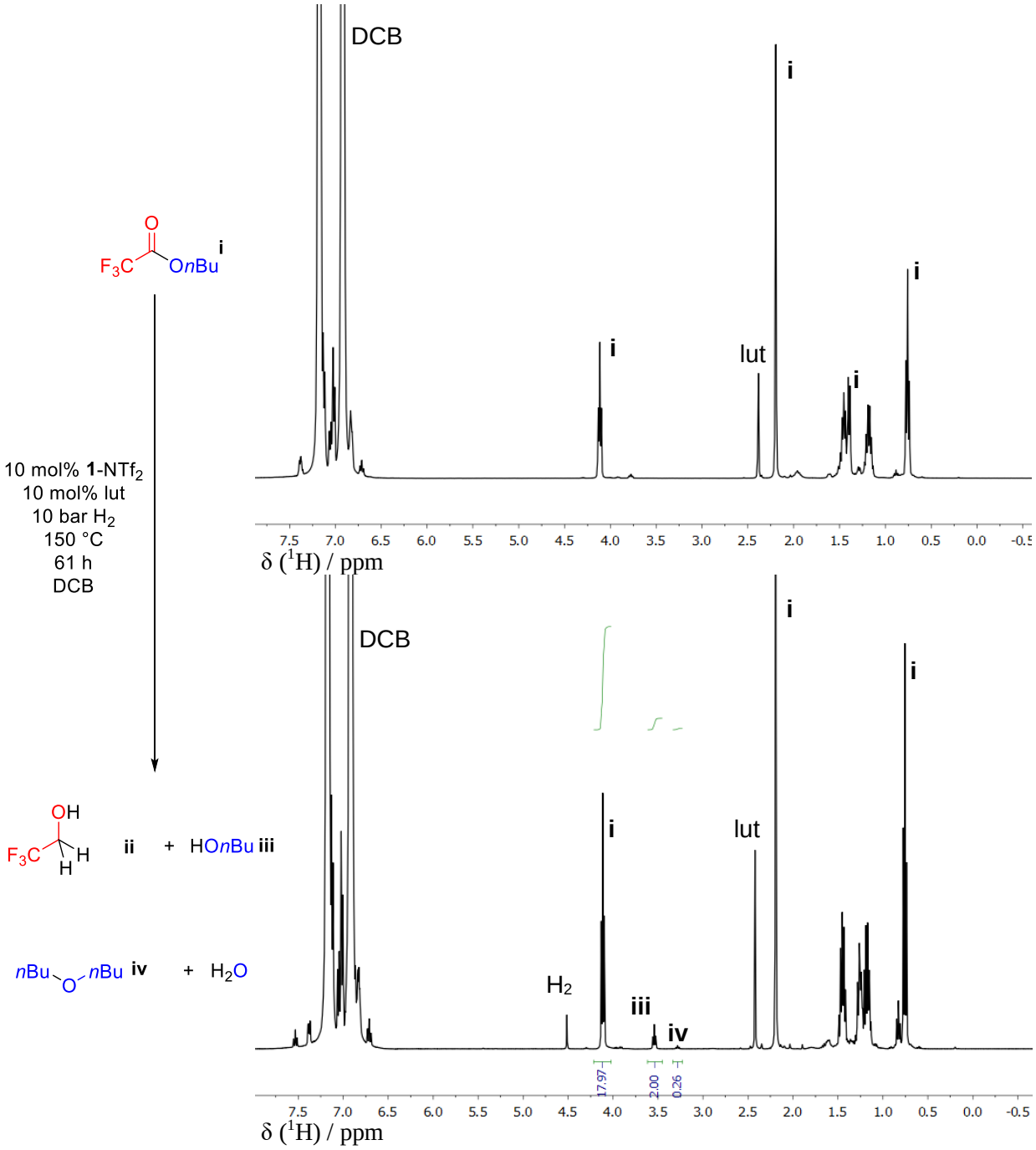

Figure S17 ^{1}H NMR spectra supporting the hydrogenation of $CF_3COOnBu$ with **1**-NTf_2/lut. All species were assigned based on the shifts of authentic samples in DCB (except **iv**[12]). The CH_2 resonance of **ii** is too broad to be observed in the ^{1}H NMR spectrum, but its formation is confirmed by ^{19}F{^{1}H} NMR spectroscopy.

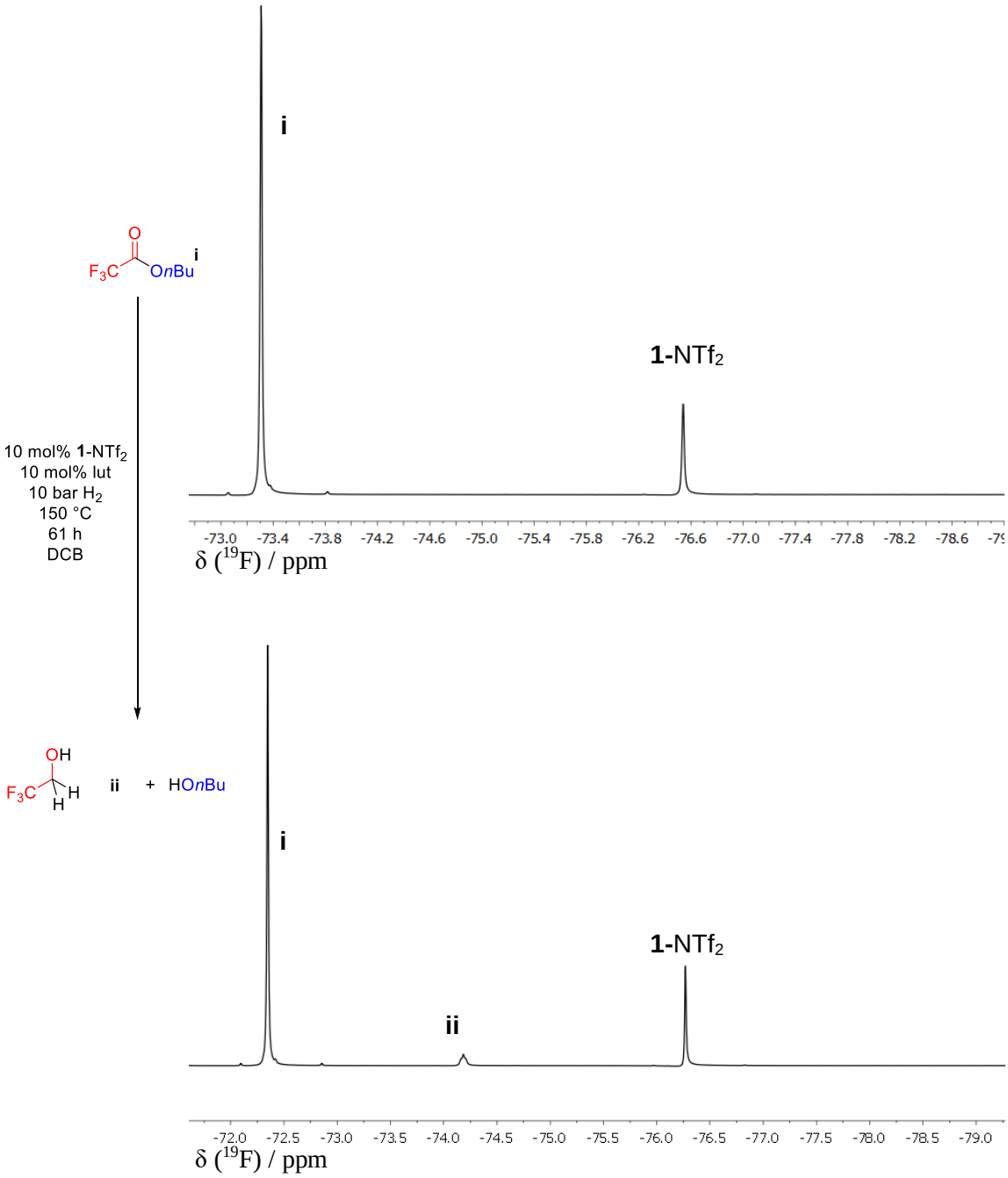

Figure S18 $^{19}F\{^{1}H\}$ NMR spectra supporting the hydrogenation of $CF_3COOnBu$ with **1**-NTf_2/lut. All species were assigned based on the shifts of authentic samples in DCB.

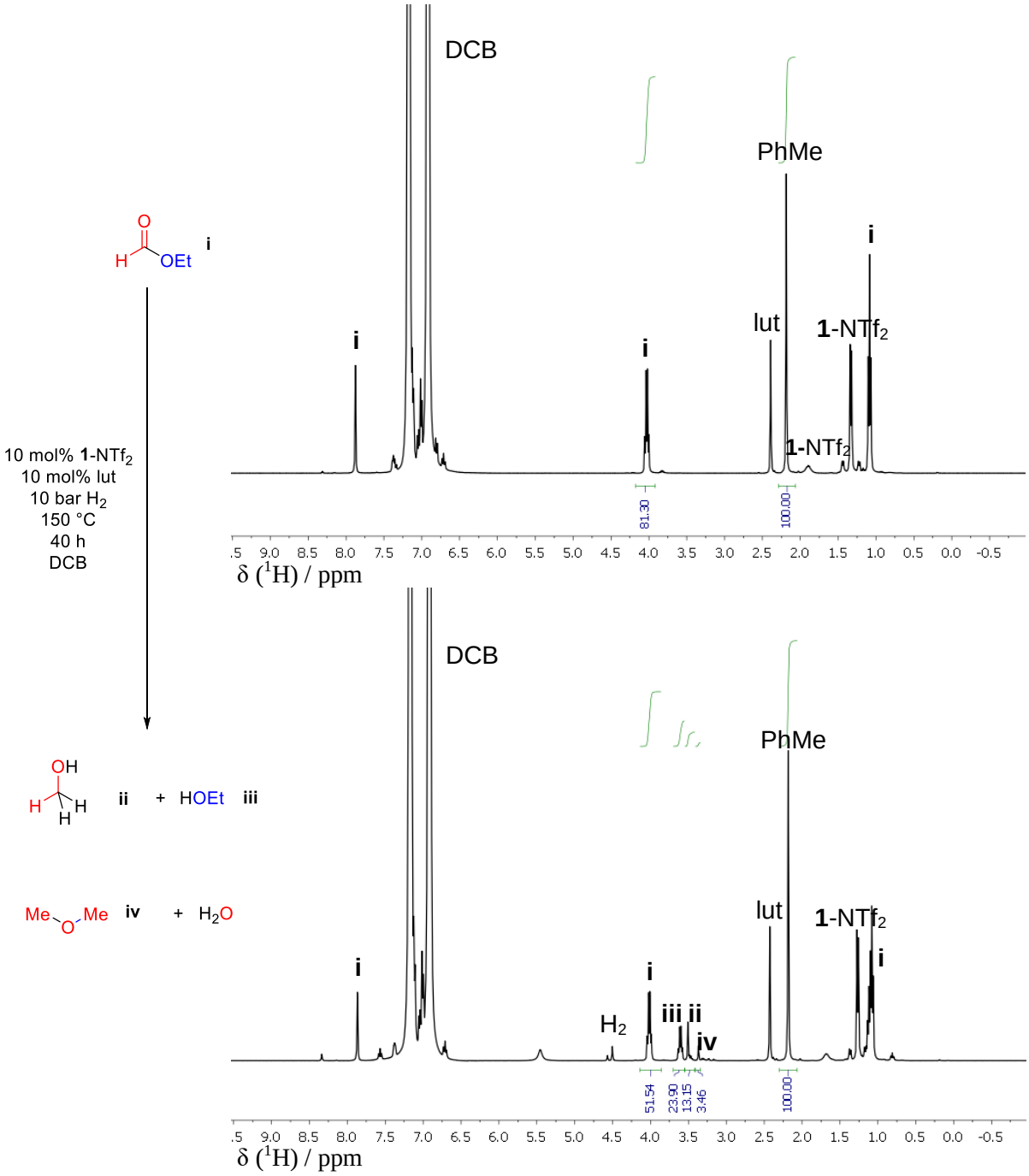

Figure S19 ^{1}H NMR spectra supporting the hydrogenation of HCOOEt with **1**-NTf_2/lut. All species were assigned based on the shifts of authentic samples in DCB. Integrals for this reaction were measured relative to the internal PhMe standard.

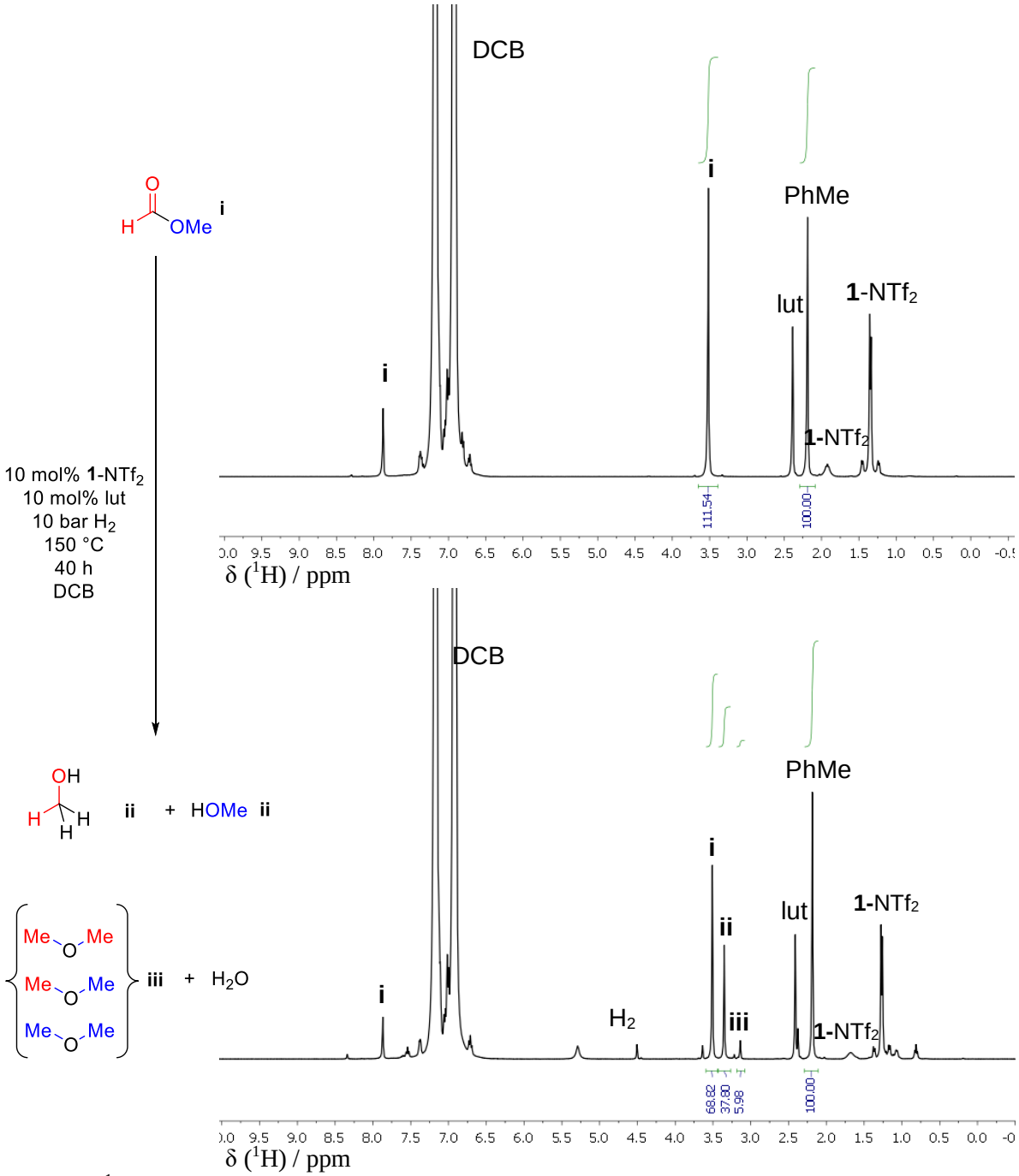

Figure S20 ^{1}H NMR spectra supporting the hydrogenation of HCOOMe with **1**-NTf$_2$/lut. All species were assigned based on the shifts of authentic samples in DCB (except for **iii**, the shift of which is consistent with that previously reported[13]). Integrals for this reaction were measured relative to the internal PhMe standard.

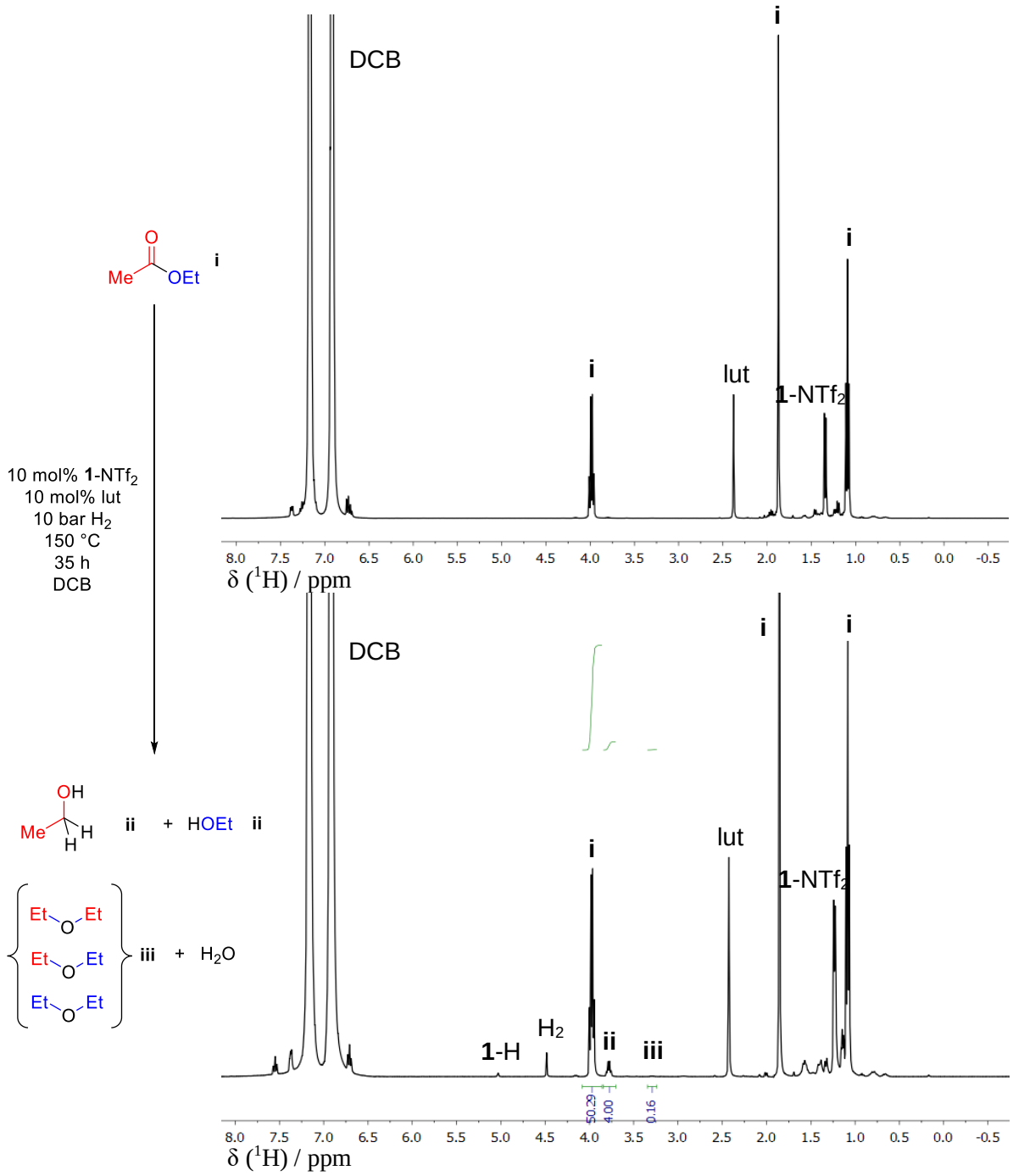

Figure S21 ^{1}H NMR spectra supporting the hydrogenation of MeCOOEt with **1**-NTf$_2$/lut. All species were assigned based on the shifts of authentic samples in DCB. Note the appearance of **1**-H in the reaction (see Section 12.5 for further discussion).

7. Condensation of EtOH to Et_2O mediated by 1-NTf_2

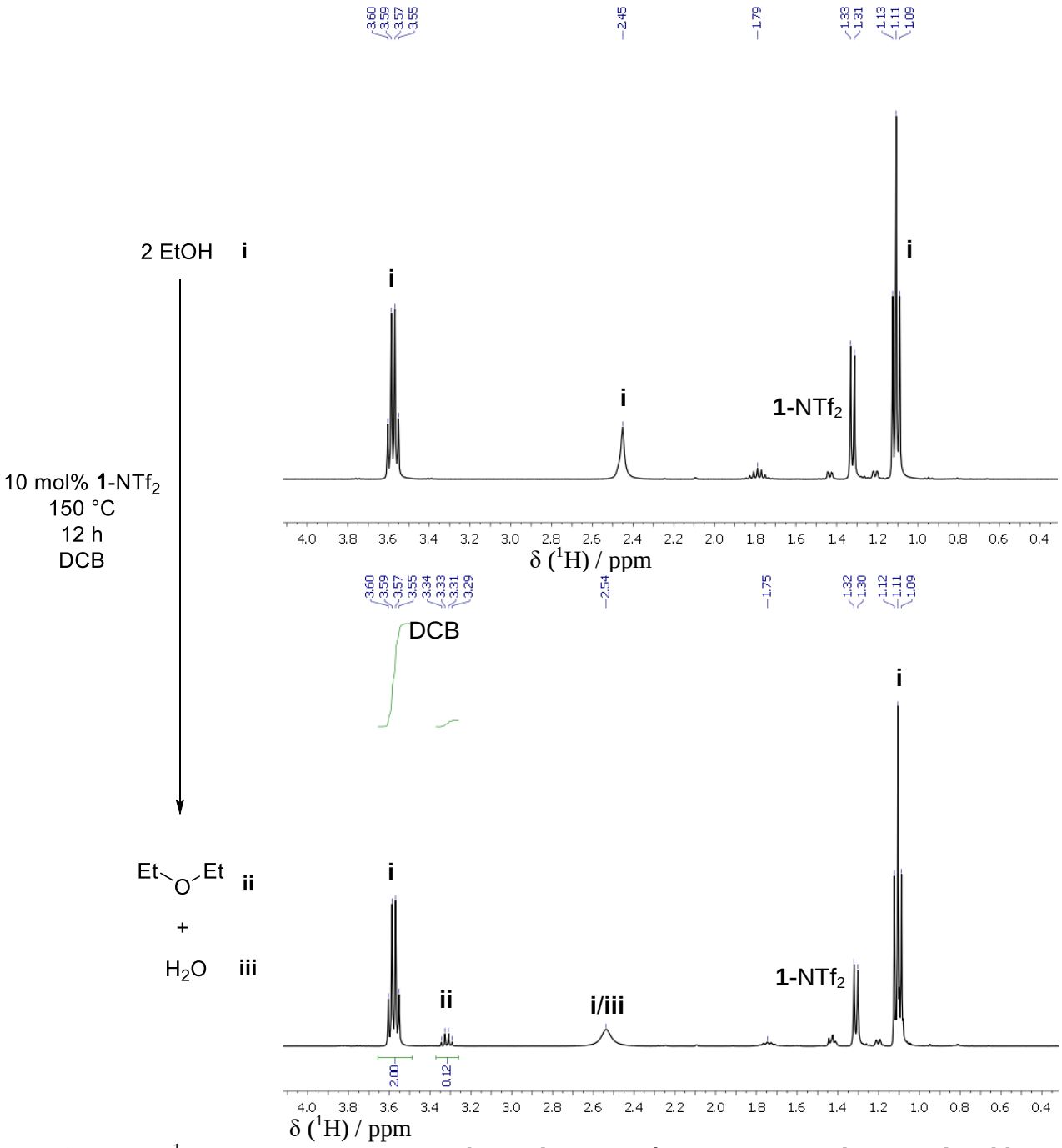

Figure S22 ^1H NMR spectra supporting the condensation of EtOH to Et_2O and H_2O mediated by **1**-NTf_2/lut. All species were assigned based on the shifts of authentic samples in DCB.

8. Ester hydrostannations using 1-H

Hydrostannations of ester using authentic **1**-H were performed to probe the reduction step during hydrogenation catalysis.

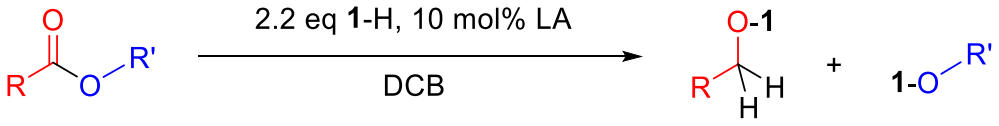

8.1. Procedure for hydrostannations of esters

An ester (0.020 mmol) and **1**-H (11.0 mg, 0.044 mmol) were combined in DCB (0.5 mL) in an NMR tube fitted with a J Youngs tap with a C_6D_6 capillary insert. The solution was left at RT, or heated for a specified period of time, until reaction was observed. **1**-NTf_2 (0.002 mmol) was subsequently added, and some tubes were heated at increasingly elevated temperatures.

The NMR spectra were acquired throughout the reactions.

8.2. NMR spectra of ester hydrostannations

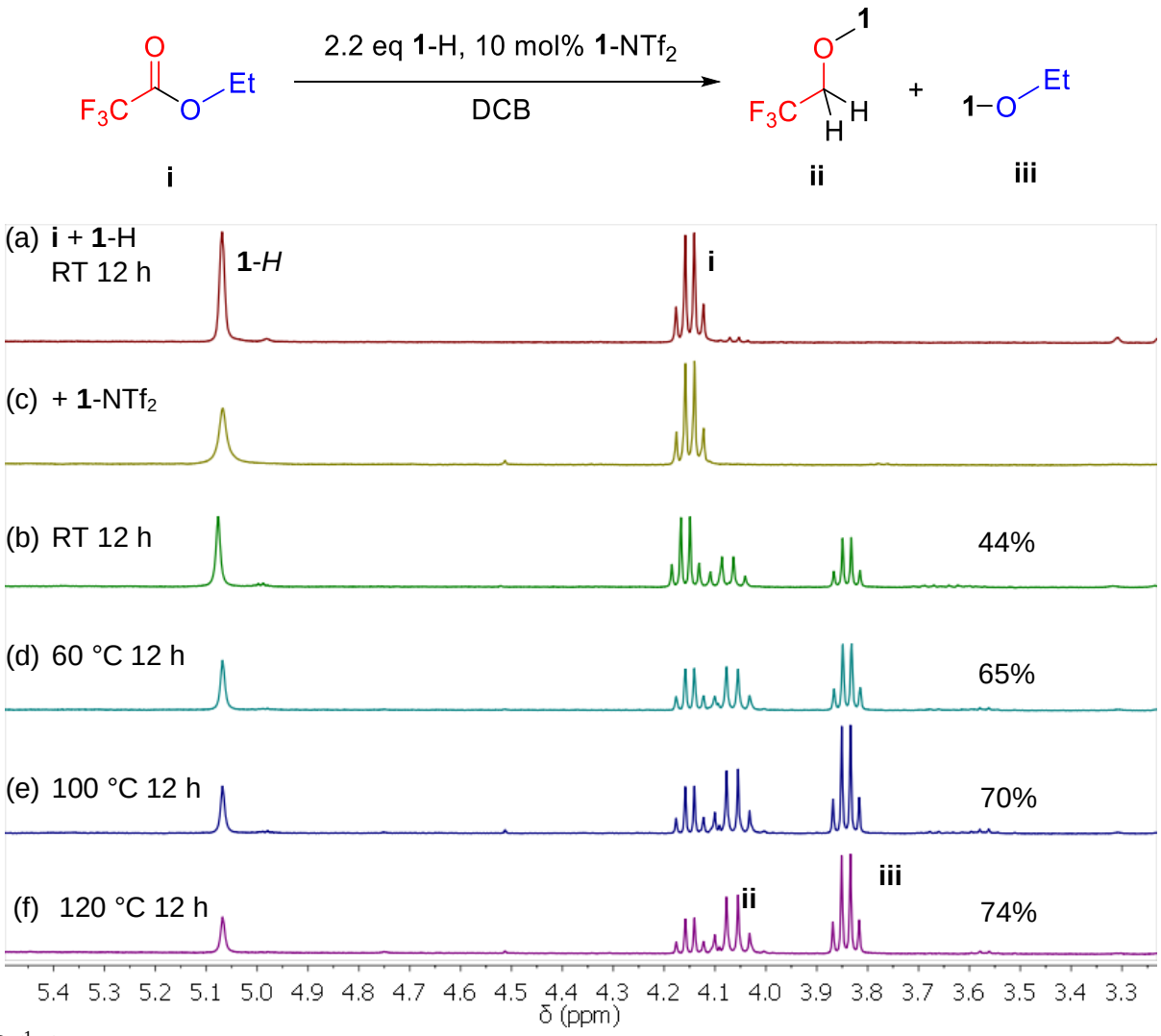

Figure S23 ^{1}H NMR spectra supporting the hydrostannation of CF_3COOEt with **1**-NTf_2.

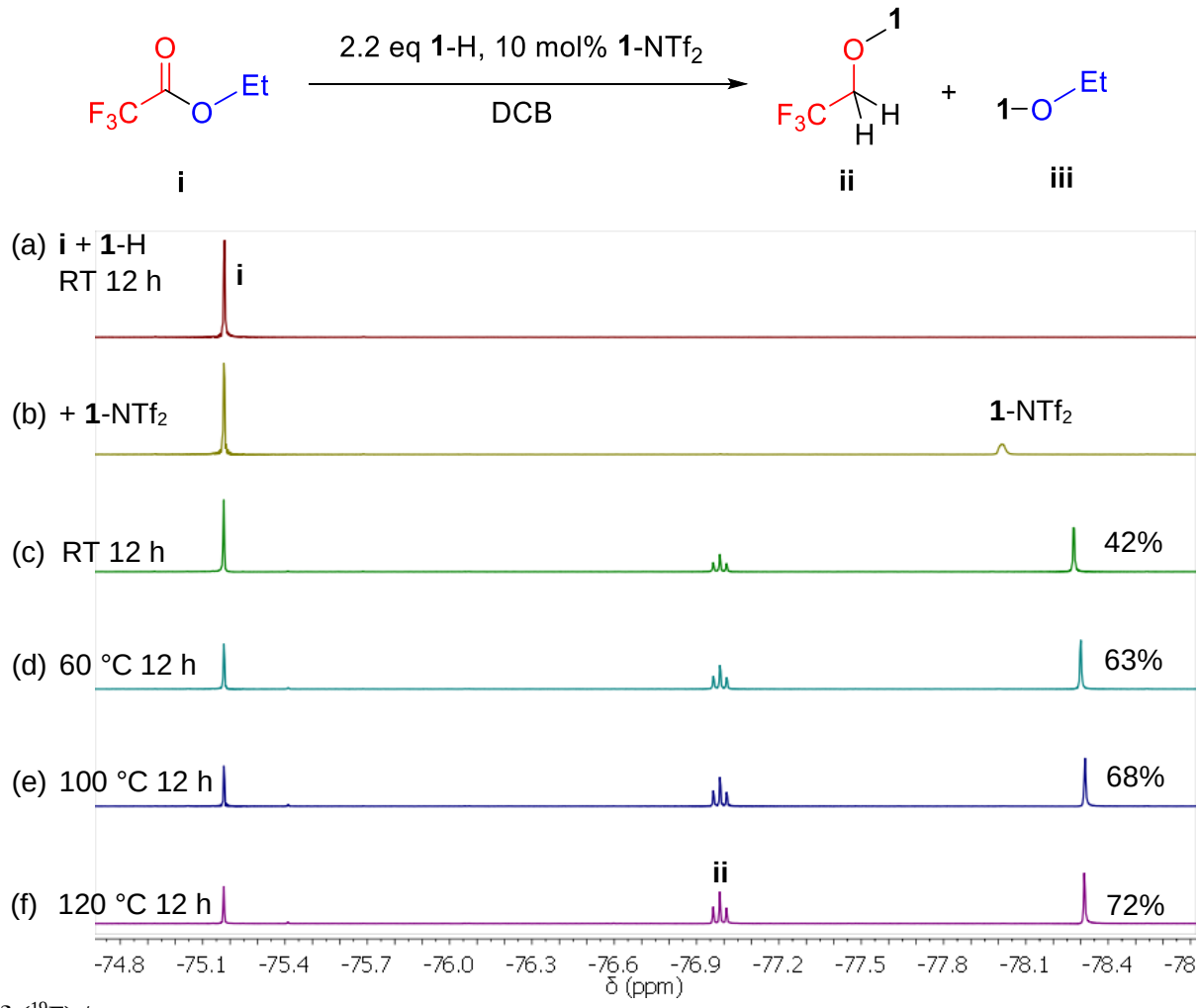

Figure S24 ^{19}F NMR spectra supporting the hydrostannation of CF_3COOEt with **1**-NTf_2.

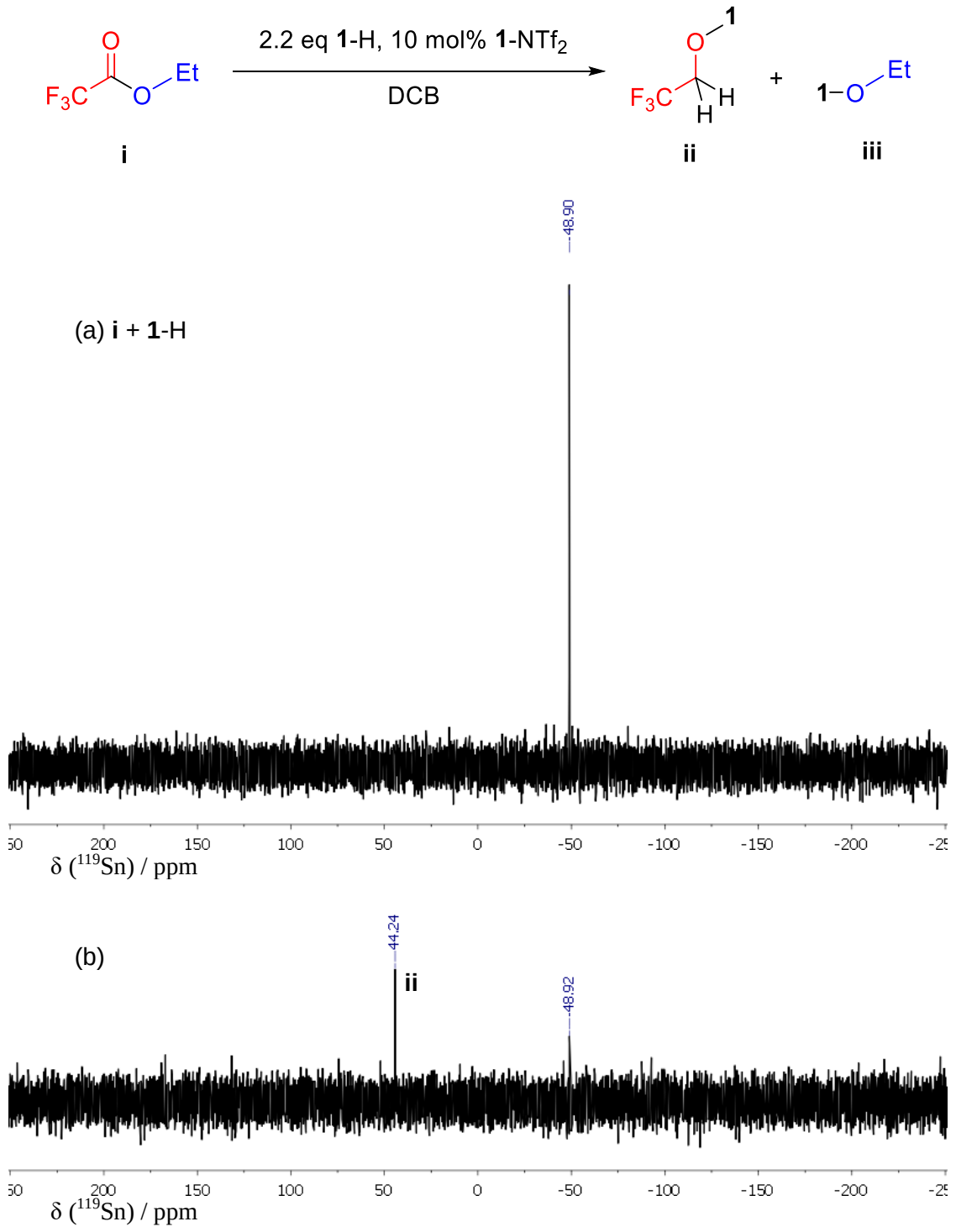

Figure S25 $^{119}Sn\{^{1}H\}$ NMR spectra supporting the hydrostannation of CF_3COOEt with **1**-NTf_2. Spectrum (b) shows the end of the reaction after heating at the temperatures and times given in the previous figure. Specie **ii** was assigned based on the outcome of the analogous hydrogenation reaction.

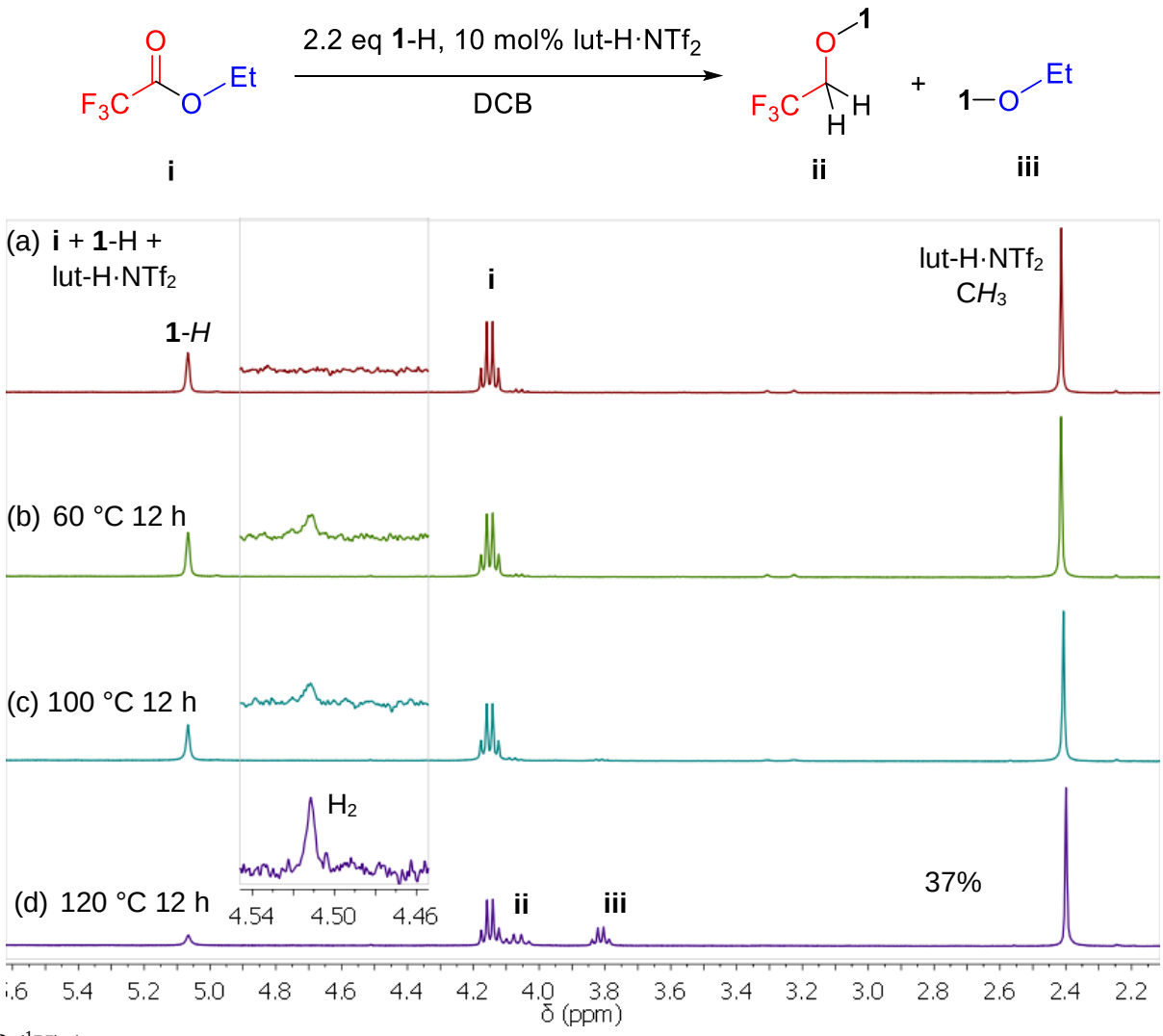

Figure S26 ^{1}H NMR spectra supporting the hydrostannation of CF_3COOEt with lut-H·NTf_2. Inset provides an expanded view of the resonance attributed to H_2, which forms by reaction of **1**-H and lut-H^+ NTf_2^- to form **1**-NTf_2 and H_2.

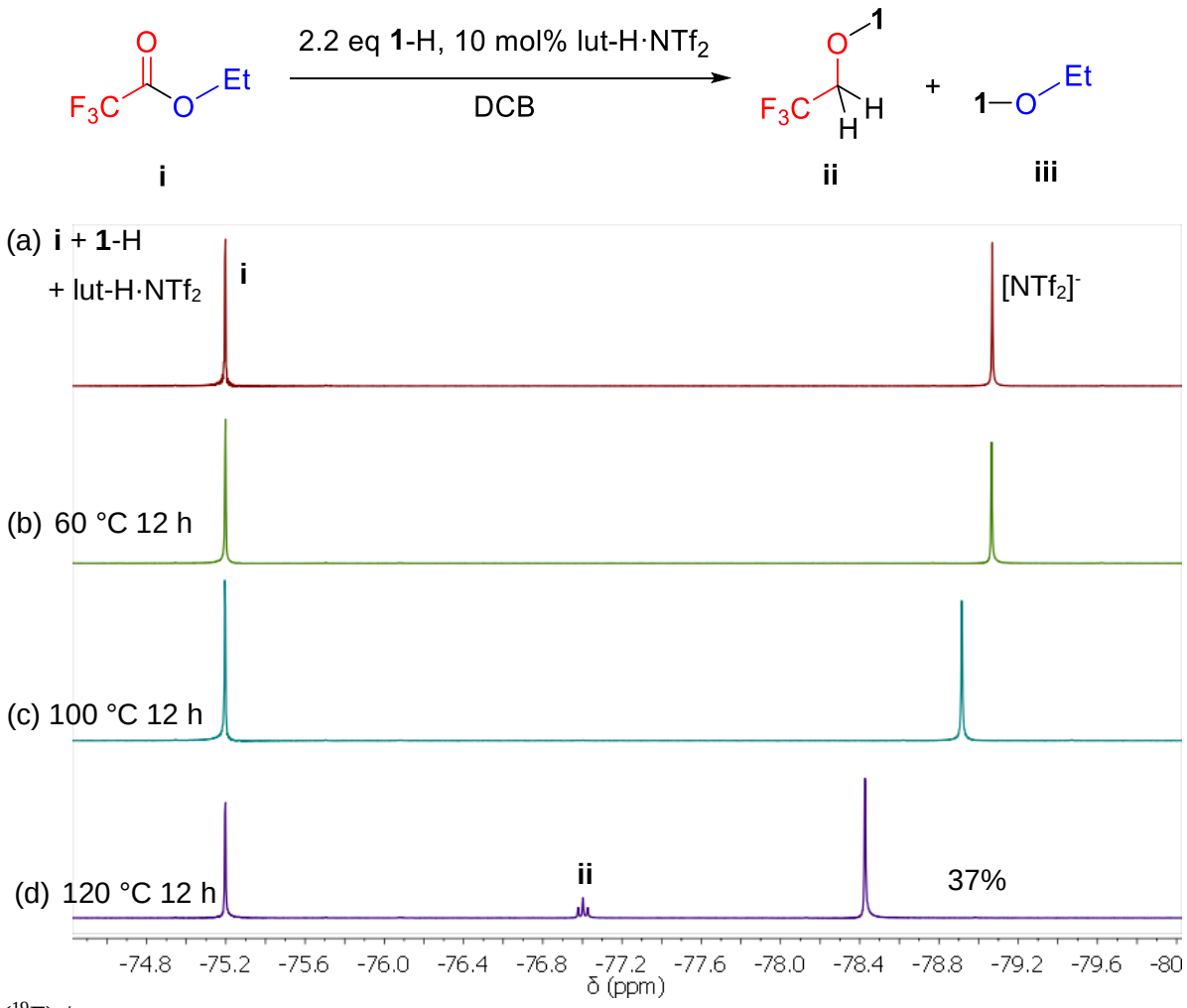

Figure S27 ^{19}F NMR spectra supporting the hydrostannation of CF_3COOEt with lut-H·NTf_2.

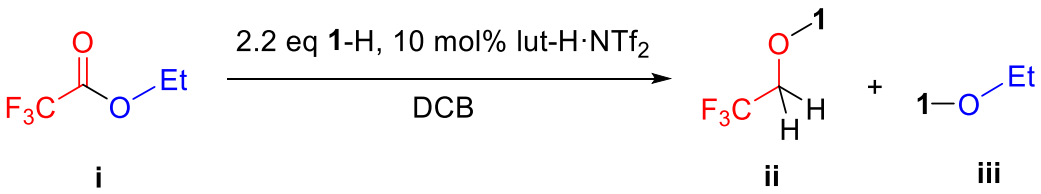

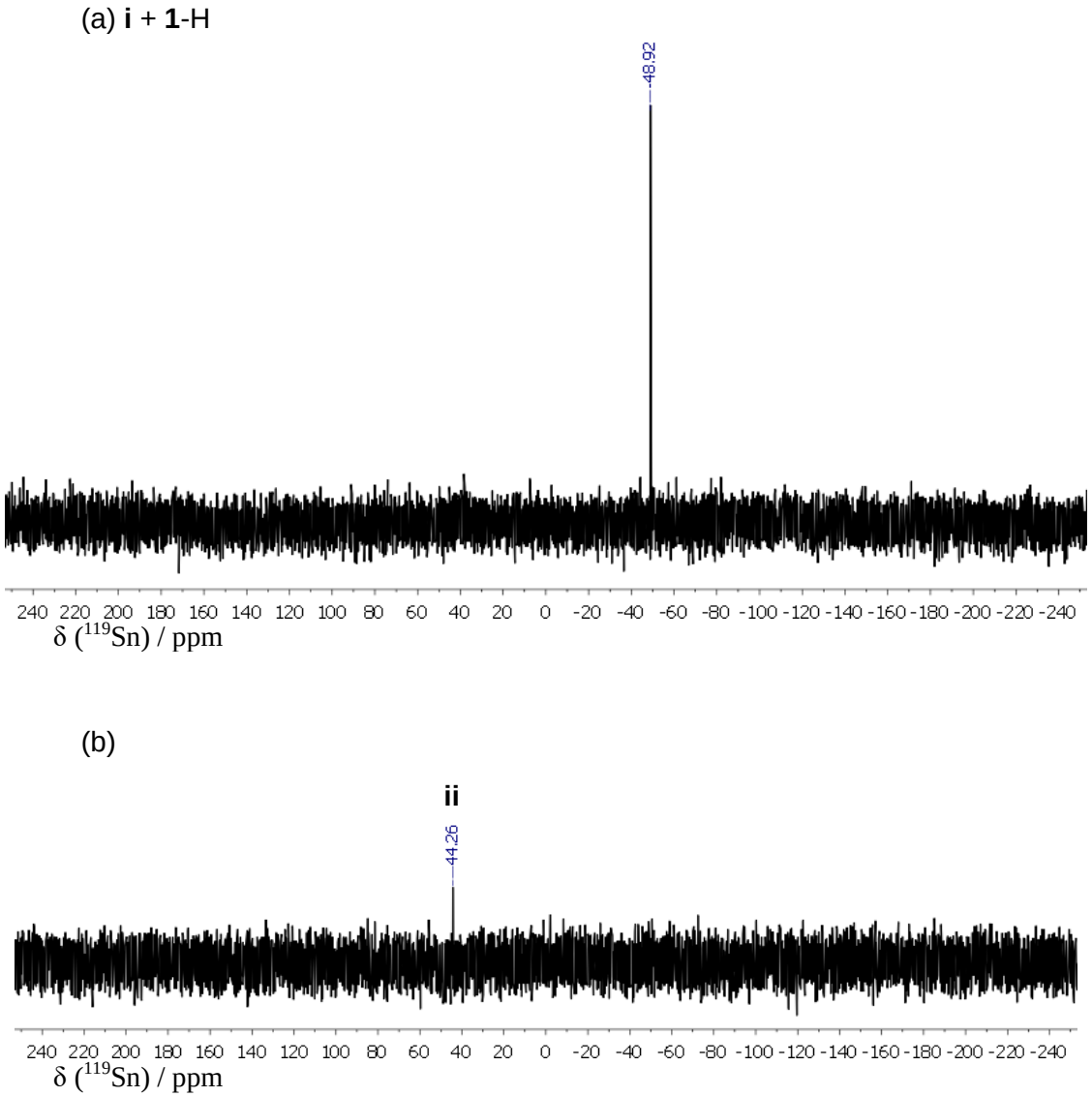

Figure S28 $^{119}Sn\{^{1}H\}$ NMR spectra supporting the hydrostannation of CF_3COOEt with lut-H·NTf_2. Spectrum (b) shows the end of the reaction after heating at the temperatures and times given in the previous figure. Specie **ii** was assigned based on the outcome of the analogous hydrogenation reaction.

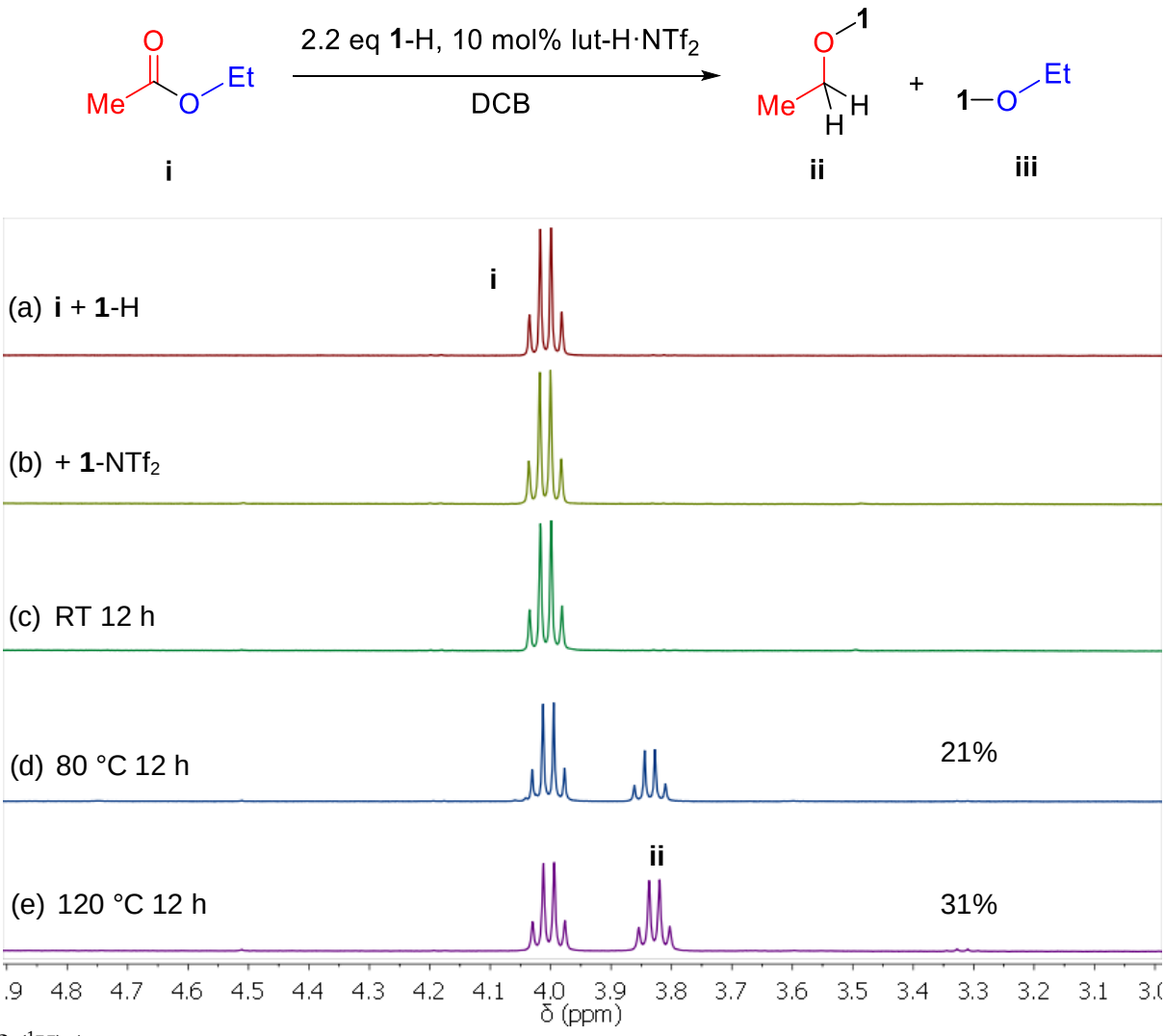

Figure S29 ^{1}H NMR spectra supporting the hydrostannation of MeCOOEt with lut-H·NTf$_2$.

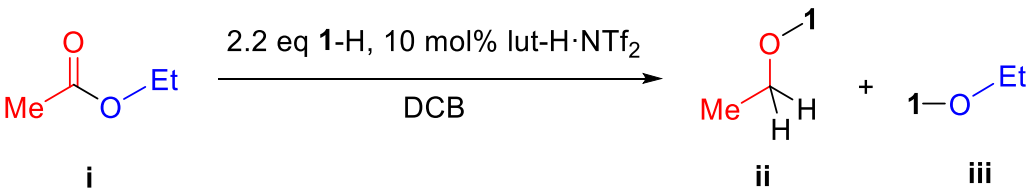

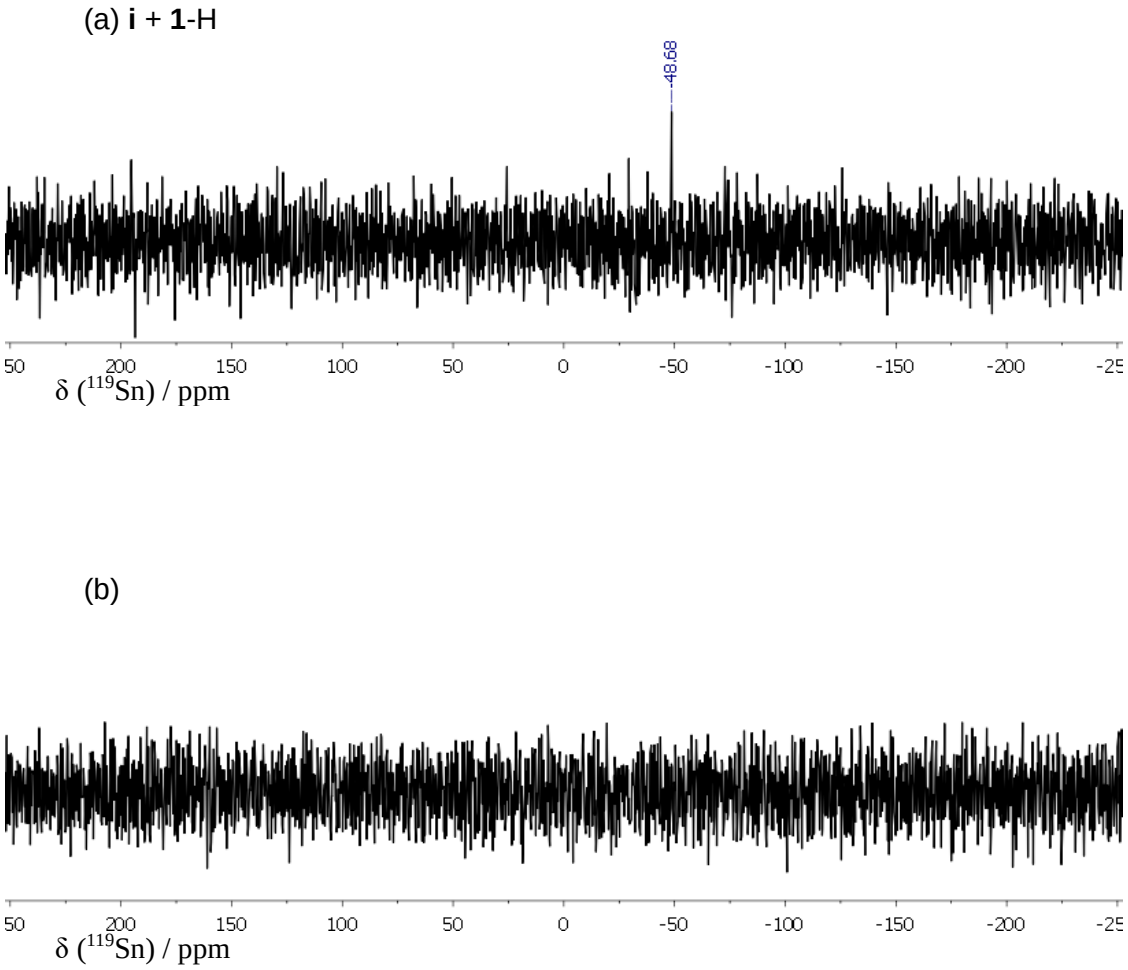

Figure S30 $^{119}Sn\{^{1}H\}$ NMR spectra supporting the hydrostannation of MeCOOEt with lut-H·NTf_2. Spectrum (b) shows the end of the reaction after heating at the temperatures and times given in the previous figure.

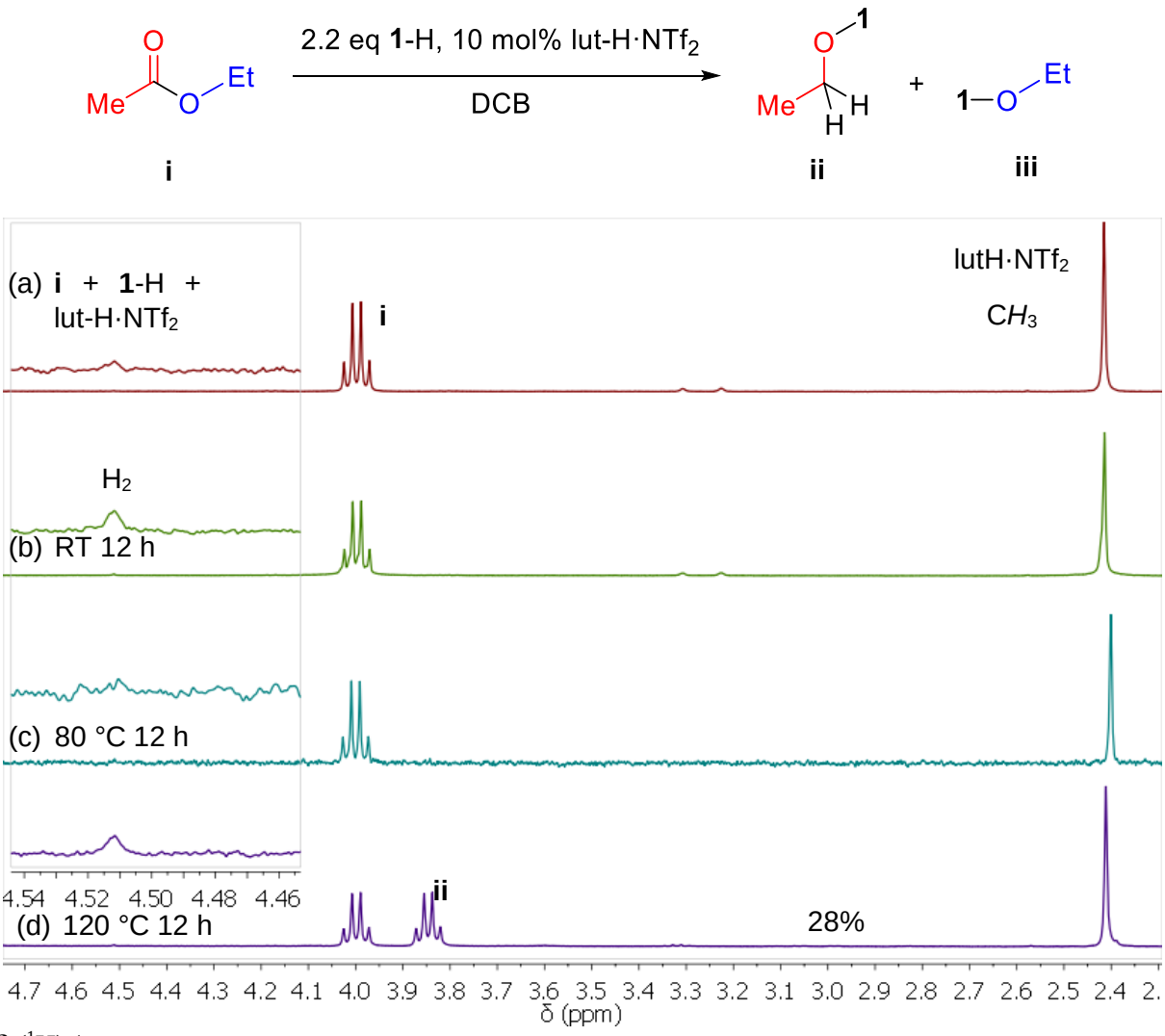

Figure S31 ^{1}H NMR spectra supporting the hydrostannation of MeCOOEt with lut-H·NTf$_2$. Inset provides an expanded view of the resonance attributed to H_2, which forms by reaction of **1**-H and lut-H$^+$ NTf$_2^-$ to form **1**-NTf$_2$ and H_2.

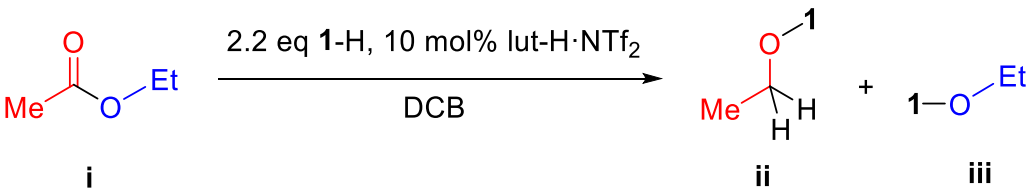

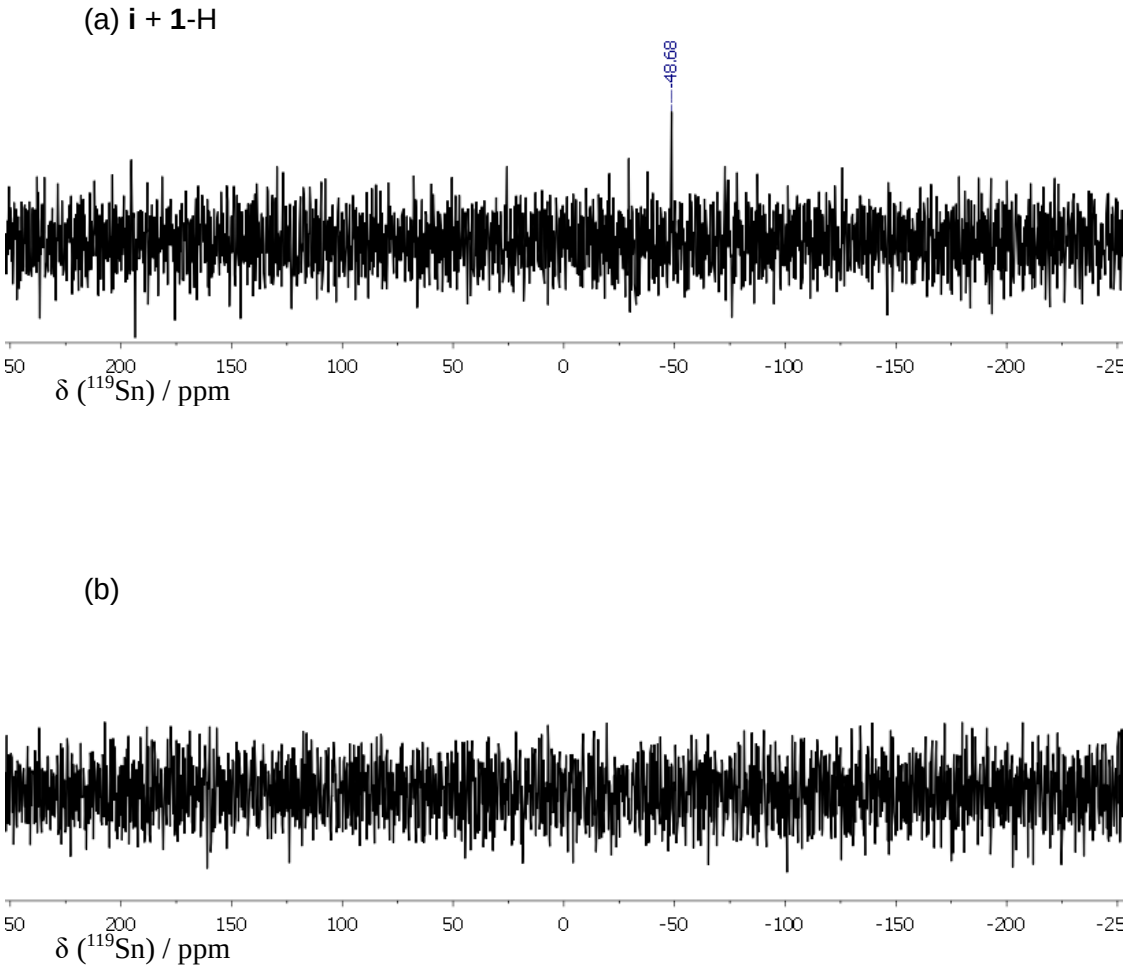

Figure S32 $^{119}Sn\{^{1}H\}$ NMR spectra supporting the hydrostannation of MeCOOEt with lut-H·NTf_2. Spectrum (b) shows the end of the reaction after heating at the temperatures and times given in the previous figure.

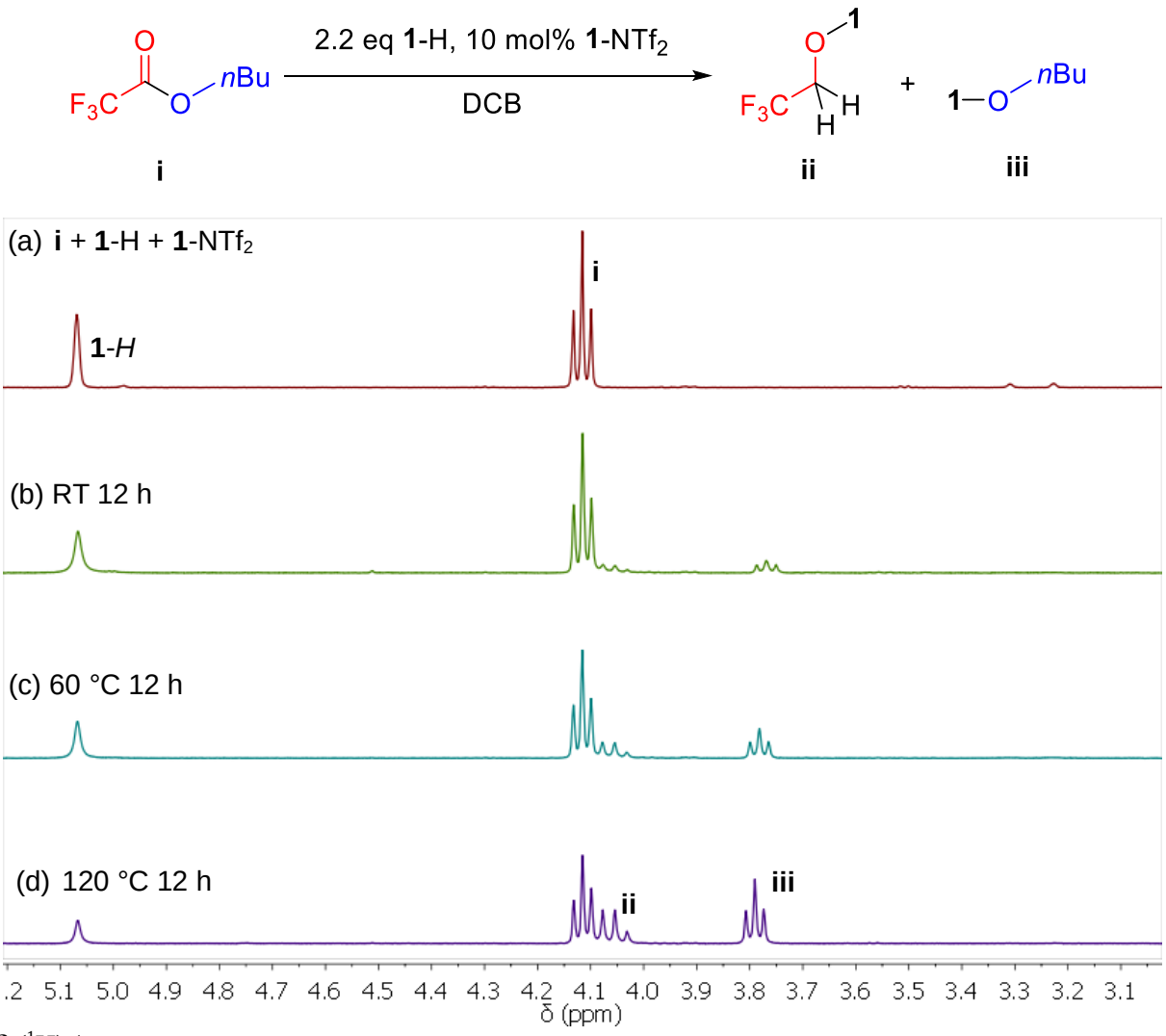

Figure S33 ^{1}H NMR spectra supporting the hydrostannation of $CF_3COOnBu$ with **1**-NTf_2. % conversions are not given due to overlap between the **i** and **ii** peaks.

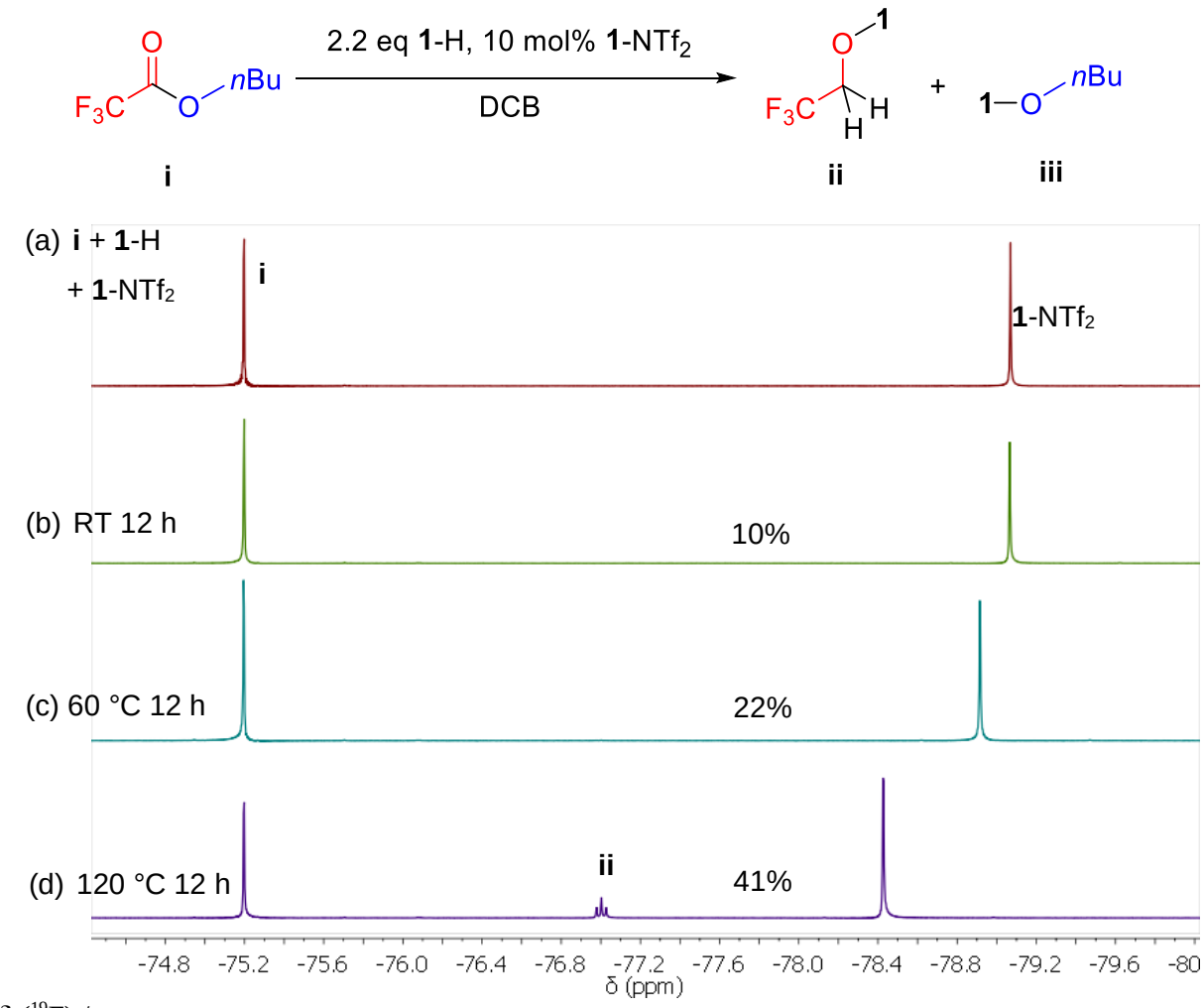

Figure S34 ^{19}F NMR spectra supporting the hydrostannation of $CF_3COOnBu$ with **1**-NTf_2.

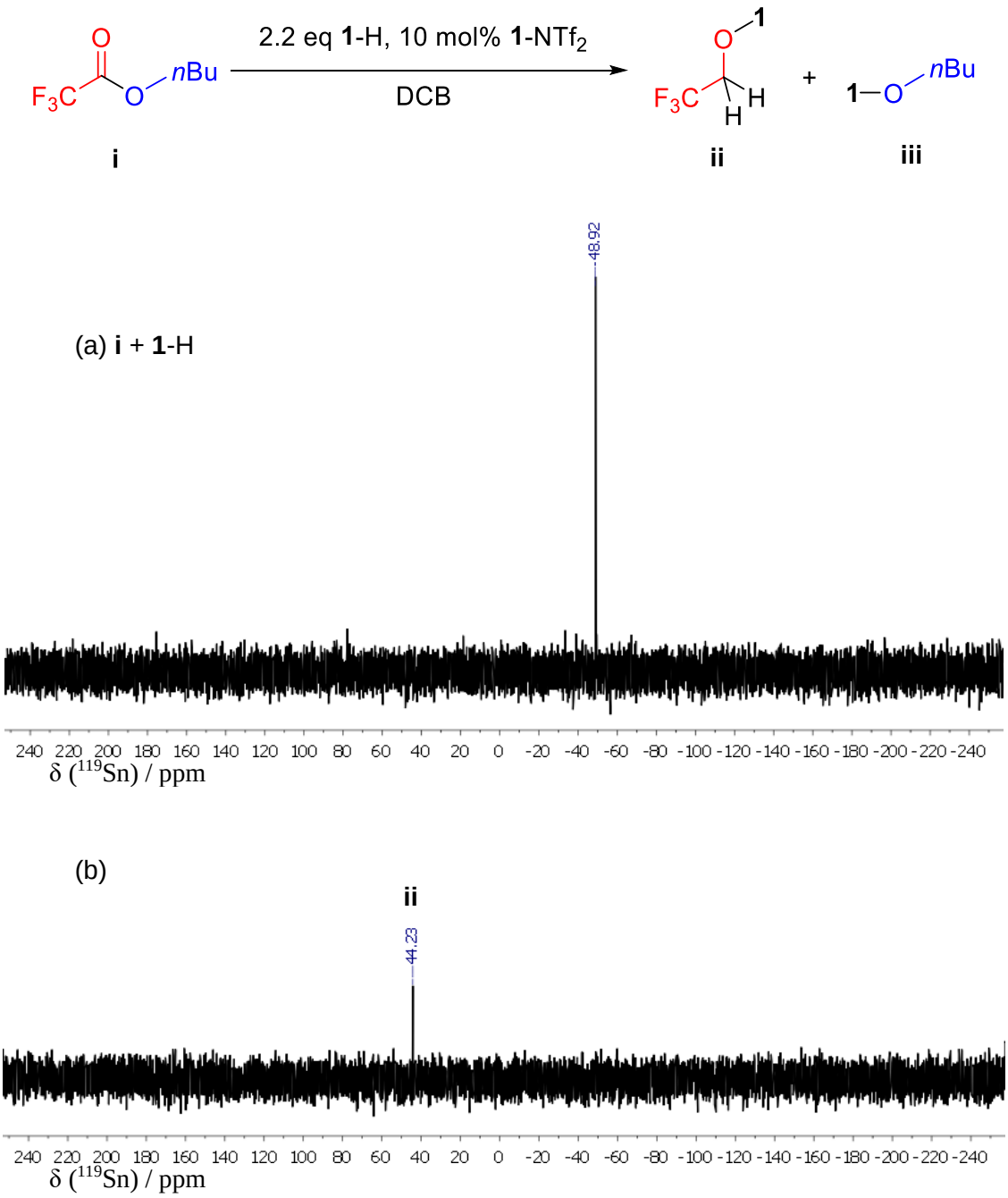

Figure S35 $^{119}Sn\{^{1}H\}$ NMR spectra supporting the hydrostannation of $CF_3COOnBu$ with **1**-NTf_2. Spectrum (b) shows the end of the reaction after heating at the temperatures and times given in the previous figure. Specie **ii** was assigned based on the outcome of the analogous hydrogenation reaction.

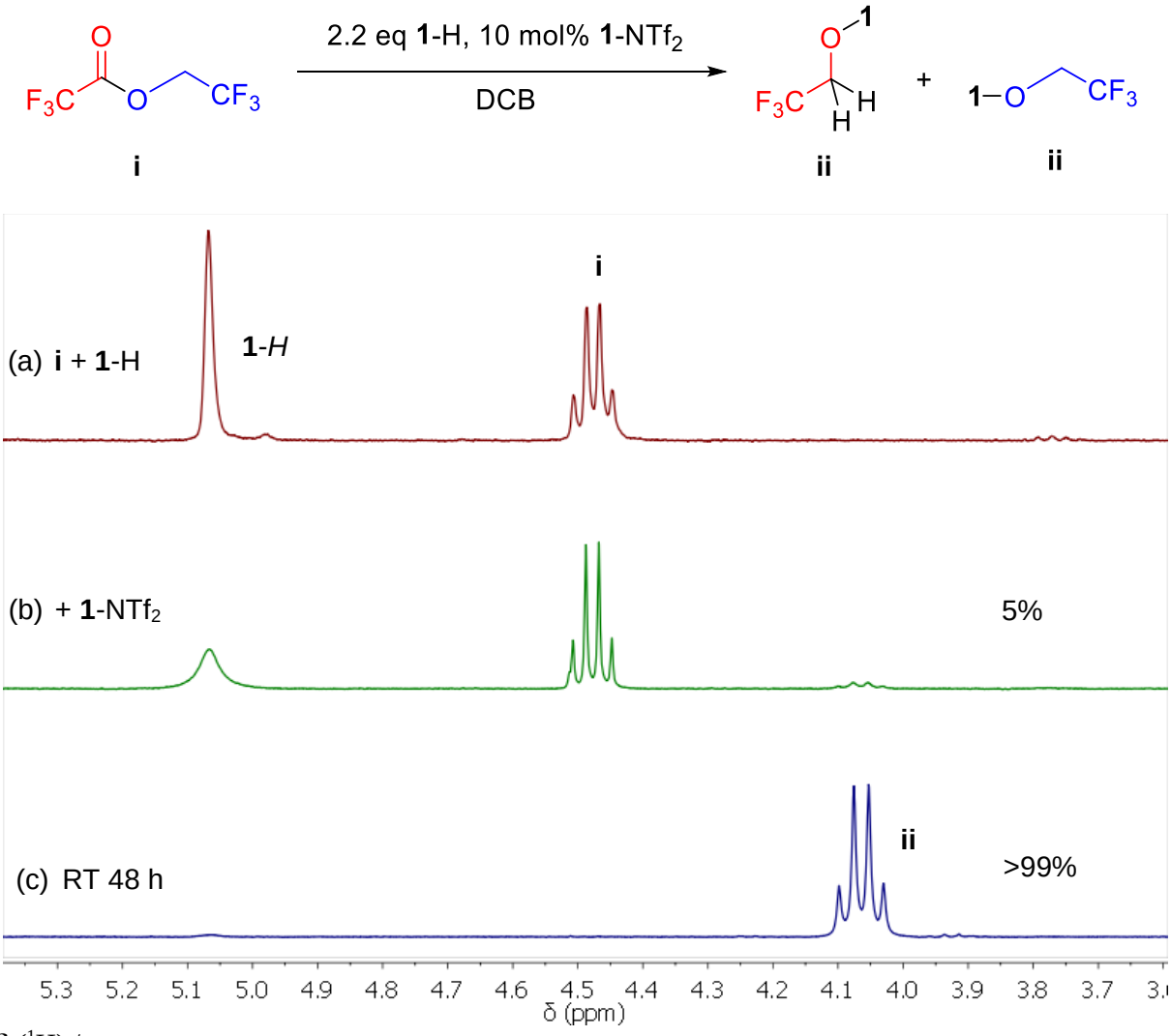

Figure S36 ^{1}H NMR spectra supporting the hydrostannation of $CF_3COOCH_2CF_3$ with **1**-NTf_2.

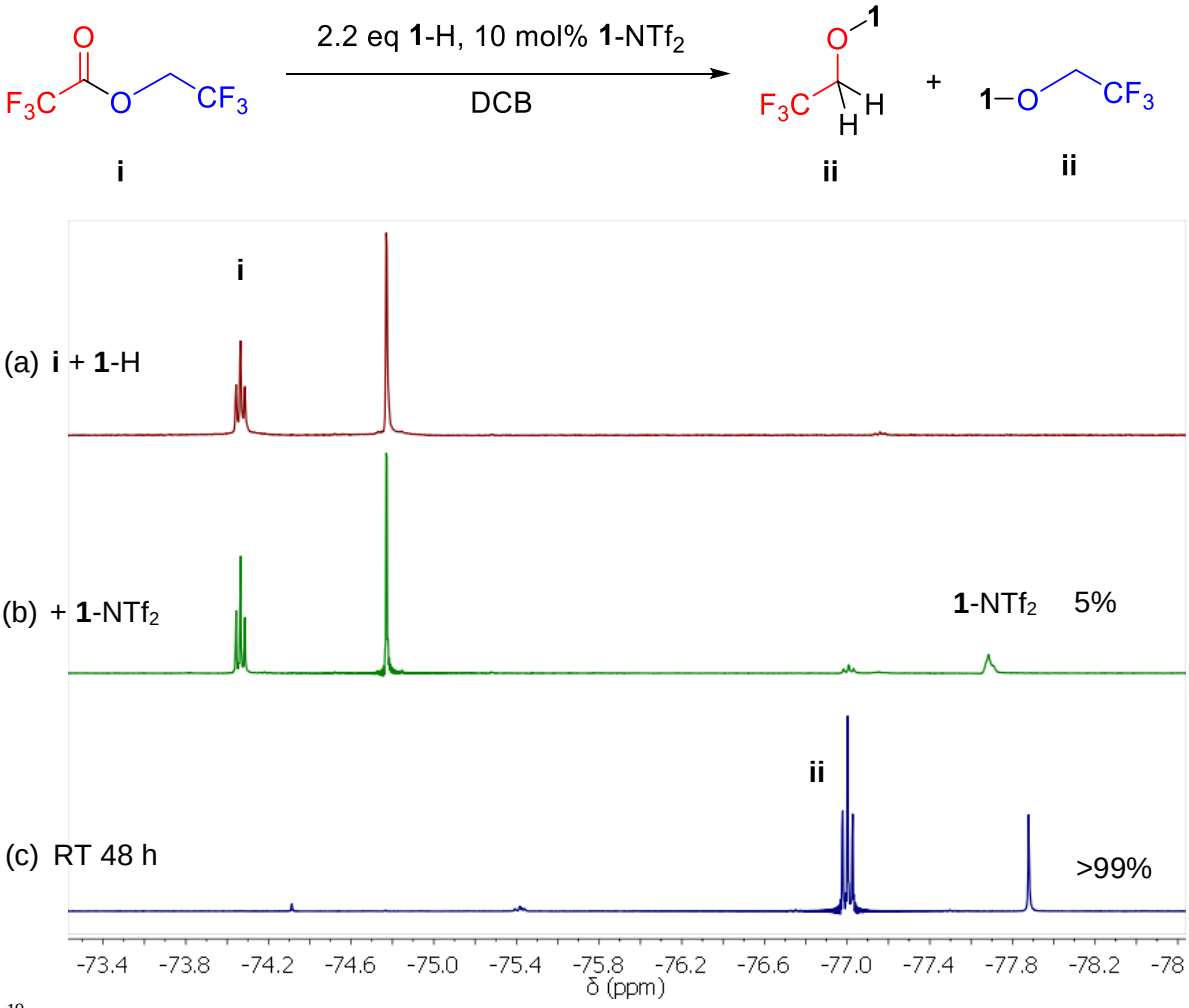

Figure S37 ^{19}F NMR spectra supporting the hydrostannation of $CF_3COOCH_2CF_3$ with **1**-NTf_2.

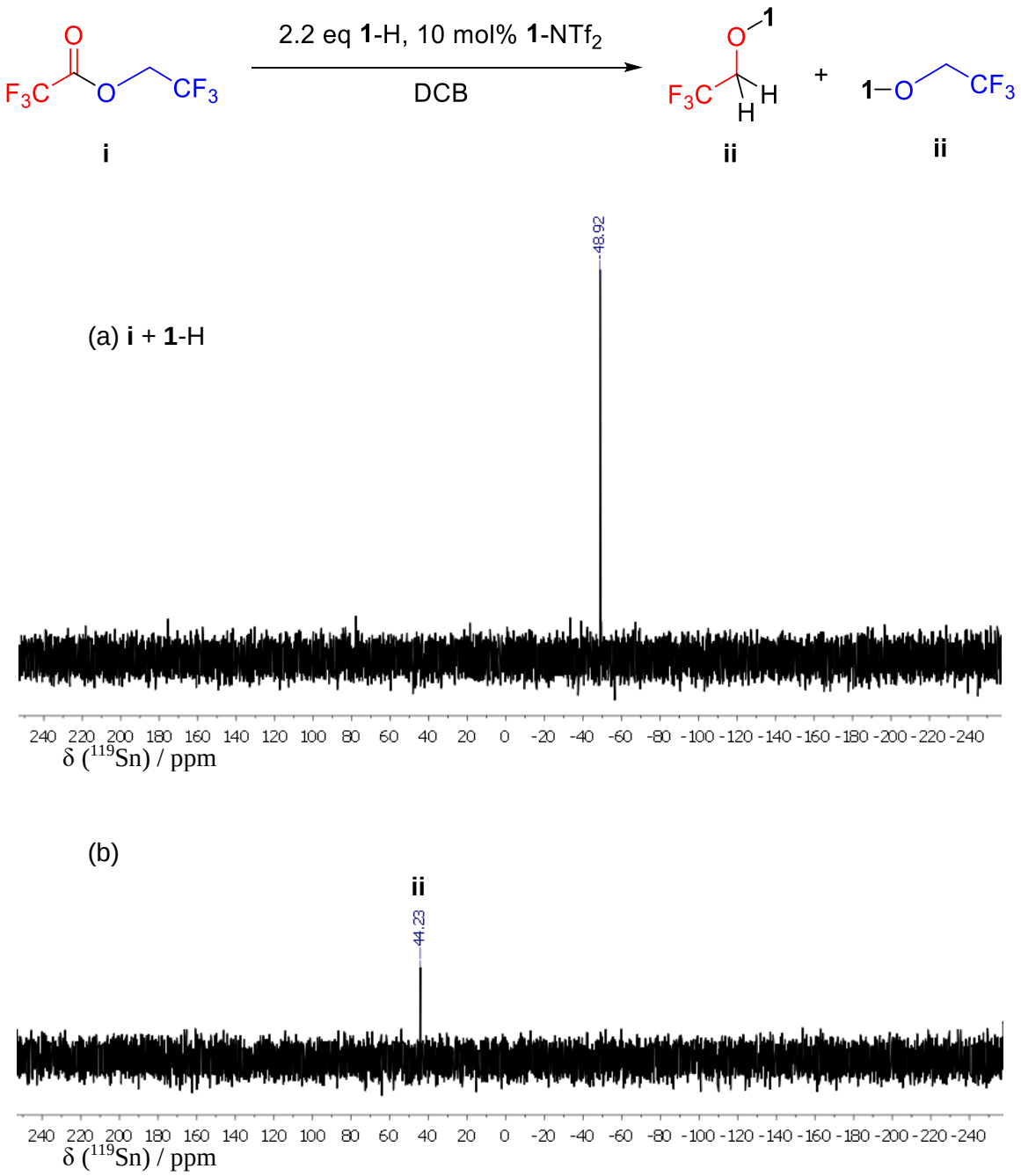

Figure S38 $^{119}Sn\{^{1}H\}$ NMR spectra supporting the hydrostannation of $CF_3COOCH_2CF_3$ with **1**-NTf_2. Spectrum (b) shows the end of the reaction after heating at the temperatures and times given in the previous figure. Specie **ii** was assigned based on the outcome of the hydrogenation reactions of CF_3COOEt and CF_3COO*n*Bu.

9. Additions of donors to 1-NTf_2

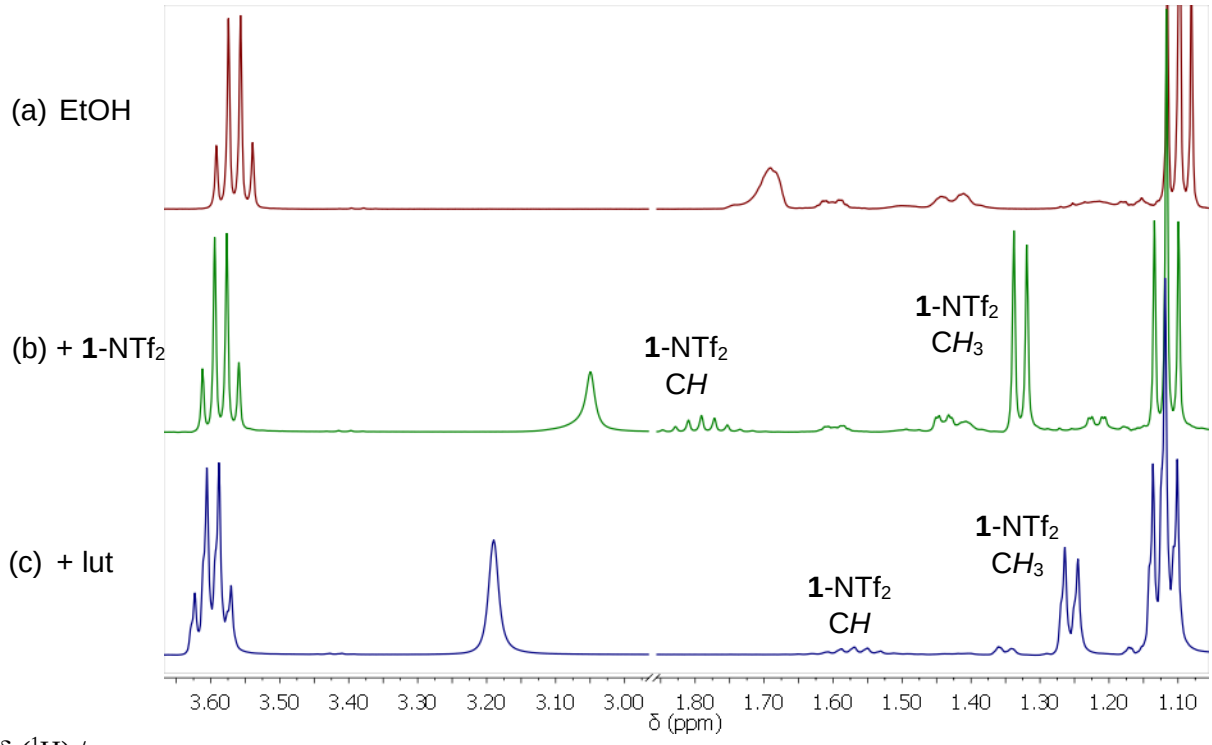

Figure S39 ^{1}H NMR spectra of the stepwise combination of EtOH, **1**-NTf_2 and lut (2:1:1) in DCB.

(a) EtOH + **1**-NTf_2

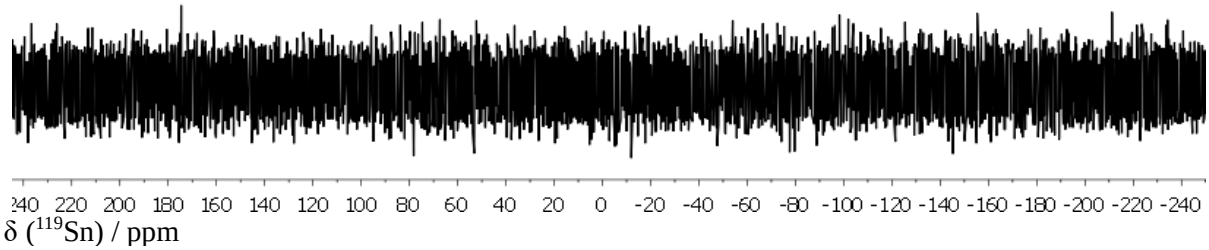

(b) + lut

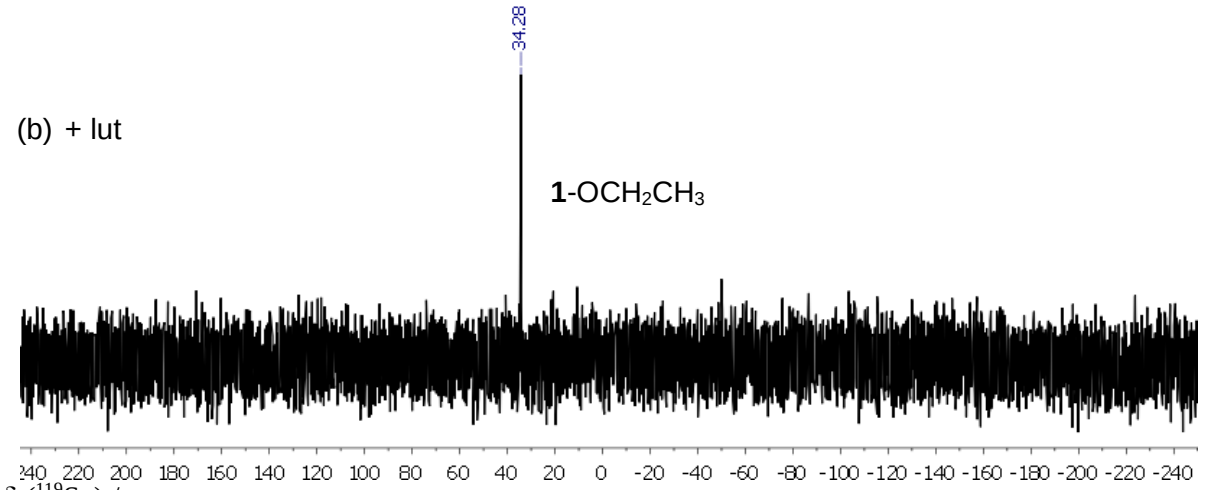

Figure S40 $^{119}Sn\{^1H\}$ NMR spectra of the stepwise combination of EtOH, **1**-NTf_2 and lut (2:1:1) in DCB.

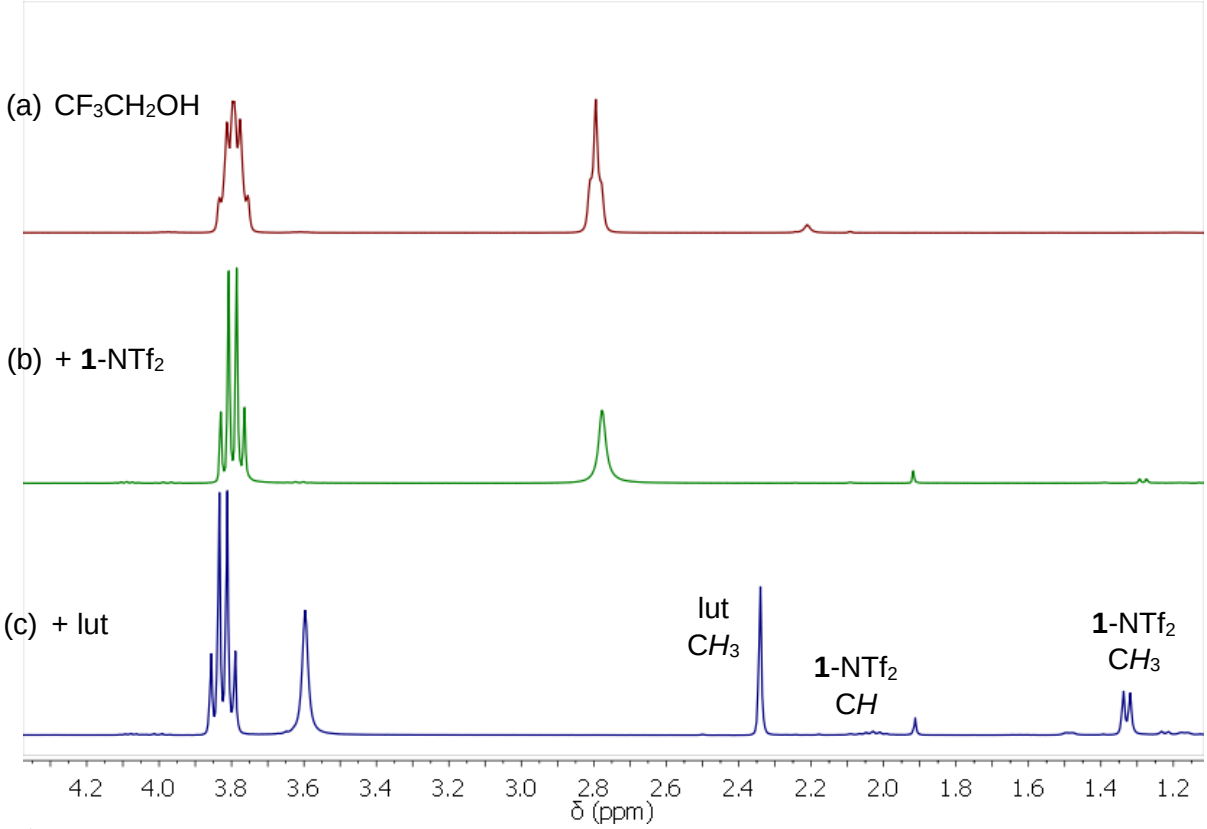

Figure S41 ^{1}H NMR spectra of the stepwise combination of CF_3CH_2OH, **1**-NTf_2 and lut (2:1:1) in DCB.

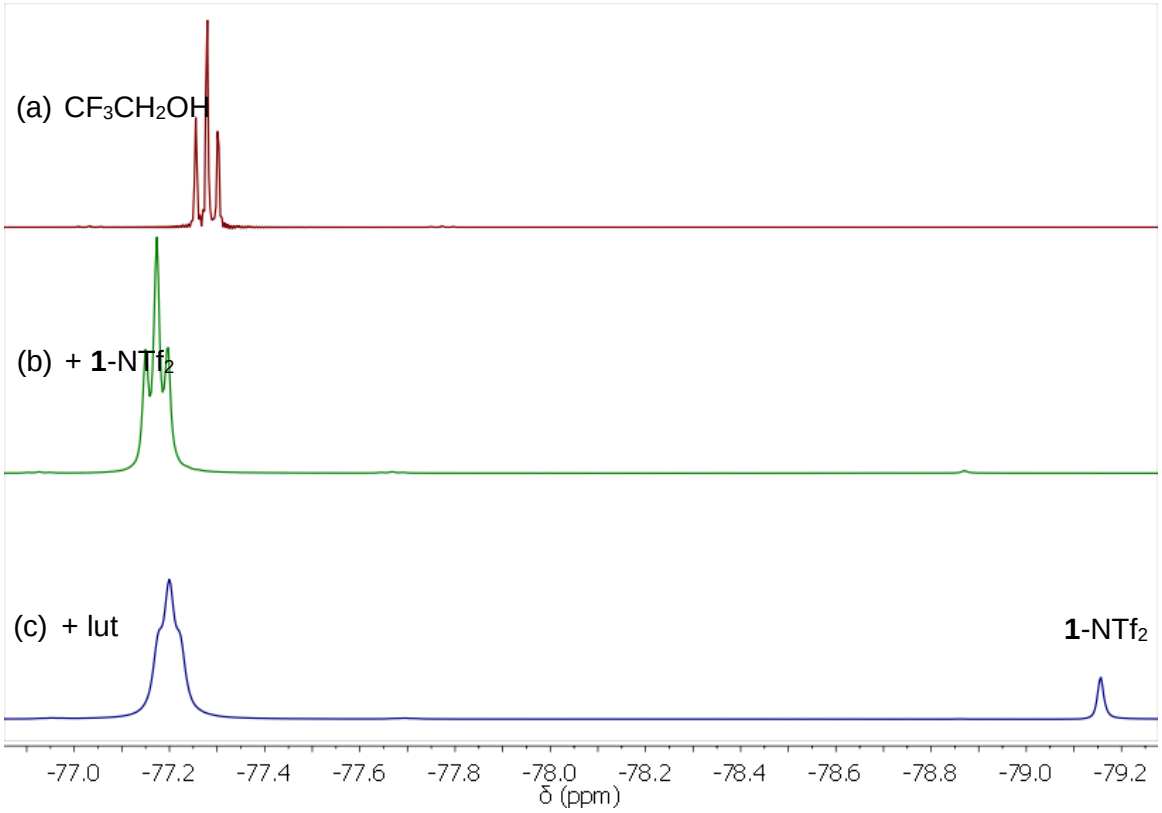

δ (^{1}H) / ppm

Figure S42 ^{19}F NMR spectra of the stepwise combination of CF_3CH_2OH, **1**-NTf_2 and lut (2:1:1) in DCB.

(a) CF_3CH_2OH + **1**-NTf_2

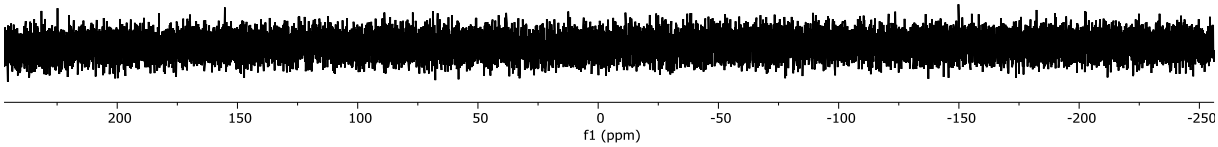

(b) + lut

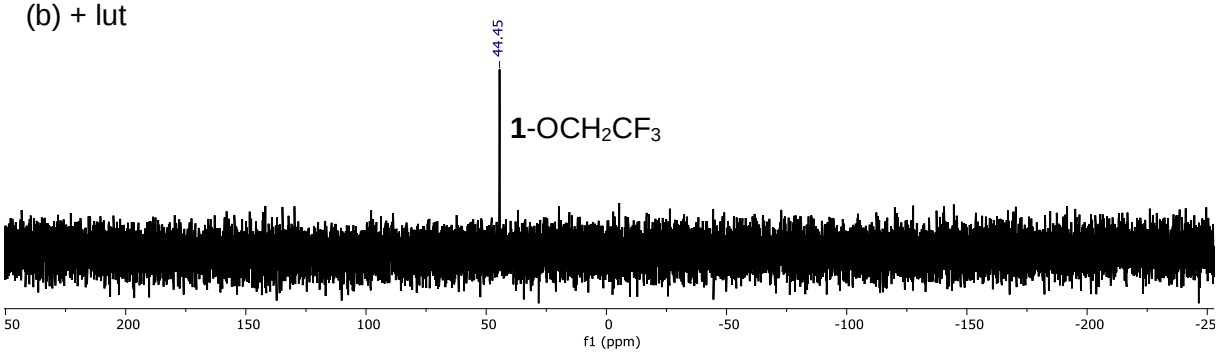

δ (^{119}Sn) / ppm

Figure S43 ^{119}Sn{^{1}H} NMR spectra of the stepwise combination of CF_3CH_2OH, **1**-NTf_2 and lut (2:1:1) in DCB.

10. H_2 activation by 1-NTf_2/lut in presence of EtOH or CF_3CH_2OH

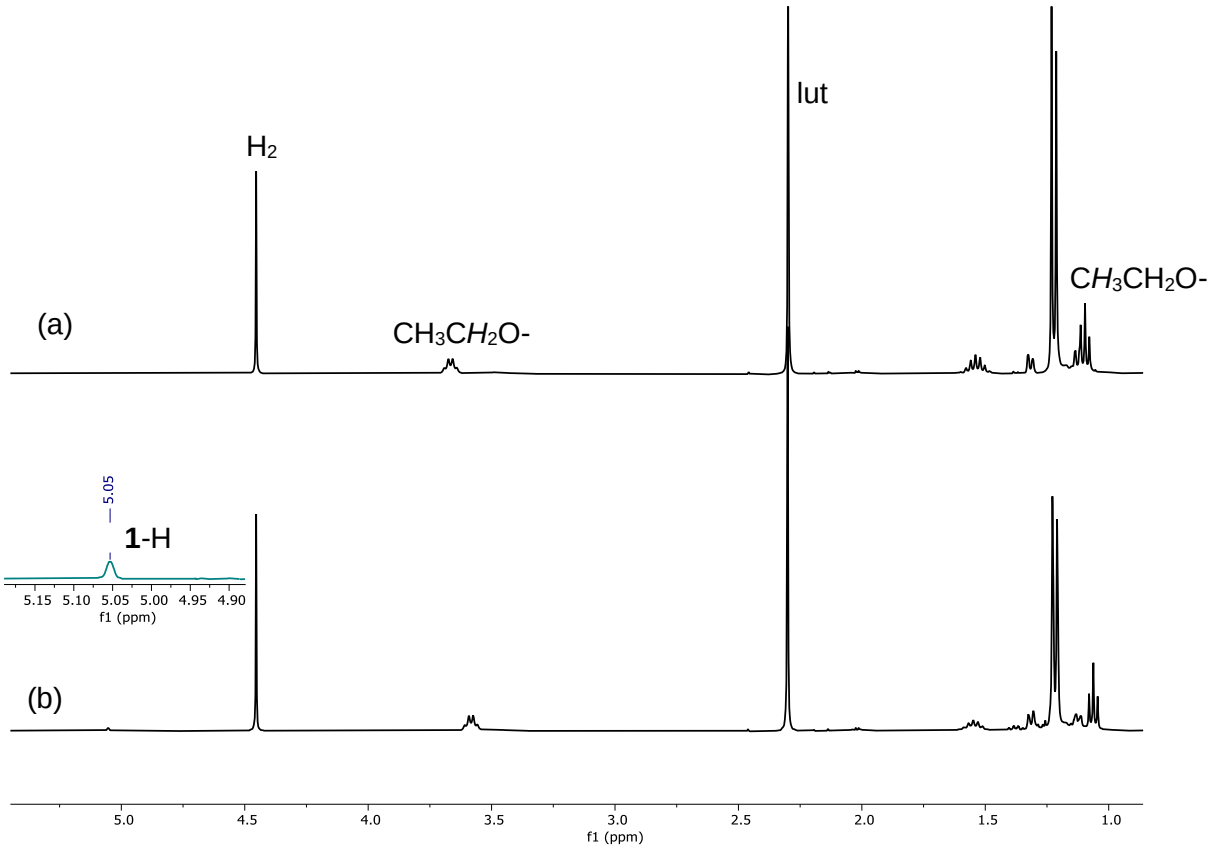

Figure S44 ^{1}H NMR spectra of EtOH, **1**-NTf_2 and lut (1:1:1) under H_2 (10 bar) in DCB solution. (a) after 7 days at room temperature; H_2 activation does not proceed, compared to successful H_2 activation within 1 day when EtOH is not present, under otherwise identical conditions; (b) after heating 2 h at 150°C, where inset shows formation of **1**-H.

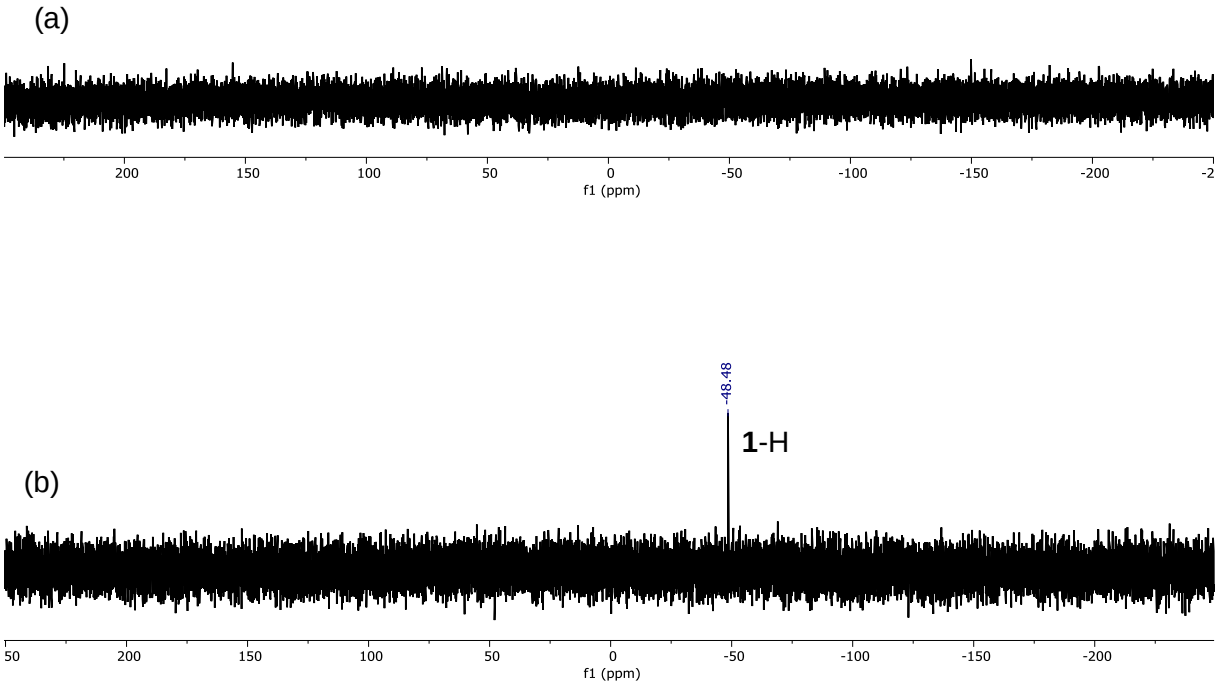

Figure S45 $^{119}Sn\{^{1}H\}$ NMR spectra of EtOH, **1**-NTf_2 and lut (1:1:1) under H_2 (10 bar) in DCB solution. (a) after 7 days at room temperature; H_2 activation does not proceed, compared to successful H_2 activation within 1 day when EtOH is not present, under otherwise identical conditions; (b) after heating 2 h at 150°C, showing formation of **1**-H.

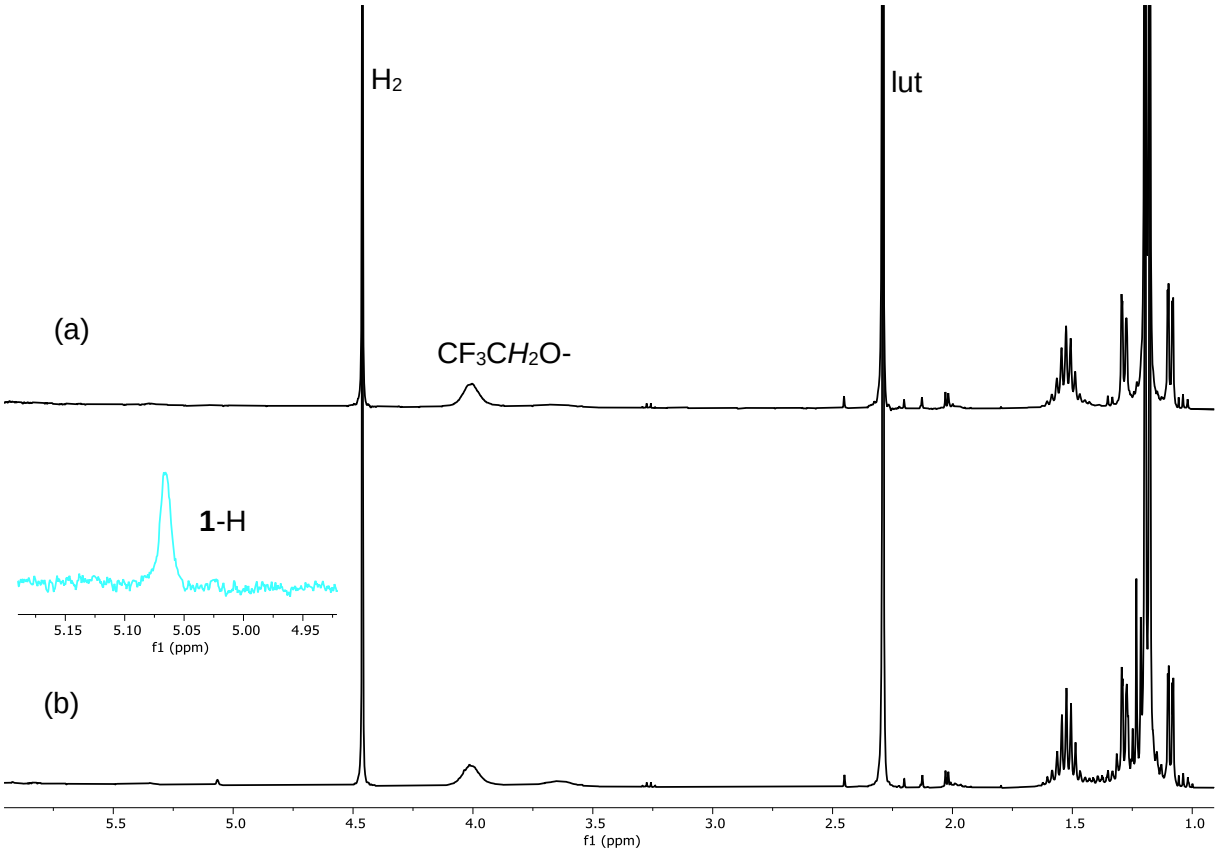

Figure S46 ^{1}H NMR spectra of CF_3CH_2OH, **1**-NTf_2 and lut (1:1:1) under H_2 (10 bar) in DCB solution. (a) after 7 days at room temperature; H_2 activation does not proceed, compared to successful H_2 activation within 1 day when CF_3CH_2OH is not present, under otherwise identical conditions; (b) after heating 2 h at 150°C, where inset shows formation of **1**-H.

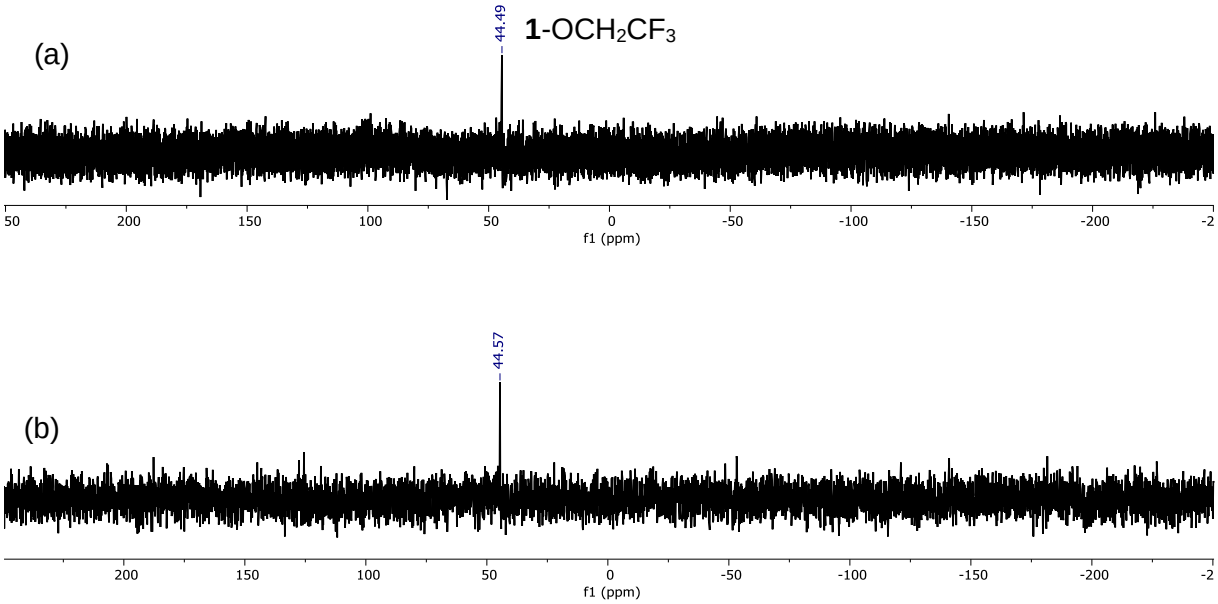

Figure S47 $^{119}Sn\{^{1}H\}$ NMR spectra of CF_3CH_2OH, **1**-NTf_2 and lut (1:1:1) under H_2 (10 bar) in DCB solution. (a) after 7 days at room temperature; H_2 activation does not proceed, compared to successful H_2 activation within 1 day when CF_3CH_2OH is not present, under otherwise identical conditions. (b) after heating 2 h at 150°C. **1**-H could not be observed using this method, possibly because its concentration was too low, or exchange broadened through interaction with **1**-NTf_2; its presence was corroborated however using ^{119}Sn-^{1}H HMBC correlation experiment.

11. X-ray diffraction data for 1-NTf_2

Crystals of **1**-NTf_2 suitable for single crystal X-ray diffraction studies were grown by layering a saturated solution of **1**-NTf_2 in $CHCl_3$ with pentane and cooling from room temperature to -40 ºC.

Table S4 Crystal data and structure refinement for ASH1608 (CCDC 2072866)

Identification code	ASH1608; CCDC 2072866
Empirical formula	$C_{11}H_{21}F_6NO_4S_2Sn$
Formula weight	528.10
Temperature/K	172.95(10)
Crystal system	tetragonal
Space group	$I4_1/acd$
a/Å	16.7483(4)
b/Å	16.7483(4)
c/Å	28.9201(7)
α/°	90
β/°	90
γ/°	90
Volume/Å^3	8112.2(4)
Z	16
ρ_{calc}g/cm^3	1.730
μ/mm^{-1}	1.533
F(000)	4192.0
Crystal size/mm^3	0.5171 × 0.4833 × 0.2545
Radiation	MoKα (λ = 0.71073)
2Θ range for data collection/°	5.618 to 56.542
Index ranges	$-21 \le h \le 20$, $-21 \le k \le 21$, $-35 \le l \le 31$
Reflections collected	21697
Independent reflections	2359 [R_{int} = 0.0305, R_{sigma} = 0.0272]
Data/restraints/parameters	2359/0/132
Goodness-of-fit on F^2	1.036
Final R indexes [I>=2σ (I)]	R_1 = 0.0390, wR_2 = 0.0817
Final R indexes [all data]	R_1 = 0.0686, wR_2 = 0.0973
Largest diff. peak/hole / e Å^{-3}	0.41/-0.41

Crystal Data for $C_{11}H_{21}F_6NO_4S_2Sn$ (M =528.10 g/mol): tetragonal, space group $I4_1/acd$ (no. 142), a = 16.7483(4) Å, c = 28.9201(7) Å, V = 8112.2(4) Å^3, Z = 16, T = 172.95(10) K, μ(MoKα) = 1.533 mm^{-1}, *Dcalc* = 1.730 g/cm^3, 21697 reflections measured ($5.618° \le 2\Theta \le 56.542°$), 2359 unique ($R_{int}$ = 0.0305, R_{sigma} = 0.0272) which were used in all calculations. The final R_1 was 0.0390 (I > 2σ(I)) and wR_2 was 0.0973 (all data).

Refinement model description

Number of restraints - 0, number of constraints - unknown.

Details:

1. Fixed Uiso
 At 1.2 times of:
  All C(H) groups
 At 1.5 times of:
  All C(H,H,H) groups
2. Others
 Fixed Sof: C7(0.5) H5A(0.5) H5B(0.5) H5C(0.5) C6(0.5) H6A(0.5) H6B(0.5)
 H6C(0.5) C5(0.5) H7(0.5)
3.a Ternary CH refined with riding coordinates:
 C2(H2), C5(H7)
3.b Idealised Me refined as rotating group:
 C3(H3A,H3B,H3C), C4(H4A,H4B,H4C), C7(H5A,H5B,H5C), C6(H6A,H6B,H6C)

Table S5 Bond Lengths for ASH1608.

Atom	Atom	Length/Å	Atom	Atom	Length/Å
Sn(1)	O(1)[1]	2.346(3)	F(2)	C(1)	1.301(6)
Sn(1)	O(1)	2.346(3)	N(3)	S(1)[2]	1.564(2)
Sn(1)	C(2)	2.137(5)	F(4)	C(1)	1.301(6)
Sn(1)	C(2)[1]	2.137(5)	F(1)	C(1)	1.325(6)
Sn(1)	C(7)	2.115(15)	C(2)	C(3)	1.516(9)
S(1)	O(0AA)	1.401(4)	C(2)	C(4)	1.506(10)
S(1)	N(3)	1.564(2)	C(5)	C(7)	1.74(4)
S(1)	C(1)	1.835(6)	C(6)	C(7)	1.38(2)
S(1)	O(1)	1.431(4)			

Table S6 Bond Angles for ASH1608.

Atom	Atom	Atom	Angle/°	Atom	Atom	Atom	Angle/°
O(1)	Sn(1)	O(1)[1]	178.6(2)	O(1)	S(1)	C(1)	100.6(2)
C(2)[1]	Sn(1)	O(1)	88.39(17)	S(1)	N(3)	S(1)[2]	124.1(3)
C(2)[1]	Sn(1)	O(1)[1]	90.99(16)	F(2)	C(1)	S(1)	110.8(4)
C(2)	Sn(1)	O(1)[1]	88.39(17)	F(2)	C(1)	F(1)	108.8(5)
C(2)	Sn(1)	O(1)	90.99(16)	F(4)	C(1)	S(1)	111.3(4)
C(2)[1]	Sn(1)	C(2)	127.2(4)	F(4)	C(1)	F(2)	108.8(5)
C(7)	Sn(1)	O(1)	78.5(6)	F(4)	C(1)	F(1)	109.0(5)
C(7)	Sn(1)	O(1)[1]	102.9(6)	F(1)	C(1)	S(1)	108.2(4)
C(7)	Sn(1)	C(2)	117.7(11)	S(1)	O(1)	Sn(1)	148.9(2)
C(7)	Sn(1)	C(2)[1]	113.9(10)	C(3)	C(2)	Sn(1)	110.1(4)
O(0AA)	S(1)	N(3)	117.2(3)	C(4)	C(2)	Sn(1)	111.8(5)
O(0AA)	S(1)	C(1)	107.0(3)	C(4)	C(2)	C(3)	114.6(7)
O(0AA)	S(1)	O(1)	118.1(3)	C(5)	C(7)	Sn(1)	106.4(15)
N(3)	S(1)	C(1)	104.97(18)	C(6)	C(7)	Sn(1)	116.4(13)
O(1)	S(1)	N(3)	107.0(2)	C(6)	C(7)	C(5)	105.7(17)

12. General computational methodology

To gain insight into the mechanism of the H_2 splitting as well as the reduction of ester substrates, we performed DFT calculations with the *Gaussian 16* suite of programs (Revision A.03).[14] The conformational analysis was carried out in the *MacroModel* software (Release 2017-1).[15] The molecular structures were rendered using *CYLview* (version 1.0) and non-essential hydrogen atoms were omitted for clarity. [16]

In our previous study, the computational methodology described below showed a good correlation with experimental results, hence we applied the same computational strategy in the present study.[17] The calculations were performed using dispersion-corrected ωB97X-D exchange-correlation functional.[18] The global solvation effects were taken into account by computing the solvation free energies employing SMD continuum solvation model (*o*-Dichlorobenzene; ε = 9.9949).[19] The ultrafine integration grid was employed in all electronic structure calculations to increase the accuracy of the numerical integration.[20] The DFT optimizations of the structures were carried without symmetry constraints, employing default convergence criteria for the SCF procedure.

To locate transition states, constrained geometry optimizations (energy scans) were performed starting from the reactant side and gradually reducing the distances between the corresponding atoms. We used the structures corresponding to the energy maxima on the potential energy curves as initial geometries in transition location procedures without constraint. All converged gas-phase geometries were checked by harmonic vibrational frequency calculations to characterize the nature of the obtained structures. The vibrational analysis revealed that no imaginary frequencies were found for the reported minima and all located transition states had only one imaginary frequency.

The reported Gibbs free energies were obtained by combining ωB97X-D/Def2TZVPP electronic energies with the thermal and solvation contributions computed at the ωB97X-D/Def2SVP level, according to the following formula:

$$G = E_0' + (G_0 - E_0) + (G_{sol} - E_0) + \Delta G_{conc}.$$

In this formula, E_0' and E_0 are electronic energies obtained using Def2TZVPP and Def2SVP basis sets,[21] respectively. G_0 is the gas-phase Gibbs free energy obtained from ωB97X-D/Def2SVP calculations (T = 298.15 K, or T = 423.15 K following the respective experimental conditions). The thermal and entropic contributions were estimated within the ideal gas−rigid rotor−harmonic oscillator (RRHO) approximation. The G_{sol} is the solution-phase Gibbs free energy, which was derived from a single point energy calculation at the ωB97X-D/Def2SVP level using the implicit SMD solvation model. The value of ΔG_{conc} (0.003019 Hartree at 298.15 K and 0.0047534 Hartree T = 423.15 K) corresponds to concentration correction to the Gibbs free energy when switching from ideal gas standard state (p = 1 atm) to the standard concentration in solution phase (c = 1 mol/dm^3).

For conformational analysis, we applied Monte Carlo sampling using the OPLS_2005 force field. The applied force field has no defined set of parameters for molecules which contain a tin atom. To deal with this, the tin atom was replaced with silicon (but keeping the Sn-C bond lengths) that has a defined parameter set in the applied force field. After generating possible structures at the molecular mechanics level, we changed the silicon atom back to tin and those structures were optimized at DFT level. Parameters of the conformational analysis are the followings: Solvent: none, Optimization method: PRCG, Maximum iteration of optimization: 15 000, Convergence threshold of optimization: 0.05 Maximum number of steps: 10 000 (300 steps per rotatable bond), CSearch method: Mixed torsional/Low-mode sampling, Energy window: 40 kJ/mol.

The most stable conformer was used as a reference state to estimate the reaction barriers of the reactions, similarly to the methodology presented in our previous study.[17]

12.1 Lewis acidity of 1-NTf_2 and 1-OTf

First, we calculated the hydride affinities of **1**-NTf_2 and **1**-OTf to compare the Lewis acidity of the two species. The hydride affinity was computed based on the **1**-X + H^- → **1**-H + X^- (X = $[NTf_2]^-$ and $[OTf]^-$) equation. The obtained free energy changes of this hypothetical processes are shown in Figure S47. The hydride affinity was found to be -43.9 kcal/mol and -34.8 kcal/mol for **1**-NTf_2 and **1**-OTf, respectively.

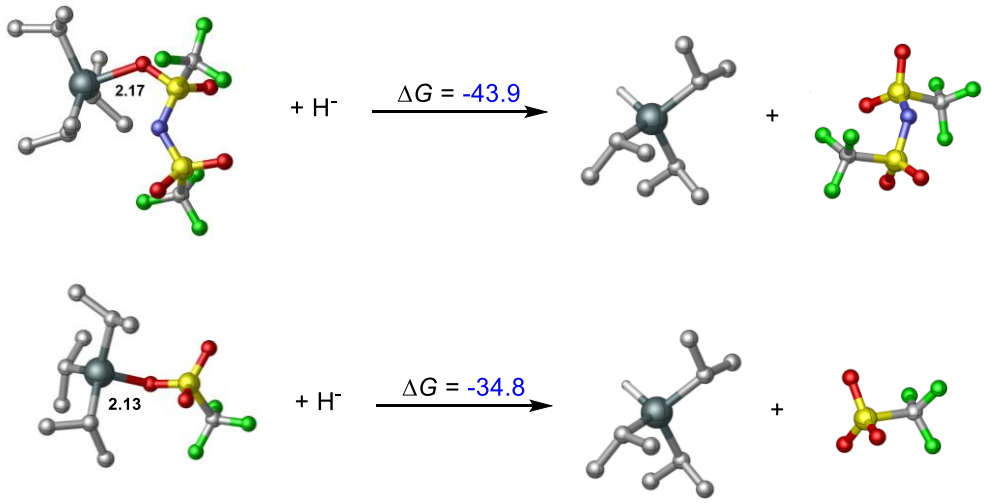

Figure S47 The measure of hydride affinity defined by the equations (given in kcal/mol).

As revealed by hydride affinities, **1**-NTf_2 possesses a more strongly hydridophilic character in comparison with **1**-OTf. We performed an energy decomposition analysis in pursuit of a deeper understanding of the difference in Lewis acidity. With this approach, we investigated the hypothetical dissociation of **1**-NTf_2 and **1**-OTf LAs to $[\mathbf{1}]^+$ + $[NTf_2]^-$/$[OTf]^-$ anions, offering insights into the energetics of the dissociation both in gas and solution phase. The relative gas (in red) and the solvent phase (in blue) Gibbs free energies for the **1**-NTf_2 and **1**-OTf species are presented in Figure S48.

The dissociation energy of **1**-OTf, leading to separated $[\mathbf{1}]^+$ cation and $[OTf]^-$, is computed to be 112.6 kcal/mol in gas phase (Figure S48, A). By contrast, the same process is found to be 95.1 kcal/mol for **1**-NTf_2, indicating that the interaction between $[\mathbf{1}]^+$ anion and $[NTf_2]^-$ is much weaker than that in the case of **1**-OTf. This energy difference ($\Delta\Delta G_{gas}$) is estimated to be 17.5 kcal/mol in gas phase. As the reaction takes place in a polar solvent and the solvation effects for the two anions are expected to differ, the solvation free energies of these liberated anions also need to be taken into account when estimating the Lewis acidity. Accordingly, the following hypothetical step is the solvation of the $[\mathbf{1}]^+$ + X^- state. The solvation of $[\mathbf{1}]^+$ and $[OTf]^-$ pair is predicted to be more favored thermodynamically as compared to that of $[\mathbf{1}]^+$ + $[NTf_2]^-$. As the solvation free energy of $[\mathbf{1}]^+$ is identical in both hypothetical processes, the energy difference in solvation arises from the differing solvation effects for $[NTf_2]^-$ and $[OTf]^-$. The ΔG_{solv} value for $[\mathbf{1}]^+$ + $[OTf]^-$ pair, is predicted to be -95.8 kcal/mol, while this free energy change is only -88.6 kcal/mol in the case of $[\mathbf{1}]^+$ + $[NTf_2]^-$ pair. The computed difference in solvation free energies indicates that the solvation of $[OTf]^-$ is energetically is a more favorable process, reducing the magnitude of free energy difference ($\Delta\Delta G_{gas}$ = 17.5 kcal/mol) obtained in gas phase to $\Delta\Delta G_{solv}$ = 7.2 kcal/mol. The latter value is the solvation free energy difference between $[OTf]^-$ and $[NTf_2]^-$ anions. For the sake of clarity, in Figure S48 B, we present the solvation free energy of each individual species used in this analysis. It can be seen that the free energy changes associated with the solvation of $[OTf]^-$ and $[NTf_2]^-$ anions are -42.8 kcal/mol and -35.6 kcal/mol, respectively. The next hypothetical step to reach the solvated LAs is the association of $[\mathbf{1}]^+$ and $[X]^-$ ions. The DFT calculations predicts a ΔG_r = -24.1 kcal/mol free energy change for the reaction between $[\mathbf{1}]^+$ and $[OTf]^-$, whilst ΔG_r is estimated to be -

15.0 kcal/mol for $[\mathbf{1}]^+ + [NTf_2]^-$. The $\Delta\Delta G_r$ = - 9.1 kcal/mol derived from the present analysis is evidently equal to the difference of hydride affinities. It is worth pointing out that the solvation free energies of **1**-OTf and **1**-NTf_2 are nearly identical ($\Delta\Delta G_{solv}$ = -1.2 kcal/mol in favor of **1**-NTf_2), therefore, the solvation effects for those hardly affect the calculated free energy difference related to the dissociation reactions.

Insight into the origin of the increased stability of **1**-OTf was sought by assessing the net atomic charges obtained from NBO analysis. The obtained NBO charges of oxygen atoms are shown in Figure S48 C. The difference in the anionic character of oxygen atoms in the two anions is well demonstrated by net atomic charges obtained from NBO analysis. The computed charge points to an increased electron density on the oxygen atom in $[OTf]^-$ (-0.993) as compared to those (-0.933, -0.928) in $[NTf_2]^-$ anion. Consequently, the increased dissociation energy for **1**-OTf can be ascribed to the greater electrostatic interaction between $[\mathbf{1}]^+$ and $[OTf]^-$.

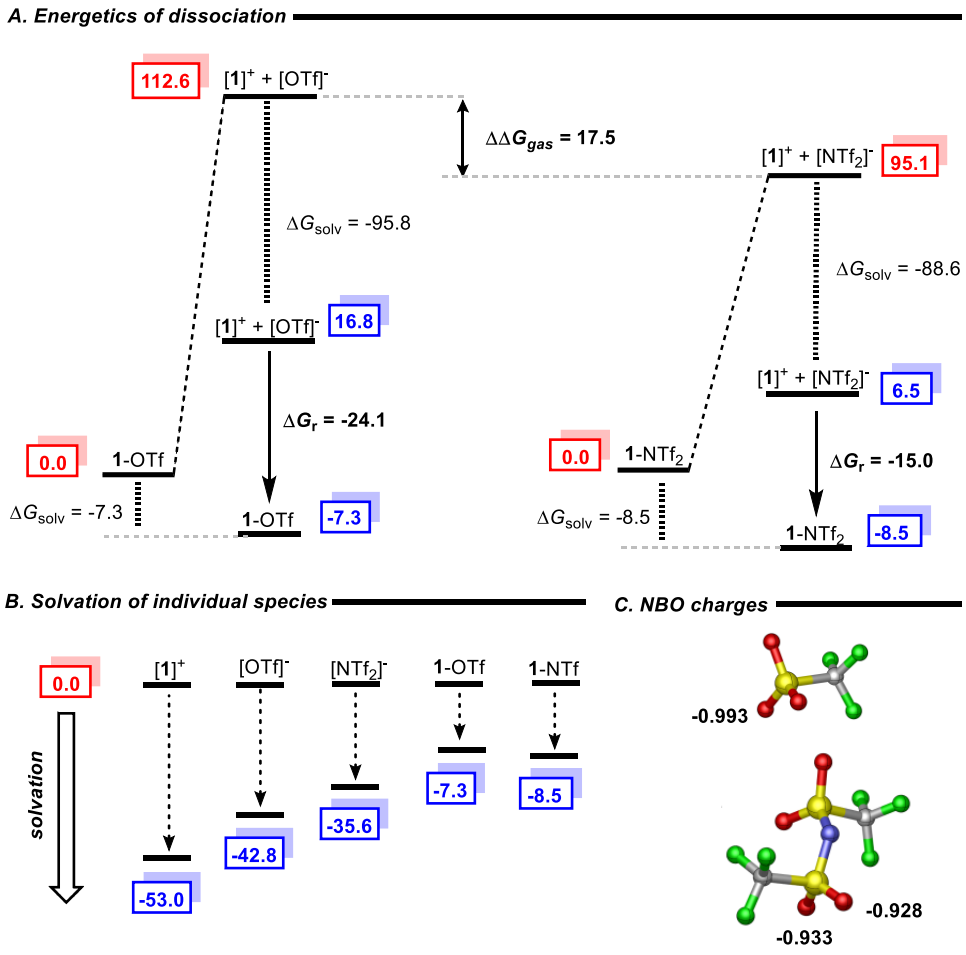

Figure S48 (A) Computed thermodynamics of the hypothetical dissociation process at RT. Note that the gas phase free energies do not contain the ΔG_{conc} (This correction was added to the solvation free energies – see details in General computational methodology). (B) Solvation free energies of the species used for energy decomposition analysis. (C) NBO charges of oxygen atoms in the anions (calculated at ωB97X-D/Def2TZVPP level). The relative free energies are given in kcal/mol.

12.2 Mechanism of H_2 activation

12.2.1 Speciation for 1-NTf_2/col

DFT calculations were performed to estimate the relative stability of possible complexes that can form upon reacting **1**-NTf_2 with col in solution phase. The obtained relative free energy data are shown in Figure S49. Calculations predicts that $[\mathbf{1}\cdot(col)]^+$ is the most stable form at RT by 2.6 kcal/mol with respect to **1**-NTf_2 + col reactant state (the latter represents a complex in which the oxygen binds to the cationic tin centre). The complex **1**-NTf_2' wherein the nitrogen atom of $[NTf_2]^-$ binds to the cationic tin center is found to be slightly less stable as compared to **1**-NTf_2 + col, only by 0.5 kcal/mol. These computations suggest that the dominant pair in the solution is $[\mathbf{1}\cdot(col)]^+ + [NTf_2]^-$.

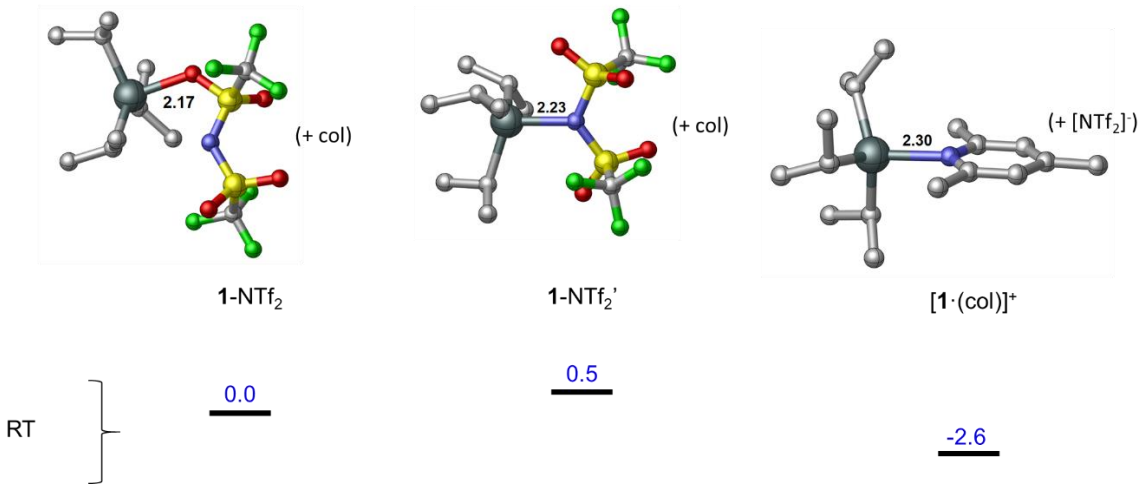

Figure S49 The most stable conformers of the species originated from **1**-NTf_2/col pair along with relative stabilities computed at RT. The relative stability (in blue) is given in kcal/mol with respect to **1**-NTf_2 + col reference state. Selected bond distances are given in Å.

12.2.2 Comparison between 1-NTf_2/col and 1-OTf/col in H_2 activation

We recently reported a combined experimental and computational study on **1**-OTf/col pair along with other [**1**]-based congeners. In that contribution, possible ground state adducts were probed and we could obtain reliable estimates on the ground state speciation as well as the reaction barrier for H_2 activation at the ωB97X-D/Def2TZVPP//ωB97X-D/Def2SVP(SMD) level of theory.[17] Here, we compare the energetics of the H_2 cleavage process for **1**-OTf/col and **1**-NTf_2/col FLP-systems. Note that the two free energy profiles were computed at the same level of DFT theory, hence permitting a direct comparison of the energetics obtained for the two systems (Figure S50). As reported in our recent study, the formation of $[\mathbf{1}\cdot(col)]^+ + [OTf]^-$ pair appeared thermodynamically rather unfavored with respect to **1**-OTf + col (+6.9 kcal/mol). In contrast, $[\mathbf{1}\cdot(col)]^+ + [NTf_2]^-$ pair was suggested to be the predominant state when **1**-NTf_2/col pair was applied for activation, being favored by -2.6 kcal/mol in free energy. This notable difference in the ground state speciation for the **1**-OTf/col and **1**-NTf_2/col pairs clearly indicates that $[NTf_2]^-$ is more loosely bound to $[\mathbf{1}]^+$ and an exchange reaction with a suitable donor molecule may occur with ease.

The barrier of H_2 activation was estimated by computing the standard free energy difference between the respective TS and the most stable reactant state. The energy barriers associated with the most favored transition states (20.2 kcal/mol for $\mathbf{TS}_{OTf\text{-}col}$ and 19.8 kcal/mol for $\mathbf{TS}_{NTf\text{-}col}$) leading to **1**-H product point to kinetically feasible H_2 activation events. The slightly lower barrier to generation of **1**-H is in a qualitative agreement with increased reactivity observed with **1**-NTf_2/col pair at RT. The origin of the increased reactivity lies in the enhanced Lewis acidity of **1**-NTf_2, and it is equally important to recognize

that the reactant-state stabilization through replacing NTf_2 with col is energetically less pronounced (as compared to that with quinuclidine (qui) as reported previously).[17] The previous calculations indicated that the H_2 activation reaction mediated by **1**-OTf/col pair is slightly endergonic, with a free energy difference of 1.7 kcal/mol, which gave a qualitative reproduction of the experimentally observed conversion. In stark contrast, H_2 cleavage with **1**-NTf_2/col pair is computed to be a thermodynamically favorable process with a free energy of $\Delta G = -4.7$ kcal/mol with respect to the $[\mathbf{1}\cdot(\text{col})]^+ + [NTf_2]^-$ state. This extent of exergonicity suggested by the calculated free energy data concurs with the high experimental conversion.

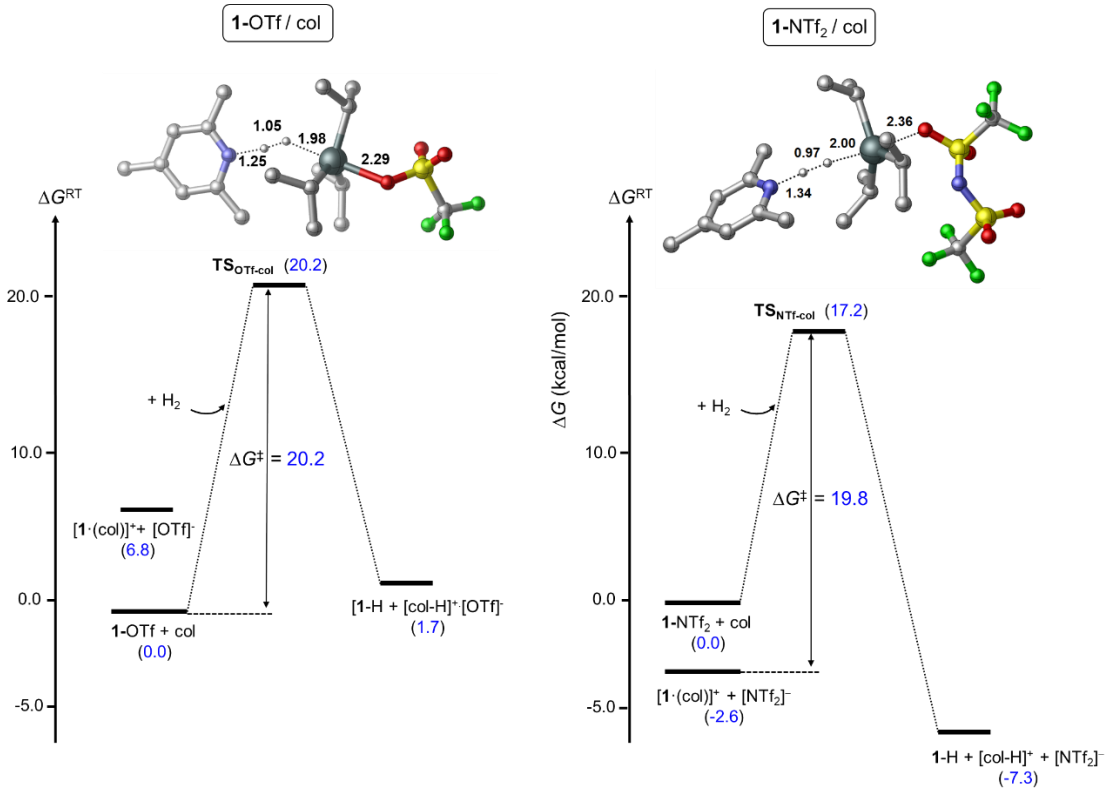

Figure S50 Relative Gibbs free energy profile for H_2 activation by **1**-OTf /col and by **1**-NTf_2/col pairs at RT. Computationally identified transition states are shown along with selected bond distances given in Å.

In our previous paper, we reported that association of $[\text{col-H}]^+\cdot[OTf]^-$ was computed to be slightly more favored (0.3 kcal/mol at RT) over the separated pair $[\text{col-H}]^+ + [OTf]^-$ (Figure S51). In contrast, it appears from the free energy data obtained using the same level of theory as previously that the dissociation of the $[\text{col-H}]^+\cdot[NTf_2]^-$ ion pair is favored by 0.9 kcal/mol (in the case of $[NTf_2]^-$ anion different forms of the ion pair were considered; for details see anion speciation section below).

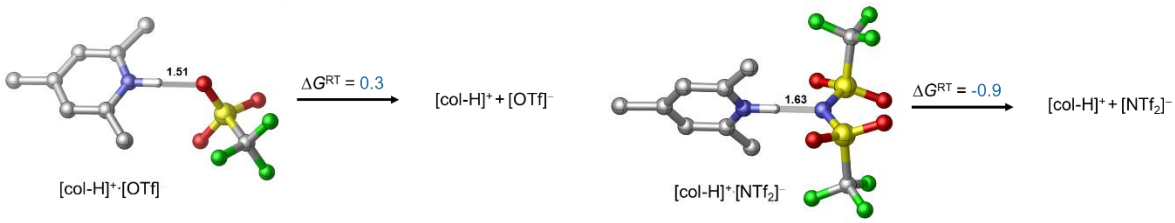

Figure S51 Calculated Gibbs free energy change (at RT) for the dissociation of ion pairs bound through H-bonding. Bond distances of $NH^{+\cdots}O/N$ are given in Å.

12.2.3 Speciation for 1-NTf_2/lut

After computationally examining the Lewis acidity of **1**-NTf_2 compound, we performed further DFT calculations to gain an insight into the ground state speciation at room temperature and at 150 °C, as the latter temperature was applied in ester reductions. We probed the **1**-NTf_2/lut system as this pair proved to be the most efficient in the reduction of the ester compounds. The results obtained with lutidine were also used to examine the H_2 activation pathway by **1**-NTf_2/lut and to make comparison with **1**-OTf/col. We again probed three possible species (Figure S52): one wherein the oxygen atom of $[NTf_2]^-$ binds to the cationic tin center (**1**-NTf_2), the second where the coordination is realized through the nitrogen atom of $[NTf_2]^-$ (**1**-NTf_2'), and third one which forms upon exchanging the anion with lutidine ($[\mathbf{1}\cdot(lut)]^+$). Again, note that the most stable conformer was used as a reference state to estimate the relative stability of these species. The DFT-computed stabilities are shown in Figure S52. The small free energy gap suggests that neither species is present exclusively. Thus, the data obtained from DFT computations alludes to a rapid equilibrium consisting of three possible species depicted in Figure S52. At room temperature, the $[\mathbf{1}\cdot(lut)]^+ + [NTf_2]^-$ pair appears to be dominant in the solution (-1.1 kcal/mol in relative to **1**-NTf_2 + lut pair) as compared to the other two states, however, the stability trend changes at elevated temperature. Computations suggests that the most stable state at 150 °C is the **1**-NTf_2 + lut pair, albeit by a small margin (-0.6 kcal/mol in relative to $[\mathbf{1}\cdot(lut)]^+ + [NTf_2]^-$ pair). Consequently, a rapid equilibrium between these adducts is also expected to be present at 150 °C.

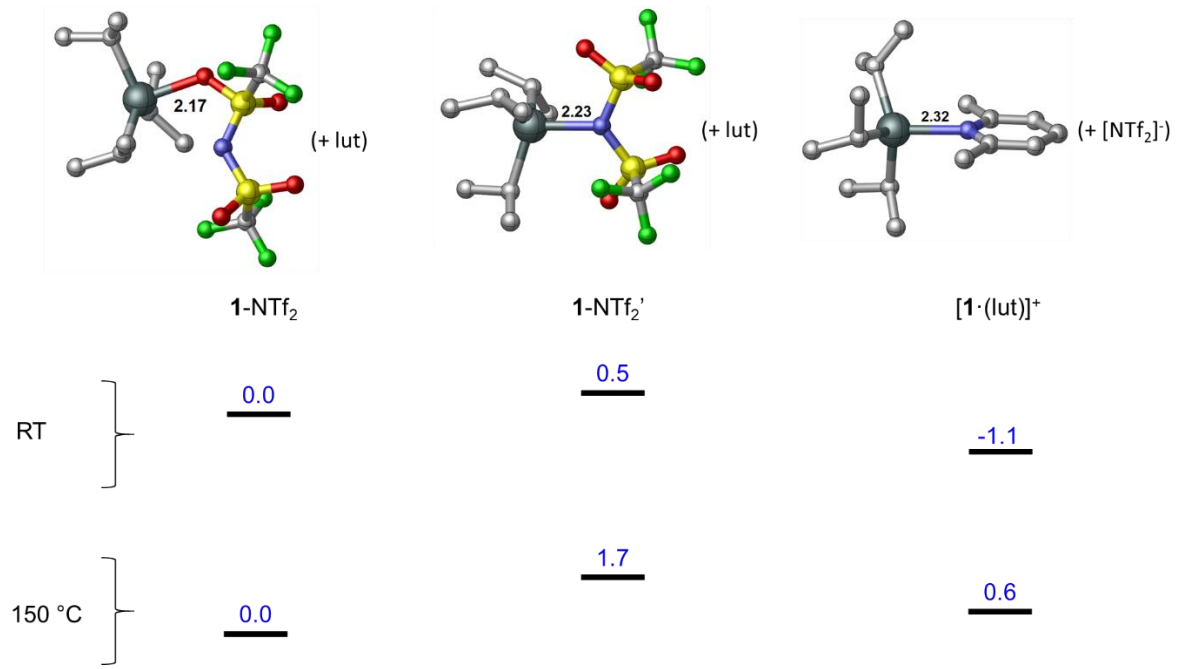

Figure S52 The most stable conformers of the three possible species and their relative stabilities at RT and 150 °C. The relative stability (in blue) is given in kcal/mol with respect to **1**-NTf_2 + lut state at both temperatures. Selected bond distances are given in Å.

12.2.4 H_2 activation with 1-NTf_2/lut at RT

After gaining insights into the ground state speciation, we examined the mechanism of H_2 activation. The relative Gibbs free energy profile obtained at RT and the transition state of H_2 splitting are shown in Figure S53. Similar to **1**-OTf + qui/col systems,[17] the H_2 cleavage with assistance of **1**-NTf_2 + lut pair is a concerted but asynchronous process (the $[NTf_2]^-$ anion is not completely dissociated in the transition state). The transition state $\mathbf{TS}_{NTf\text{-}lut}$ is found to lie 16.7 kcal/mol above the **1**-NTf_2 + lut state, hence the reaction barrier related to H_2 activation is estimated to be 17.8 kcal/mol at RT. The H_2 cleavage leading

to **1**-H is computed to be an exergonic process. Interestingly, on the product side of the reaction with **1**-NTf_2/lut pair, the association of the $[lut\text{-}H]^{+}\cdot[NTf_2]^{-}$ was thermodynamically less favored than the respective separated state $[lut\text{-}H]^{+}$ + $[NTf_2]^{-}$. This observation stands in contrast to the computational results obtained in the case of $[OTf]^{-}$ + $[qui–H]^{+}$ or $[col\text{-}H]^{+}$ where the formation of $[qui–H]^{+}\cdot[OTf]^{-}$ and $[col–H]^{+}\cdot[OTf]^{-}$ adducts gave rise to notable stabilization on the product side. However, this concurs with the observation of the reduced coordinative ability of $[NTf_2]^{-}$ anion. At RT, the separated state was computed to be 1.3 kcal/mol more stable than the adduct.

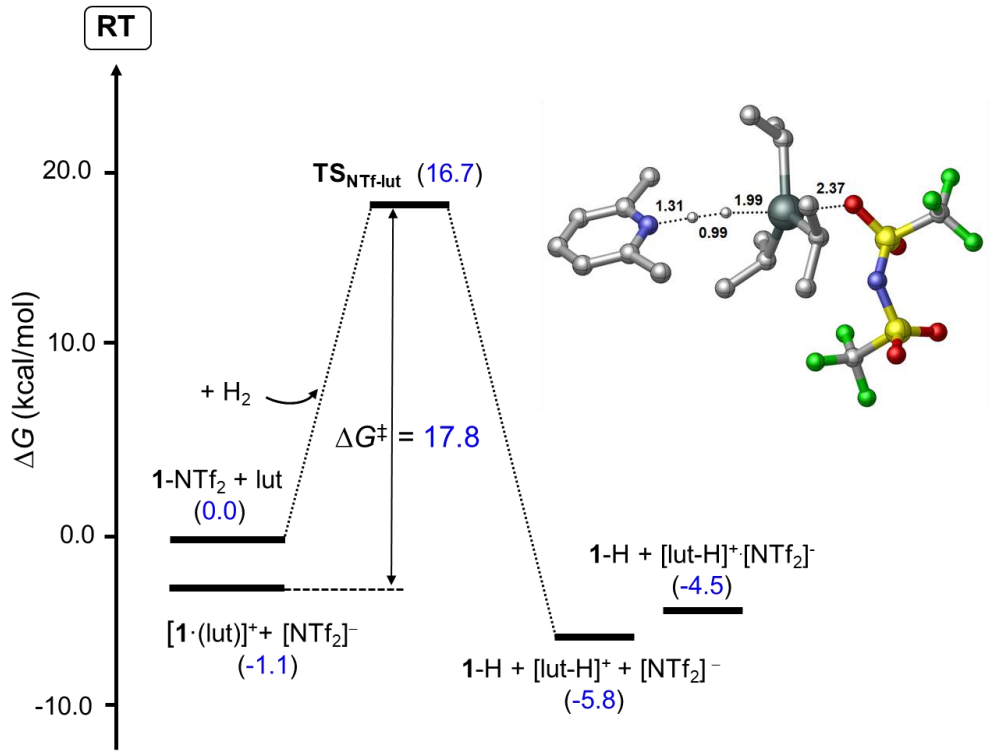

Figure S53 Relative Gibbs free energy profile for H_2 activation by **1**-NTf_2/lut at room temperature. Relative stabilities (in kcal/mol) are shown in parentheses with respect to $[\mathbf{1}\cdot(lut)]^{+}$ + $[NTf_2]^{-}$. Selected bond distances of $\mathbf{TS}_{NTf\text{-}lut}$ are given in Å.

12.2.5 H_2 activation with 1-NTf_2/lut at 150 °C

Given that the *in situ* ester reduction occurs at 150 °C, we examined the relative free energy profile of H_2 activation at this temperature as well. As shown in Figure S54, the barrier predicted for the H_2 activation increased by 6.0 kcal/mol ($\Delta G^{‡}$ = 23.8 kcal/mol), which is in line with the expectation that higher temperature raises a transition state in free energy when the molecularity decreases, and this is due to the substantial entropy loss that the transition state suffers. Note that the overall reaction rate is determined by the Eyring-Polanyi equation, therefore elevating the temperature may give rise to rate acceleration even though the barrier in question noticeably increased. It is also worth pointing out that the ground state at 150 °C is different compared to that at RT. The **1**-NTf_2 + lut state is found to be slightly more stable than $[\mathbf{1}\cdot(lut)]^{+}$ + $[NTf_2]^{-}$ at 150 °C. Formation of **1**-H intermediate on this pathway is still exergonic, and the dissociation of the $[lut\text{-}H]^{+}\cdot[NTf_2]^{-}$ ion pair is thermodynamically even more favored as the higher temperature facilitates processes associated with entropy production.

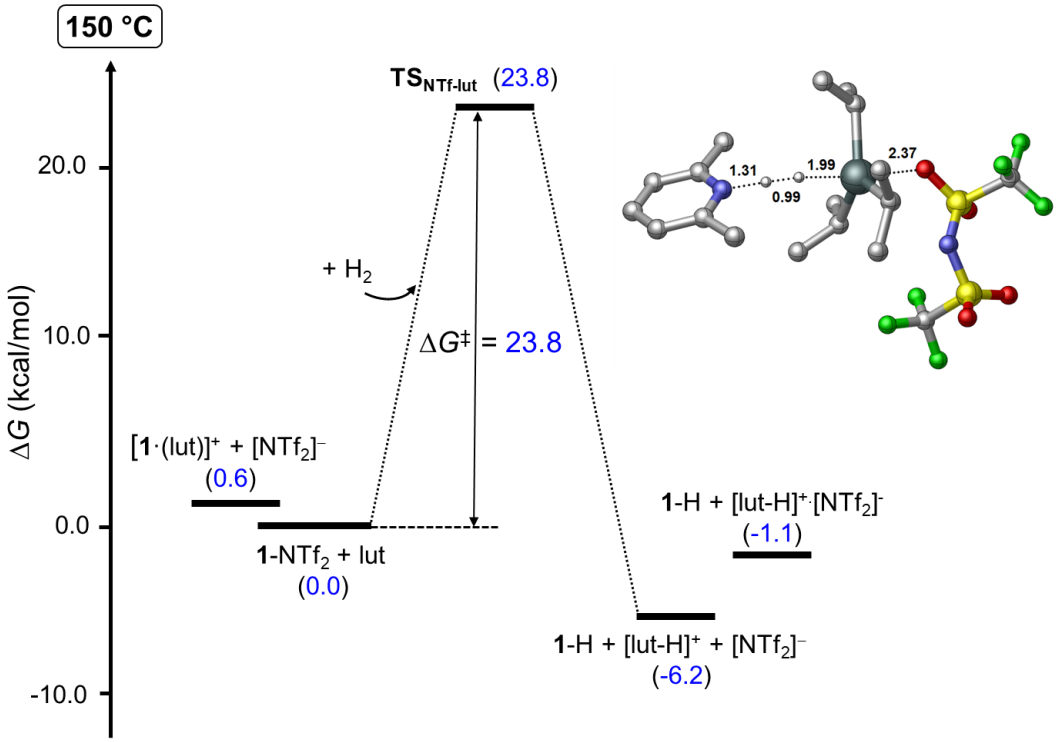

Figure S54 Relative Gibbs free energy profile for H_2 activation by **1**-NTf_2/lut at 150 °C. Relative stabilities (in kcal/mol) are shown in parentheses with respect to **1**-NTf_2 + lut.

We also probed the effect of changing the Lewis base to weaker, yet structurally related 2-methyl-6-chloropyridine (MeCl-pyr) and 2,6-dichloropyridine (diCl-pyr), upon H_2 heterolysis; in both cases H_2 cleavage was endoergic (+5.3 and +16.2 kcal/mol, respectively), which likely explains their inability to hydrogenate $MeCO_2Et$. Furthermore our procedures to locate the TS structures for H_2 cleavage, which were successful for {**1**-NTf_2/**1**-OTf + lut/col} Lewis pairs, does not work for the {**1**-NTf_2 + 2-methyl-6-chloropyridine/2,6-dichloropyridine} combinations; instead we observe spontaneous H_2 elimination from the proposed **1**-H + [LB-H]$^+$[NTf_2]$^-$ product structures, indicating that H_2 splitting is also kinetically disfavoured (Figure S55).

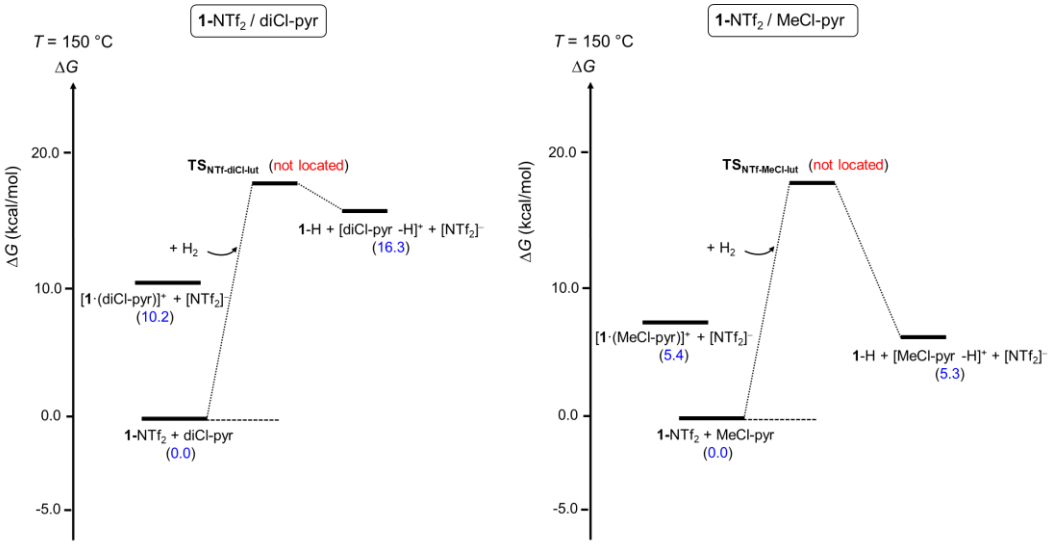

Figure S55. Relative Gibbs free energy profile for H_2 activation by **1**-NTf_2 and either 2-methyl-6-chloropyridine (MeCl-pyr) or 2,6-dichloropyridine (diCl-pyr) at 150 °C. Relative stabilities (in kcal/mol) are shown in parentheses with respect to **1**-NTf_2 + respective Lewis base.

12.2.6 Additional pathways for H_2 activation

We also probed further mechanistic possibilities with respect to the H_2 activation, as illustrated in Figure S55. Although the O-coordinated complex (see **1**-NTf_2 in Figure S52) is predicted to be 0.5 kcal/mol more stable than the N-coordinated form (**1**-NTf_2'), it was necessary to computationally examine the transition state **TS'**$_{NTf\text{-}lut}$ in which the N atom departs from the [**1**]-center upon H_2 cleavage. The reaction barrier associated with the mechanism involving **TS'**$_{NTf\text{-}lut}$ is predicted to be disfavored by ~ 6 kcal/mol at both temperatures ($\Delta G^{\ddagger}$ = 23.9 kcal/mol at RT, $\Delta G^{\ddagger}$ = 30.9 kcal/mol at 150 °C). We also examined a mechanistic scenario in which a [**1**·(lut)]$^+$/lut pair participates in H_2 activation via transition state **TS**$_{lut\text{-}lut}$, but this pathway becomes even less accessible kinetically, as demonstrated by the high reaction barriers ($\Delta G^{\ddagger}$ = 27.0 kcal/mol at RT, $\Delta G^{\ddagger}$ = 34.8 kcal/mol at 150 °C). It needs to be pointed out that in this route the reference state differs from that in the case of **TS**$_{NTf\text{-}lut}$ and **TS'**$_{NTf\text{-}lut}$, as the activation with the [**1**·(lut)]$^+$/lut pair requires two equivalents of lutidine (for reference states see Figure S53 caption).

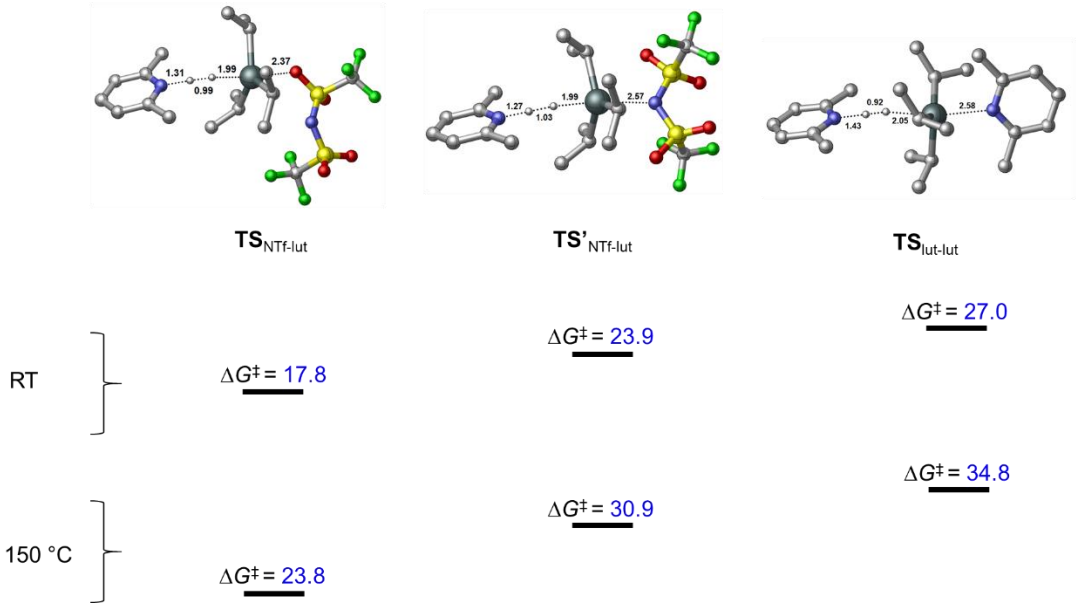

Figure S56 Computationally identified transition states for H_2 activation. Relative stabilities are given in kcal/mol (in blue). The calculated stabilities of **TS**$_{NTf\text{-}lut}$ and **TS'**$_{NTf\text{-}lut}$ at RT are given with respect to [**1**·(lut)]$^+$ + $[NTf_2]^-$ + H_2, and at 150 °C with respect to **1**-NTf_2 + lut + H_2. In the case of **TS**$_{NTf\text{-}lut}$, the reference states are the followings: [**1**·(lut)]$^+$ + lut + $[NTf_2]^-$ + H_2 at RT, and **1**-NTf_2 + 2 lut + H_2 at 150 °C.

12.2.7 Anion association

As noted above, the association of the $[lut\text{-}H]^+\cdot[NTf_2]^-$ was thermodynamically less favored than the separated state $[lut\text{-}H]^+ + [NTf_2]^-$. In the $[NTf_2]^-$ anion, both the N- and O-center can participate in H-bonding interactions with $[lut\text{-}H]^+$. The orientations identified computationally are displayed in Figure S56. In general, the $NH^{+}\cdots N$ H-bonding interaction appears favored over the $NH^{+}\cdots O$. The two structures encompassing $NH^{+}\cdots N$ bonding differs from one another by the orientation of $[NTf_2]^-$ anion relative to lutidine. Similarly, the difference between $[lut\text{-}H]^+\cdot[NTf_2]^-$ (I) and $[lut\text{-}H]^+\cdot[NTf_2]^-$ (III) arises from the relative orientation of the anion.

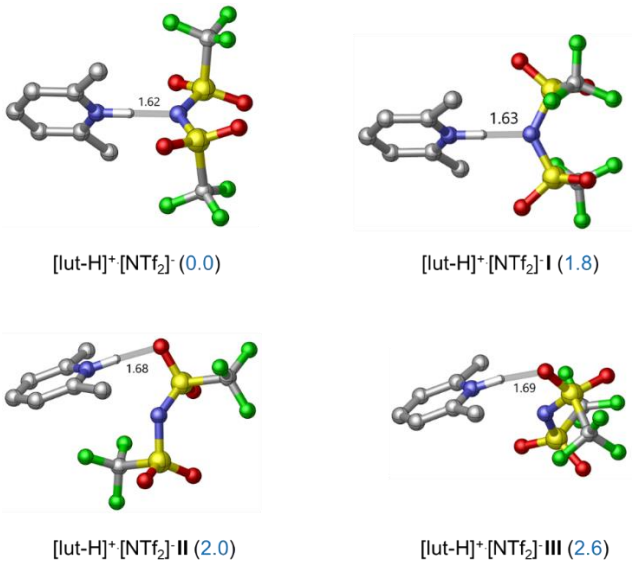

Figure S57 Computationally identified $[lut\text{-}H]^+ \cdot [NTf_2]^-$ adducts. Relative stabilities (in kcal/mol, at RT) are shown in parentheses with respect to $[lut\text{-}H]^+ \cdot [NTf_2]^-$. Bond distances of $NH^{+\cdots}N/O$ are given in Å.

12.4 Inhibition

We first investigated the stability of three relevant species in which EtOH binds to the Sn centre in [**1**]. The free energy changes of the following reactions were calculated at RT and at 150 °C as well. As the NMR experiments were performed at RT, we herein discuss the thermodynamics computed at RT. Additionally, the free energy changes corresponding to 150 °C are also shown underneath the reaction arrow.

The reaction between EtOH and **1**-NTf_2 forming a ternary complex ((EtOH)·**1**-NTf_2) is predicted to be slightly endergonic (1.7 kcal/mol) (Figure S57 A. Eq. 1), the dissociation of $[NTf_2]^-$ anion results in complex $[\mathbf{1}\cdot(EtOH)]^+$ that is more stable than EtOH + **1**-NTf_2 starting state by 1 kcal/mol (Figure S57 A, Eq. 2). This is in agreement with the NMR experiment as the ^1H NMR peaks of EtOH were only slightly perturbed when EtOH was administered to a solution of **1**-NTf_2 (see Figure S39). Overall, for this mixture, the relatively small free energy difference (2.7 kcal/mol free energy window) suggests that all the possible species are in equilibrium with one another but $[\mathbf{1}\cdot(EtOH)]^+$ is the dominant species. Upon addition of lut, further movement of the peak was seen in the ^1H NMR spectrum, however, a much more dramatic change in the $^{119}Sn\{^1H\}$ NMR spectrum is evident with the appearance of a sharp peak at δ = 34.28 ppm (see Figure S40). The calculations indicate that the deprotonation event by lutidine is thermodynamically rather favored (-8.6 kcal/mol), furnishing species **1**-OEt. Furthermore, the association of **1**-OEt and lut-H^+ via H-bonding interaction was estimated to be favored by 2 kcal/mol. The free energy difference between the **1**-OEt and [lut-H^+]·[**1**-OEt] adduct is relatively small, suggesting these two species are in equilibrium.

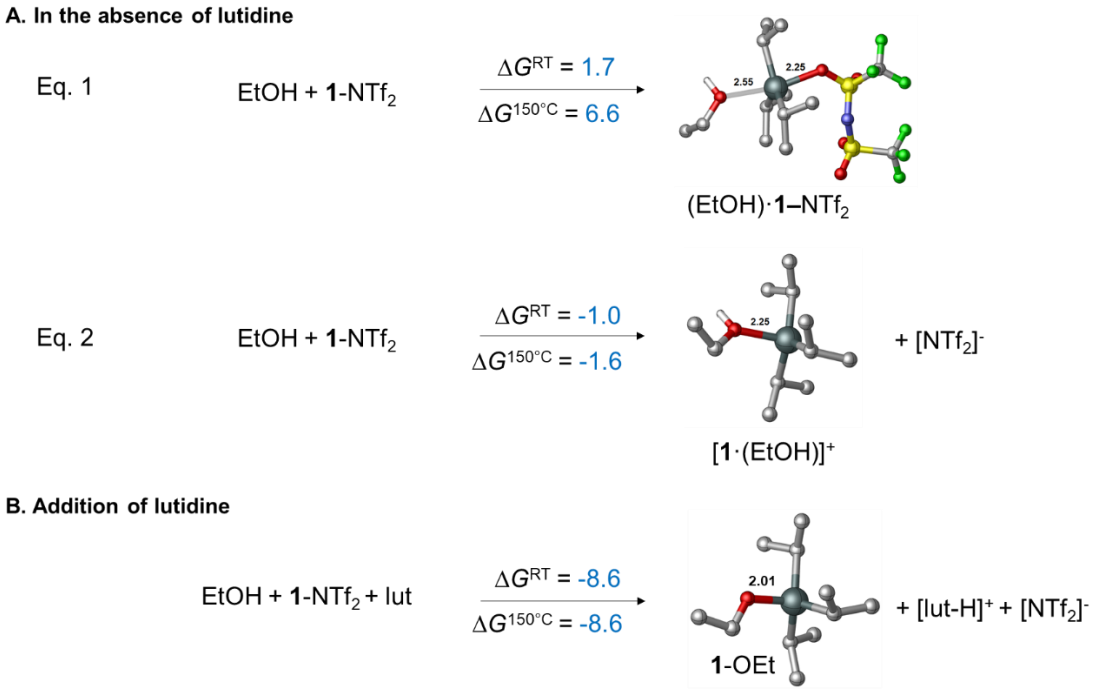

Figure S58 Computed free energy change of reactions between EtOH, **1**-NTf_2 and lut (in kcal/mol).

By comparison, when the alcohol is CF_3CH_2OH the thermodynamics of these reactions is different. The binding of CF_3CH_2OH to **1**-NTf_2 is endergonic (computed to be +4.2 kcal/mol; Figure S58 **A**, Eq. 1), suggesting that the $(CF_3CH_2OH)\cdot$**1**-NTf_2 ternary adduct is in an undetectable concentration. The dissociation of $[NTf_2]^-$ anion is unfavored (A. Eq. 2), with the formation of $[\mathbf{1}\cdot(CF_3CH_2OH)]^+$ calculated to be even more endergonic than formation of the ternary adduct (+8.1 kcal/mol). The high endergonicity

of the reaction indicates that the CF_3-substituted alcohol is far less prone to coordinate to cationic [**1**]$^+$, likely due to the electron-deficient nature of the oxygen atom reducing its basicity.

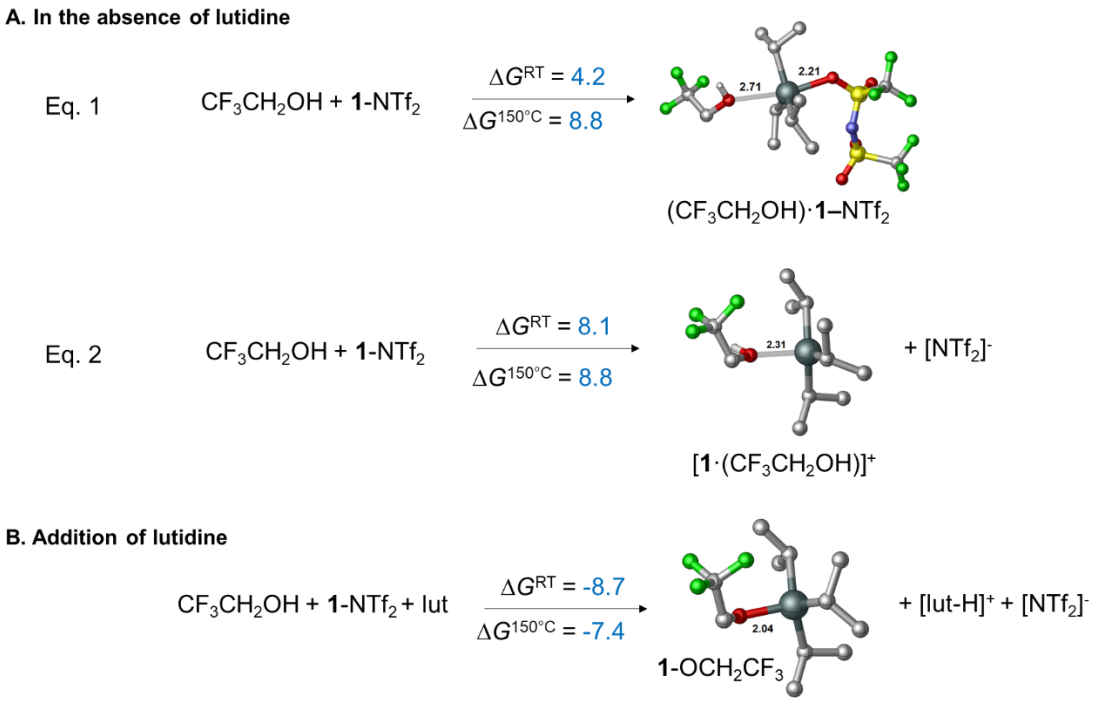

Figure S59 Computed free energy change of reactions between CF_3CH_2OH, **1**-NTf_2 and lut (in kcal/mol).

At first glance, it may appear unexpected that ΔG^{RT} values of the third reactions (when lutidine is present) is nearly identical (-8.6 kcal/mol for EtOH, -8.7 kcal/mol for CF_3CH_2OH), but the $CF_3CH_2O^-$ anion is expected to display a weaker interaction with fragment [**1**]$^+$. Note that two factors should be taken into account here; first, how acidic the alcohol is, and second, how strong the interaction between RO^- and [**1**]$^+$ is. Clearly, the electron withdrawing group in CF_3CH_2OH weakens the alcohol binding to **1**-NTf_2, which in this case is entirely counterbalanced by the lower pKa of the adduct, rendering deprotonation more favorable.

We have also examined the coordination of the catalyst to to the Sn-alkoxides **1**-OCH_2R and found that such adducts may exist in their dissociated form, [**1**·(**1**-OCH_2R)]$^+$ + $[NTf_2]^-$ (Figure S59). Formation of the trifluoroethoxy species is endoergic, whereas the more basic ethoxy derivative forms a stronger adduct; accordingly **1**-OCH_2CF_3 and [**1**·(**1**-OCH_2CH_3)]$^+$ + $[NTf_2]^-$ are the lowest energy Sn-containing states in their respective catalytic cycles.

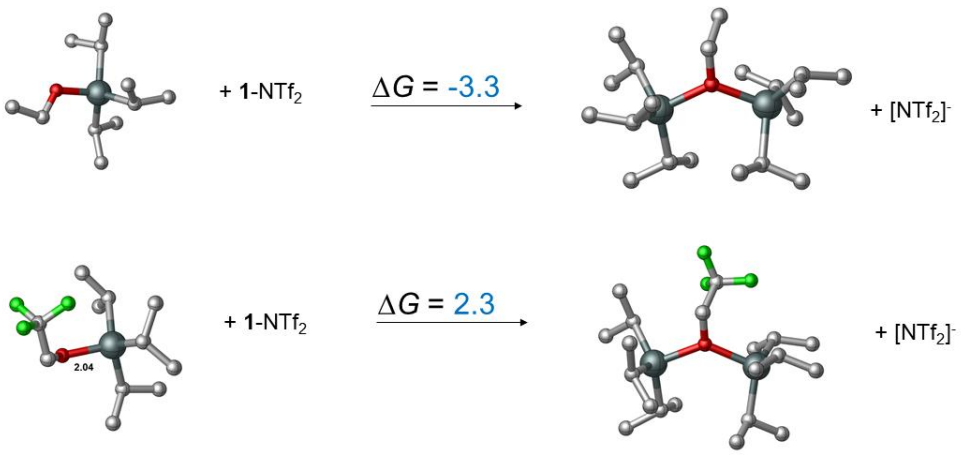

Figure S60 Computed free energy change of reactions between **1**-OCH_2R (R = CF_3 and CH_3) and **1**-NTf_2 (in kcal/mol).

Relevance to the catalytic ester reduction

These results imply that **1**-NTf_2 is converted into **1**-OR in the early-phase of the reaction i.e. **1**-OR becomes a reservoir for the most Lewis acidic $[\mathbf{1}]^+$ fragment, in active **1**-NTf_2. It follows that in the ensuing cycles the reaction barriers increase by the free energy of **1**-OR + $[lut\text{-}H]^+$ + $[NTf_2]^-$ → **1**-NTf_2 + ROH + lut exchange reaction (by about 9 kcal/mol) as the elementary steps of the reduction remain unchanged, which requires the involvement of **1**-NTf_2 Lewis acid. This explains the necessity of the high temperature and prolonged reaction time needed for the successful reduction of the CF_3CO_2Et substrate.

12.5 Mechanism of ester reduction

12.5.1 Proton-catalyzed pathway

Ethyl trifluoroacetate (CF_3CO_2Et) in the presence of **1**-NTf_2/lut + H_2 gave reduction products with appreciable conversion (80%) and was the first substrate used to probe the mechanism of ester reduction. We first considered pathways where the ester substrate was activated via protonation. Upon H_2 cleavage, the reaction mixture consists of $[NTf_2]^-$ + **1**-H + CF_3CO_2Et + $[lut\text{-}H]^+$ species. It has been previously suggested that an anion being in close proximity to **1**-H is required for H^- transfer to be initiated as the anion sequesters the forming $[\mathbf{1}]^+$, which would otherwise result in the formation of a prohibitively high-energy $[\mathbf{1}]^+$ 'free' cation.[22] With this in mind a transition state could be identified wherein the protonation of CF_3CO_2Et and H^- transfer take place in a synchronous manner (Figure S60). The computed barrier was rather high as $\mathbf{TS_{red\text{-}prot}}$ was found to be 50.2 kcal/mol above the reactant state. The stepwise version of the proton-catalyzed ester reduction can be undoubtedly ruled out based on the computed ΔG = +49.0 kcal/mol free energy change of CF_3CO_2Et + $[lut\text{-}H]^+$ = $[CF_3(C{=}O\text{-}H)OEt]^+$ + lut protonation process, strongly indicating that the protonation of the ester by $[lut\text{-}H]^+$ is thermodynamically highly unfavored, in line with the strongly disparate pK_a(H_2O) values of protonated esters (~ -7) and $[lut\text{-}H]^+$ (6.72). Taken together, these results suggest that the reduction of the ester substrate is not a H^+-mediated process.

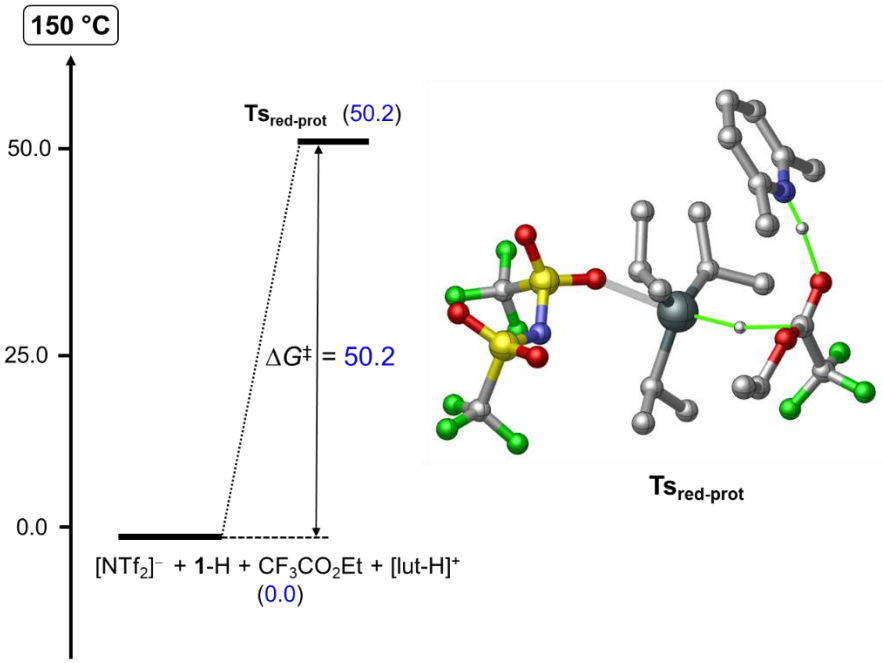

Figure S61 Calculated reaction barrier for the synchronous proton-catalyzed ester reduction at 150 °C. Relative stabilities are given in kcal/mol (in blue) with respect to $[NTf_2]^-$ + **1**-H + CF_3CO_2Et + $[lut\text{-}H]^+$ reference state.

12.5.2 Reduction without activation

Various reaction pathways corresponding to the hydride transfer step were also examined in our study. In these processes depicted in Figure S61, the H^- transfer was modelled with no activation of the carbonyl group (both the ester and aldehyde were examined). The transition state **TS-1** in which the $[NTf_2]^-$ anion resides close to [**1**]-centre is predicted to be at 45.3 kcal/mol with respect to **1**-H + CF_3CO_2Et + $[NTf_2]^-$ reactant state, indicating that the first H^- transfer is very unlikely to take place in such a manner. For the CF_3CHO intermediate, the analogous transition state **TS-3** is estimated to lie 30.6 kcal/mol above the corresponding **1**-H + CF_3CHO + $[NTf_2]^-$ reactant state, which is still considered to be too high. Interestingly, the alternative pathways which disregard the assistance of $[NTf_2]^-$ were found to be slightly lower in energy in both cases (**TS-2** → $\Delta G^‡$ = 42.7 kcal/mol for CF_3CO_2Et and **TS-4** → $\Delta G^‡$ = 29.1 kcal/mol for CF_3CHO). On close inspection of the located transition states **TS-2** and **TS-4**, the concomitant formation of **1**-OCH_2CF_3 can be seen on these pathways, sequestering the resultant $[\mathbf{1}]^+$ cation, yet these modes of reduction are still unlikely to operate based on the computed

barriers. Overall, the free energy data obtained for reduction were completely consistent with the stoichiometric **1**-H + CF_3CO_2Et experiments as no reduction products (**1**-OCH_2CF_3/CF_3CH_2OH or **1**-OEt/EtOH) were observed in the absence of Lewis acidic **1**-NTf_2.

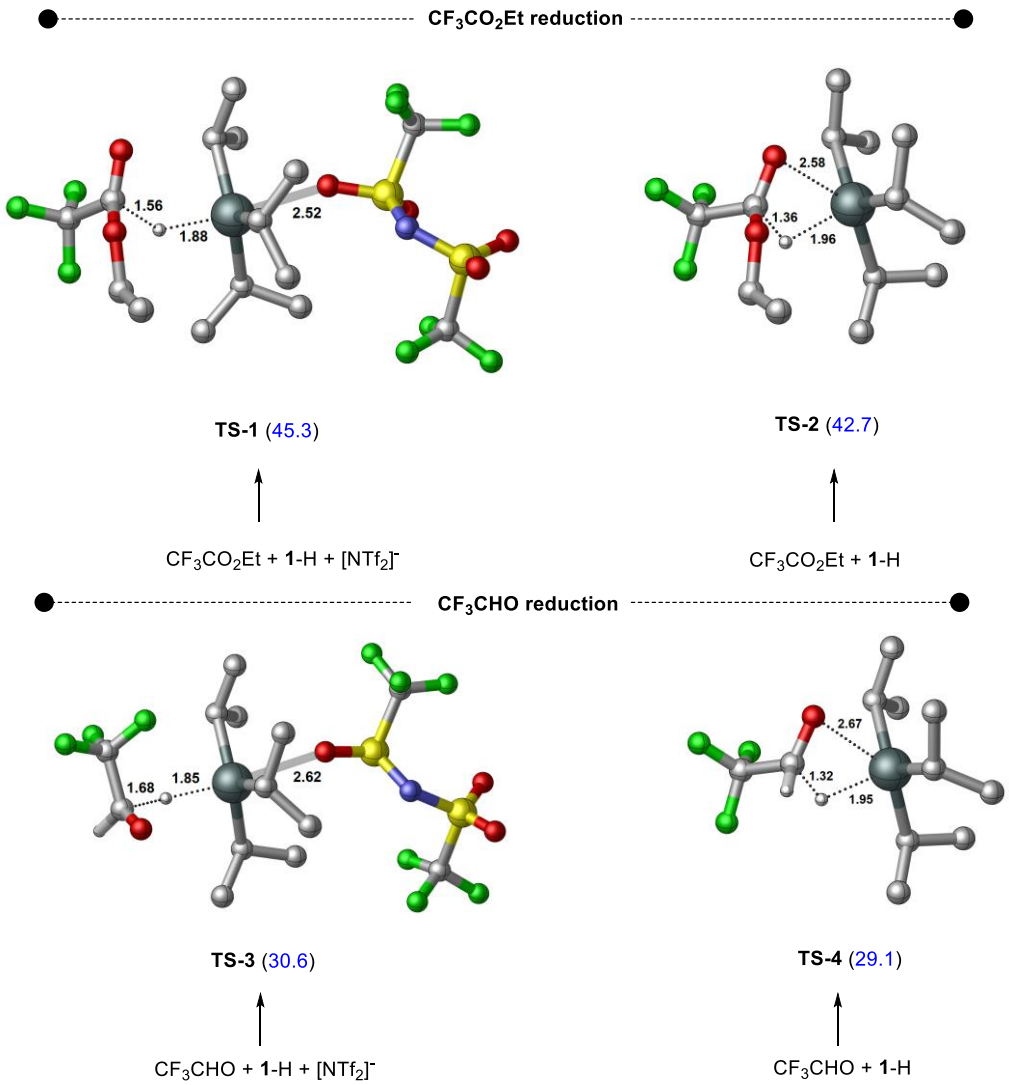

Figure S62 Computationally identified transition states for H^- transfer when ester substrate is CF_3CO_2Et. Computed barriers are given in kcal/mol (in blue) with respect to the corresponding reactant states indicated below TS structures. Selected bond distances of TSs are given in Å.

The analogous pathways for EtOAc reduction were considered for comparison (Figure S62). For the first H^- transfer, the **TS-6** in which the $[NTf_2]^-$ anion is absent was predicted to be favored over **TS-5**, with a free energy difference of 7.5 kcal/mol. Nevertheless, **TS-6** was estimated to lie at 52.6 kcal/mol, hence this barrier is insurmountable under the applied conditions. As expected, the transition states **TS-7** and **TS-8** corresponding to the reduction of MeCHO were found to be lower in free energy as compared to transition states related to EtOAc reduction. Again, the **TS-8** lacking the involvement of $[NTf_2]^-$ anion appeared kinetically more favored than **TS-7**. Based on the computed high reaction barriers, the pathways in which the carbonyl group is non-activated are even less likely in the case of EtOAc. Comparison of these transition states with the corresponding TS structures for CF_3-substituted oxo-compounds indicates that, while the electron withdrawing group CF_3-group significantly enhances the reactivity of the C=O bond, the involvement of a LA is still likely to be required for H^- transfer to occur from **1**-H.

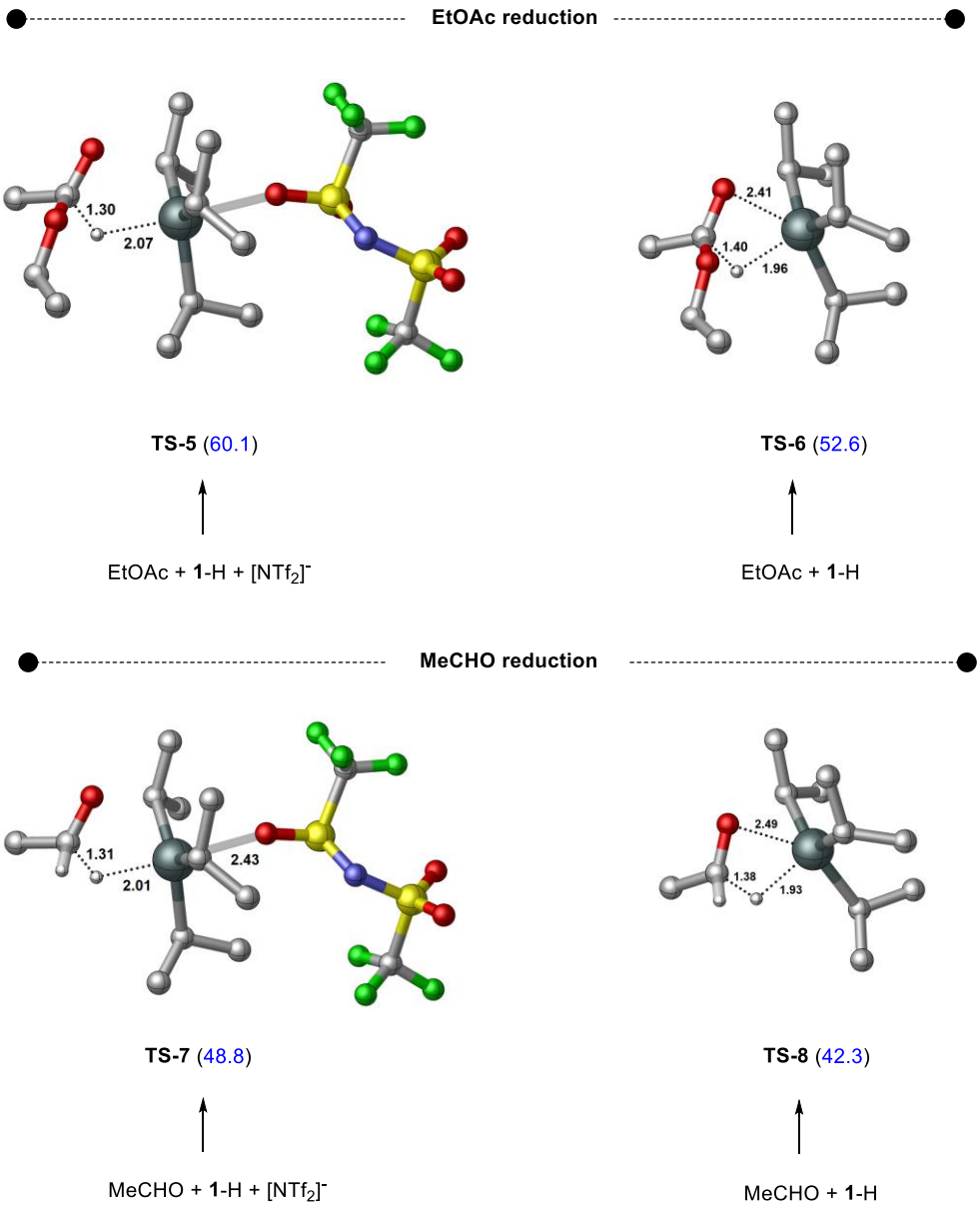

Figure S63 Computationally identified transition states for H^- transfer when ester substrate is EtOAc. Computed barriers are given in kcal/mol (in blue) with respect to the corresponding reactant states indicated below TS structures. Selected bond distances of TSs are given in Å.

12.5.3 Reduction with Lewis acid activation

A.) Reduction of ethyl trifluoroacetate

After ruling out the H^+-catalyzed and non-activated mechanistic scenarios, we next examined a reaction pathway which involves the activation of the carbonyl group (in both esters and aldehydes) by the Lewis acidic **1**-NTf_2. The relative free energy diagram of the entire catalytic cycle of CF_3CO_2Et reduction is shown in Figures S63, and the most stable intermediates and TS contributing towards alcohol formation are depicted below the free energy profile. The reported Gibbs free energy values refer to 150 °C, the temperature at which catalytic reduction was carried out.

The envisioned cycle begins with the activation of two equivalents of H_2. As shown in Figure S54, H_2 cleavage proceeds via $\mathbf{TS}_{\text{NTf-lut}}$ with a free energy barrier of 23.8 kcal/mol, resulting in **1**-H reductant along with $[\text{lut-H}]^+ + [NTf_2]^-$ ions. Experimental data strongly conclusively demonstrate that ester reduction relies on the use of Lewis acidic **1**-NTf_2. This conversion is presumed to involve the formation of a $[\mathbf{1}\cdot(CF_3CO_2Et)]^+$ activated species, which has been computed to require a free energy of +13.2

kcal/mol. Additionally, as discussed above, the close proximity of $[NTf_2]^-$ anion to the [**1**]-centre appears essential to initiate a kinetically feasible H^- transfer from **1**-H. The formation of $([NTf_2]^-)\cdot$**1**-H species has a free energy penalty of +11.3 kcal/mol (see equations below reduction 1 step). Interestingly, the mechanism of the H^- transfer to the carbonyl group could not be explicitly calculated as no transition state on the potential energy surface could be located for this process. All attempts to locate a transition state for H^- transfer failed as the H^- anion shift between $([NTf_2]^-)\cdot$**1**-H and the cationic $[\mathbf{1}\cdot(CF_3CO_2Et)]^+$ species always occurred during the course of TS geometry optimization. Based on the DFT calculations, it appears that activation of the ester substrate by **1**-NTf_2 brings about an extremely reactive cationic $[\mathbf{1}\cdot(CF_3CO_2Et)]^+$ species, enabling the H^- transfers to take place without a barrier when the $([NTf_2]^-)\cdot$**1**-H + $[\mathbf{1}\cdot(CF_3CO_2Et)]^+$ pair is formed. We assume that diffusion-control is negligible at 150 °C and, therefore, the barrier heights for H^- transfer can be estimated as the sum of the free energy changes of the following two processes; CF_3CO_2Et + **1**-NTf_2 → $[\mathbf{1}\cdot(CF_3CO_2Et)]^+$ + $[NTf_2]^-$ and $[NTf_2]^-$ + **1**-H → $([NTf_2]^-)\cdot$**1**-H, which is 24.5 kcal/mol. It is worth pointing out that this estimated free energy barrier is comparable to that of H_2 activation (23.8 kcal/mol), indicating that these two processes may take place in parallel. The reduction of CF_3CO_2Et to acetal **1**-acF is found to be exergonic by -3.7 kcal/mol, by which this stage of the reduction becomes the resting-state in the cycle, lying at -16.3 kcal/mol in free energy.

Next, we explored the collapse of the acetal **1**-acF intermediate which gives rise to the formation of CF_3CHO and **1**-OEt as well as the concomitant liberation of a **1**-NTf_2 Lewis acid. This step proceeds via $\mathbf{TS}_{ald\text{-}F}$ and we obtained a barrier of 23.6 kcal/mol, which is slightly lower than that of H_2-activation, yet still comparable to the largest barrier of 24.5 kcal/mol observed for H^- transfer step. Our computational analysis indicates that the formation of CF_3CHO aldehyde is somewhat endergonic from acetal **1**-acF intermediate (+2.6 kcal/mol), but slightly exergonic with respect to CF_3CO_2Et + **1**-H state (-1.3 kcal/mol). The principal mechanistic features of the subsequent aldehyde reduction are quite similar to that observed for the first reductive step. Namely, the transition state of H^- transfer could not be found as the cationic $[\mathbf{1}\cdot(CF_3CHO)]^+$ species abstracts the H^- anion from $([NTf_2]^-)\cdot$**1**-H with no barrier. Again, we used the sum of the free energy changes of the respective two processes to estimate the reaction barrier (CF_3CHO + **1**-NTf_2 → $[\mathbf{1}\cdot(CF_3CHO)]^+$ + $[NTf_2]^-$ ΔG = 10.0 kcal/mol). Accordingly, the reduction of CF_3CHO is predicted to have a 21.3 kcal/mol energy barrier relative to the preceding reactant level, but the overall barrier of this reduction process is 23.9 kcal/mol with respect to the most stable **1**-acF intermediate state. The reduction of CF_3CHO by the second equivalent of **1**-H leading to **1**-OCH_2CF_3 is computed to be clearly exergonic. Overall, the formation of **1**-OEt and **1**-OCH_2CF_3 is thermodynamically rather favored with respect to 2 **1**-NTf_2 + 2 lut + 2 H_2 + CF_3CO_2Et reactant state, giving rise to an exergonicity of -33.5 kcal/mol.

The predicted free energy barriers of the analyzed steps are comparable and considering the accuracy of DFT methods the rate-determining step cannot be identified with complete certainty. However, the relative energies of the estimated reaction barriers are within 0.9 kcal/mol energy range and we, therefore, suggest a mechanistic sequence in which the elementary steps proceed in parallel. This parallel process is pivotal in order for the reaction to progress, and it is also important to note that in our mechanistic view the presence of **1**-NTf_2 is needed for substrate activation (as experimentally corroborated). The activation barrier represented by $\mathbf{TS}_{NTf\text{-}lut}$ is 23.8 kcal/mol, which is similar to the estimated barrier for the first H^- transfer (24.5 kcal/mol). This implies that **1**-NTf_2 Lewis acid is still available in the early phase of the reaction to activate the ester. The notably faster H_2 activation would otherwise result in the complete conversion of **1**-NTf_2 into **1**-H, and the reaction would be stranded in the state of **1**-H + $[lut\text{-}H]^+$ + $[NTf_2]^-$, which is indeed experimentally observed (see Figure S21; **1**-H: $^{119}Sn\{^1H\}$ NMR $\delta Sn\mathit{H}$ = 5.05 ppm). Such a mechanistic scenario can give a rationale for the poor performance observed with EtOAc (exacerbated by product inhibition of the **1**-NTf_2 catalyst), as discussed below.

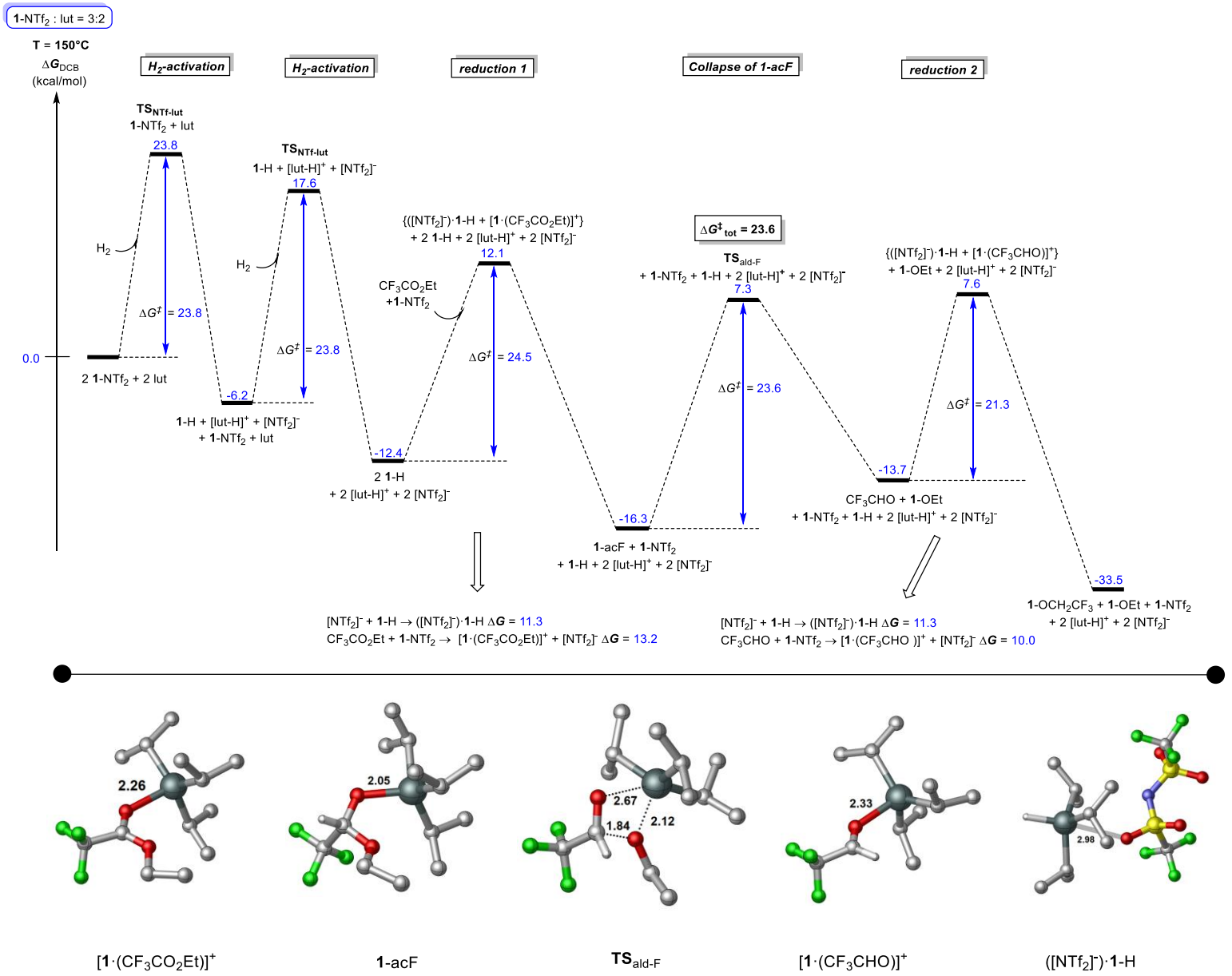

Figure S64 Computed Gibbs free energy profile (ΔG in kcal/mol) of the proposed mechanism of **1**-NTf_2-catalyzed CF_3CO_2Et reduction. The reference state is 3 **1**-NTf_2 + 2 lut + 2 H_2 + CF_3CO_2Et. Key structures involved in the mechanism are shown with selected bond distances given in Å. Non-essential H atoms are omitted for clarity.

B.) Reduction of ethyl acetate

For ethyl acetate (EtOAc) substrate, the reduction proceeded with very low conversion. To gain further insight into the reactivity difference observed between CF_3CO_2Et and EtOAc, we computed the Gibbs free energy profile for the reduction of EtOAc (Figures S64). Although the mechanism of the reduction shares common features with that of previously investigated CF_3CO_2Et substrate, the reduction of EtOAc shows a very distinct energy profile in comparison with that of CF_3CO_2Et. The computed free energy profile indicates that the explored catalytic cycle is overall thermodynamically feasible (2 **1**-NTf_2 + 2 lut + 2 H_2 + EtOAc → 2 **1**-OEt + 2 $[lut\text{-}H]^+$ + 2 $[NTf_2]^-$ ΔG = -21.4 kcal/mol), but the free energy barriers represented by the analogous transition states are less comparable as seen in the case of CF_3CO_2Et.

The H_2 cleavage process via the same $\mathbf{TS}_{NTf\text{-}lut}$ leads to the necessary **1**-H reductant. As ascertained for the reduction of CF_3CO_2Et, attempts to locate a transition state for H^- transfer to EtOAc were unsuccessful and, hence, the relative barrier height was estimated by using the aforementioned protocol. The acetal intermediate **1**-ac is calculated to be formed through a relatively small barrier of 12.2 kcal/mol, based on the sum of the free energy changes of the required processes to form the activated ion pair $([NTf_2]^-)\cdot$**1**-H + $[\mathbf{1}\cdot(EtOAc)]^+$. The free energy data for the activation of the EtOAc by **1**-NTf_2 points to an energetically more favorable process as compared to that for CF_3CO_2Et. The free energy change associated with EtOAc + **1**-NTf_2 → $[\mathbf{1}\cdot(EtOAc)]^+$ + $[NTf_2]^-$ reaction is only 0.9 kcal/mol. This is in accord with chemical intuition that the electron density around the carbonyl group of CF_3CO_2Et is significantly reduced due to the strongly electron-withdrawing CF_3-group. The formation of acetal **1**-ac is, however, found to be disfavored energetically as this intermediate is 5.9 kcal/mol less stable than the preceding EtOAc + **1**-H reactant state.

The subsequent collapse of the acetal intermediate is presented by transition state $\mathbf{TS}_{ald}$ with a free energy barrier of 27.3 kcal/mol, which is ~ 4 kcal/mol larger than the corresponding $\mathbf{TS}_{ald\text{-}F}$ (with respect to the respective most stable transient state), and it represents the highest-energy transition state on this reaction pathway. It is important to recognize that the destabilization of $\mathbf{TS}_{ald}$ arises from the appreciable endergonicity of the acetal formation. The reaction barrier for the collapse of **1**-ac is 21.4 kcal/mol with respect to the preceding reactant state, but the overall barrier is 27.3 kcal/mol as the EtOAc + **1**-H reactant state is more stable. Upon acetal collapse MeCHO and **1**-OEt are formed, which is found to be a nearly thermoneutral process. Next, MeCHO reduction is predicted to be relatively facile, via the active pair $([NTf_2]^-)\cdot$**1**-H + $[\mathbf{1}\cdot(MeCHO)]^+$, with an estimated barrier of 12.6 kcal/mol. At this stage of the reaction, two equivalents of **1**-OEt are produced and **1**-NTf_2 are expected to be liberated. However, on this reaction path, the least favored transition state, $\mathbf{TS}_{ald}$ corresponding to the collapse of acetal **1**-ac, shows a barrier of 27.3 kcal/mol. This barrier height is now lower than that for H_2 activation, and as a result of the decreased rate of the aldehyde formation (i.e. collapse of **1**-ac), **1**-NTf_2 could be fully consumed prior to the H^- transfer step, and thus the activation of the EtOAc by **1**-NTf_2 cannot be achieved.

Summary of reduction process

Our mechanistic analysis shows that the variation of ester acyl substituents could dramatically alter the reactivity and the overall thermodynamic profile of the reduction. We found a pathway accounting for the origin of the poor activity of EtOAc substrate, and trends compare very well with the experimental observations. Computational findings led to a proposal wherein the collapse of acetal has a decisive role in the entire catalytic cycle. The key element of the mechanistic view emerging from our DFT study is that the reaction barriers involved in the reduction of CF_3CO_2Et are comparable, encompassing a sufficiently low barrier for the collapse of acetal to be competent, which prevents **1**-NTf_2 Lewis acid from complete consumption in the early phase of the reaction, hence substrate activation can take place. In contrast, EtOAc displays a relatively high barrier for the collapse of the corresponding acetal, thus leading to the termination of the catalytic cycle due to the absence of **1**-NTf_2 Lewis acid needed for activation as it is transformed into **1**-H.

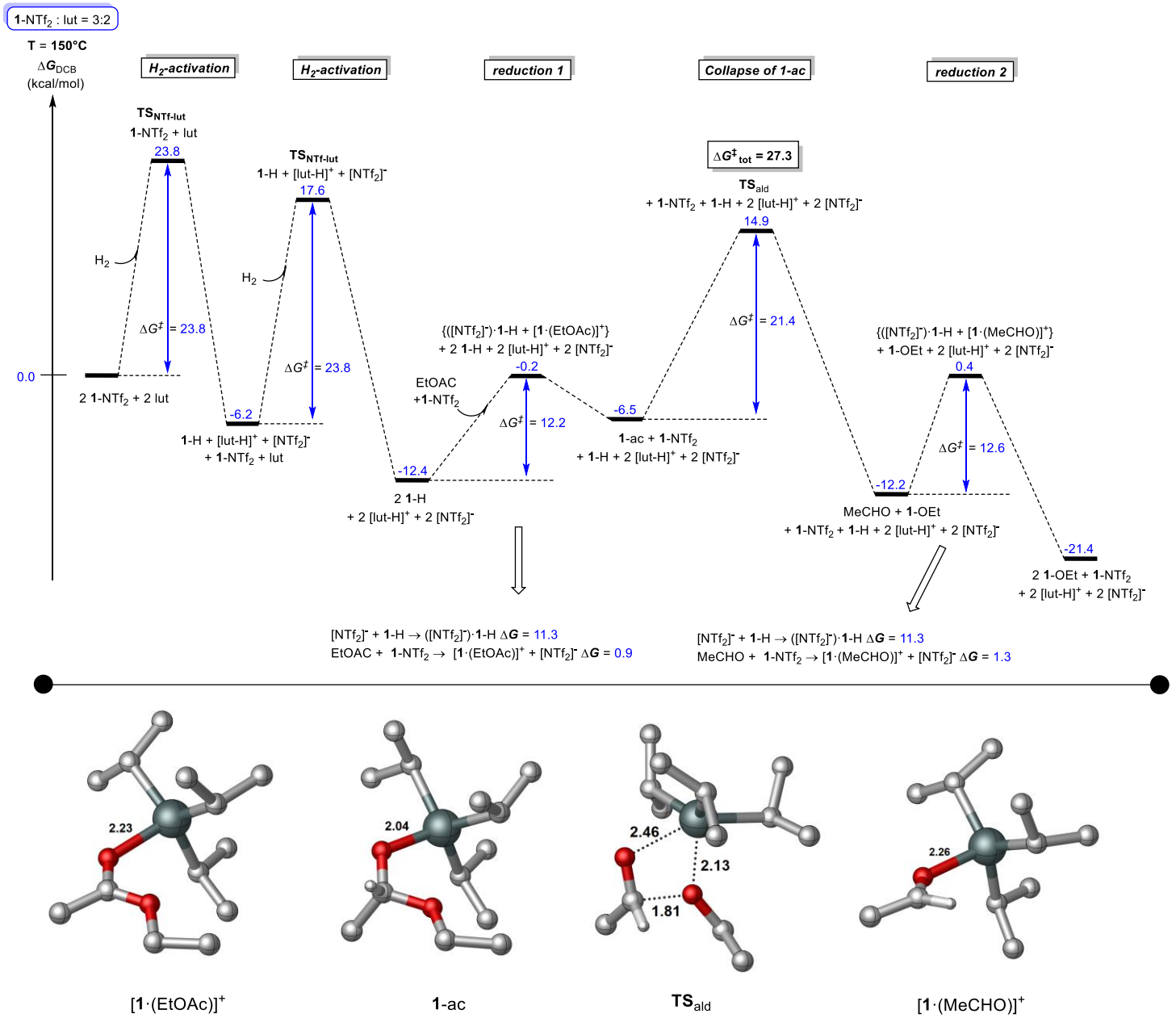

Figure S65 Computed Gibbs free energy profile (ΔG in kcal/mol) of the proposed mechanism of **1**-NTf_2-catalyzed EtOAc reduction. The reference state is 3 **1**-NTf_2 + 2 lut + 2 H_2 + EtOAc. Key structures involved in the mechanism are shown with selected bond distances given in Å. Non-essential H atoms are omitted for clarity.

12.6 Computed energy components of the reported structures.

Table S7 Summary of energy data (given in Hartree) computed for optimized structures at the ωB97X-D/Def2SVP level of theory. Note that *G* contains concentration correction. For the definition of various energy components, see Computational details section. The G_0 and *G* values marked by asterisks were obtained from calculations at 298.15 K.

Structure	E_0'	G_0	E_0	G_{sol}	*G*
1-NTf_2	-2397.4572	-2395.2099 -2395.1632*	-2395.4345	-2395.4512	-2397.2444 -2397.1994*
$[NTf_2]^-$	-1827.5270	-1825.8916 -1825.8662*	-1825.8791	-1825.9389	-1827.5945 -1827.5708*
1-OTf	-1531.6347	-1530.1075*	-1530.3594	-1530.3740	-1531.3943*
$[OTf]^-$	-961.6791	-960.7818*	-960.7778	-960.8489	-961.7513*
1-H	-570.6022	-569.9902 -569.9622*	-570.2059	-570.2124	-570.3620 -570.3883*
H^-	-0.5076	-0.4966*	-0.4866	-0.6355	-0.6634*
H_2	-1.1765	-1.1797 -1.1732*	-1.1718	-1.1712	-1.1791086 -1.1744*
col	-366.2540	-365.7249*	-365.8610	-365.8728	-366.1267*
$[\mathbf{1}\cdot(col)]^+$	-936.0863	-934.9027*	-935.3024	-935.3783	-935.7594*
$\mathbf{TS}_{NTf\text{-}col}$	-2764.8882	-2762.0273*	-2762.4724	-2762.5053	-2764.4731*
$[col\text{-}H]^+$	-366.6473	-366.1051*	-366.2550	-366.3397	-366.5790*
$[col\text{-}H]^+[NTf_2]^-$	-2194.3117	-2192.1049*	-2192.2889	-2192.3130	-2194.1488*
lut	-326.9322	-326.4878 -326.4692*	-326.5808	-326.5918	-326.8454 -326.8285*
$[\mathbf{1}\cdot(lut)]^+$	-896.7601	-895.6796 -895.6423*	-896.0178	-896.0951	-896.4944 -896.4589*
1-NTf_2'	-2397.4639	-2395.2159 -2395.1711*	-2395.4465	-2395.4596	-2397.2418 -2397.1986*
$\mathbf{TS}_{NTf\text{-}lut}$	-2725.5644	-2722.8281 -2722.7709*	-2723.1902	-2723.2237	-2725.2311 -2725.1756*
$\mathbf{TS'}_{NTf\text{-}lut}$	-2725.5602	-2722.8223 -2722.7668*	-2723.1904	-2723.2228	-2725.2197 -2725.1660*
$\mathbf{TS}_{lut\text{-}lut}$	-1224.8729	-1223.3051 -1223.2574*	-1223.7813	-1223.8540	-1224.4646 -1224.4186*
$[lut\text{-}H]^+$	-327.3192	-326.8629 -326.8437*	-326.9685	-327.0559	-327.2962 -327.2787*
$[lut\text{-}H]^{\cdot\cdot}[NTf_2]^-$	-2154.9871	-2152.8827 -2152.8460*	-2153.0062	-2153.0297	-2154.8824 -2154.8475*
$[lut\text{-}H]^{\cdot\cdot}[NTf_2]^-$ I	-2154.9836	-2152.8792	-2153.0032	-2153.0279	-2154.8795
$[lut\text{-}H]^{\cdot\cdot}[NTf_2]^-$ II	-2154.9842	-2152.8763	-2153.0016	-2153.0267	-2154.8792
$[lut\text{-}H]^{\cdot\cdot}[NTf_2]^-$ III	-2154.9799	-2152.8740	-2152.9971	-2153.0233	-2154.8783
EtOH	-155.0591	-154.8343 -154.8209*	-154.8763	-154.8816	-155.0177 -155.0060*
(EtOH)·**1**-NTf_2	-2552.5370	-2550.0394 -2549.9888*	-2550.3408	-2550.3616	-2552.2516 -2552.2028*
$[\mathbf{1}\cdot(EtOH)]^+$	-724.8691	-724.0257 -723.9899*	-724.2985	-724.3773	-724.6703 -724.6363*
1-OEt	-724.4885	-723.6505 -723.6163*	-723.9146	-723.9255	-724.2306 -724.1982*

CF_3CH_2OH	-452.8439	-452.2858 -452.2695*	-452.2979	-452.3048	-452.8340 -452.8194*
(CF_3CH_2OH)**1**-NTf_2	-2850.3180	-2847.4903 -2847.4362*	-2847.7599	-2847.7806	-2850.0644 -2850.0121*
[**1**·(CF_3CH_2OH)]$^+$	-1022.6424	-1021.4611 -1021.4245*	-1021.7113	-1021.7938	-1022.4699 -1022.4351*
1-OCH_2CF_3	-1022.2801	-1021.1042 -1021.0691*	-1021.3457	-1021.3568	-1022.0450 -1022.0116*
TS$_{red\text{-}prot}$	-3331.0798	-3327.5484	-3328.0003	-3328.0416	-3330.6644
$[CF_3COHOEt]^+$	-605.8116	-605.0457	-605.0975	-605.1805	-605.8382
CF_3CO_2Et	-605.5047	-604.7511	-604.7915	-604.7974	-605.4655
CF_3CHO	-451.6141	-451.0832	-451.0719	-451.0764	-451.6252
TS-1	-2705.8430	-2703.1292	-2703.4667	-2703.5235	-2705.5574
TS-2	-2551.9682	-2549.4773	-2549.7628	-2549.8175	-2551.7327
TS-3	-878.2831	-877.2199	-877.5381	-877.5529	-877.9749
TS-4	-724.4071	-723.5666	-723.8332	-723.8460	-724.1485
EtOAc	-307.7361	-307.3165	-307.3854	-307.3935	-307.6704
MeCHO	-153.8437	-153.6472	-153.6650	-153.6715	-153.8277
TS-5	-3003.6346	-3000.5900	-3000.8979	-3000.9520	-3003.3760
TS-6	-1176.0641	-1174.6693	-1174.9589	-1174.9749	-1175.7857
TS-7	-2849.7634	-2846.9434	-2847.1956	-2847.2484	-2849.5592
TS-8	-1022.1940	-1021.0211	-1021.2586	-1021.2738	-1021.9670
[**1**·(CF_3CO_2Et)]$^+$	-1175.3037	-1173.9253	-1174.2022	-1174.2748	-1175.0945
([NTf_2])·**1**-H	-2398.1470	-2395.8822	-2396.1144	-2396.1691	-2397.9647
1-acF	-1176.1468	-1174.7493	-1175.0431	-1175.0548	-1175.8599
TS$_{ald\text{-}F}$	-1176.1112	-1174.7111	-1175.0069	-1175.0185	-1175.8223
[**1**·(CF_3CHO)]$^+$	-1021.4021	-1020.2506	-1020.4699	-1020.5510	-1021.2593
[**1**·(EtOAc)]$^+$	-877.5538	-876.5085	-876.8135	-876.8886	-877.3190
1-ac	-878.3599	-877.2995	-877.6166	-877.6279	-878.0493
TS$_{ald}$	-878.3286	-877.2651	-877.5851	-877.5965	-878.0152
[**1**·(MeCHO)]$^+$	-233.6835	-233.3299	-233.4203	-233.4254	-233.5935
[**1**·(**1**-OEt)]$^+$	-1294.3345	-1292.8529	-1293.3713	-1293.4459	-1293.8859
[**1**·(**1**-OCH_2CF_3)]$^+$	-1592.1104	-1590.2988	-1590.7886	-1590.8641	-1591.6913

12.7 Cartesian coordinates of the reported structures

Cartesian coordinates of the optimized geometries are given below in standard XYZ format (units are in Å). The first line indicates total number of atoms, while the second line is the molecule name (as defined above in Table S7).

46
1-NTf_2
Sn 0.259336 3.003328 3.812966
C 1.975279 2.723177 2.526465
C 2.352651 1.250174 2.370173
C 3.149338 3.582693 3.003382
H 1.629813 3.104907 1.550961
H 3.162364 1.137070 1.629539
H 1.504774 0.638056 2.029921
H 2.717461 0.820916 3.316682

H	2.889068	4.651197	3.075221
H	3.997988	3.501983	2.303323
H	3.518409	3.260255	3.991002
C	0.323591	2.146385	5.799533
C	1.251065	3.009583	6.660053
C	0.711926	0.670751	5.811042
H	-0.708804	2.236948	6.165447
H	2.297283	2.970835	6.313005
H	1.246430	2.643443	7.700227
H	0.942093	4.067073	6.689879
H	0.671379	0.284036	6.842448
H	0.017590	0.065766	5.213303
H	1.735780	0.509362	5.437351
C	-0.692463	4.932280	3.589813
C	-2.163264	4.870737	4.004003
C	-0.511817	5.447131	2.160746
H	-0.153757	5.600196	4.285092
H	-2.292848	4.543601	5.045203
H	-2.630367	5.865102	3.908497
H	-2.738593	4.184343	3.363121
H	-0.976741	6.440802	2.047765
H	0.548209	5.546637	1.879111
H	-0.993816	4.777960	1.430107
O	-1.074672	1.933441	2.479092
S	-2.353114	1.214906	2.860062
O	-3.543418	1.669914	2.184853
N	-2.291299	1.139030	4.417958
C	-1.969243	-0.485026	2.199942
S	-3.450799	0.587146	5.421012
F	-1.839350	-0.412970	0.889931
F	-2.935809	-1.316663	2.510606
F	-0.831786	-0.910670	2.729928
O	-4.476722	-0.171945	4.738727
C	-4.253292	2.182045	5.940493
O	-2.795218	0.092048	6.609393
F	-4.693735	2.845171	4.885817
F	-3.377980	2.941791	6.591406
F	-5.264321	1.910755	6.742901

15

$[NTf_2]^-$

S	0.149314	0.136307	0.043113
S	0.149314	-0.508677	-2.717644
O	-1.222013	-0.331789	0.170907
O	-1.222013	-0.040582	-2.845438
F	-0.687143	2.390418	-1.080898
F	-0.687143	-2.762789	-1.593632
N	0.884164	-0.186185	-1.337265
F	1.190414	2.571039	-0.045899
F	1.190414	-2.943409	-2.628632
F	-0.643115	2.419560	1.072959
F	-0.643115	-2.791931	-3.747489
C	-0.004923	1.990408	-0.016432
C	-0.004923	-2.362778	-2.658099
O	1.078781	-0.089311	1.136542

O 1.078781 -0.283060 -3.811073

39
1–OTf
Sn 1.353828 3.122096 3.188496
C 1.101054 0.994740 3.471011
C 2.433970 0.323642 3.808861
C 0.436975 0.381822 2.235862
H 0.419229 0.890797 4.333467
H 2.296683 -0.762291 3.946803
H 2.876798 0.718937 4.736238
H 3.169909 0.459341 3.000403
H -0.544430 0.833059 2.021094
H 0.277880 -0.700307 2.379184
H 1.064150 0.510026 1.340082
C 2.715931 4.144662 4.520018
C 4.170868 3.784221 4.222673
C 2.323122 3.879244 5.975563
H 2.566408 5.212021 4.291521
H 4.373955 2.713943 4.387772
H 4.845043 4.351257 4.886741
H 4.441373 4.027935 3.186953
H 2.984391 4.436451 6.660448
H 1.289962 4.191534 6.199178
H 2.415303 2.812231 6.238670
C -0.416959 4.186409 2.540960
C -0.222609 5.701458 2.612380
C -1.648242 3.712032 3.316868
H -0.522256 3.892862 1.482808
H 0.639120 6.031868 2.014721
H -1.117414 6.220392 2.229714
H -0.065863 6.043845 3.648810
H -2.556473 4.209523 2.937194
H -1.810199 2.626106 3.229860
H -1.577013 3.955661 4.390295
C 4.340980 3.656300 -0.242741
F 4.775152 4.611480 -1.045534
F 4.192864 2.539428 -0.932235
F 5.233954 3.457260 0.715803
S 2.719826 4.176458 0.488122
O 2.443623 2.946191 1.371730
O 2.997851 5.345437 1.312154
O 1.785857 4.282230 -0.609849

8
$[OTf]^-$
C -2.359224 0.771747 3.865924
F -3.028990 1.396432 2.888231
S -0.528108 0.698179 3.520049
O -0.481290 -0.048903 2.258711
O -0.019201 -0.011622 4.698346
O -0.172946 2.118488 3.431039
F -2.628141 1.428033 5.002456
F -2.895620 -0.449964 3.985863

32
1–H
Sn -2.746392 -0.689184 0.497954
C -1.841585 0.647245 -0.965145
C -1.697547 2.064116 -0.407060
C -2.598124 0.628820 -2.293957
H -0.830517 0.236322 -1.135114
H -1.110444 2.087165 0.525131
H -1.191168 2.728183 -1.129797
H -2.680205 2.514651 -0.188593
H -2.108388 1.279408 -3.040070
H -3.632132 0.994760 -2.177478
H -2.652308 -0.382431 -2.727356
C -2.970159 -2.670667 -0.384489
C -3.900840 -3.573581 0.426914
C -1.606510 -3.322364 -0.624854
H -3.441132 -2.484627 -1.365785
H -4.898045 -3.126496 0.561430
H -3.494917 -3.781648 1.430286
H -4.040639 -4.548645 -0.072679
H -1.714225 -4.290893 -1.144334
H -1.081584 -3.524401 0.323675
H -0.944382 -2.692688 -1.240695
C -1.461204 -0.746014 2.261837
C 0.017691 -0.758908 1.867668
C -1.809133 -1.907638 3.194397
H -1.668573 0.198731 2.793761
H 0.281554 -1.666603 1.300107
H 0.291263 0.108075 1.246079
H 0.665598 -0.738910 2.761791
H -1.193091 -1.879146 4.110563
H -1.622315 -2.881999 2.713175
H -2.864874 -1.891389 3.508041
H -4.307474 -0.086745 0.934397

1
H^-
H 2.982026 0.702614 0.000000

2
H_2
H 0.000000 0.000000 0.378902
H 0.000000 0.000000 -0.378902

20
col
C 2.930862 11.444145 8.794618
C 1.979742 10.727619 9.527545
N 1.006864 11.334228 10.210440
C 0.936347 12.666789 10.196987
C 1.850559 13.451763 9.487638
C 2.874802 12.838789 8.763451
C 2.002971 9.224040 9.589397

C	-0.182093	13.285416	10.991652
H	1.762301	14.541025	9.504189
H	3.715376	10.911365	8.251281
H	2.829341	8.798961	9.003906
H	2.100185	8.892154	10.633755
H	1.053505	8.817760	9.210306
H	-0.175051	14.382052	10.930651
H	-1.151681	12.915676	10.626377
H	-0.102112	12.988021	12.047801
C	3.858708	13.645494	7.960623
H	4.828649	13.134185	7.881613
H	3.481270	13.799809	6.936771
H	4.023031	14.637439	8.405062

51

[**1**·(col)]$^{+}$

C	-6.104684	-2.065230	-1.437436
C	-4.773462	-2.307135	-2.153190
C	-4.056917	-3.566449	-1.660647
Sn	-3.439272	-0.603261	-1.967465
C	-4.065440	1.475614	-2.143918
C	-3.010193	2.352214	-2.822351
N	-2.161514	-1.102418	-3.818381
C	-2.337142	-0.646155	-0.085554
C	-1.420055	0.561518	0.108018
C	-3.418069	-0.703671	1.003010
C	-5.486792	1.726413	-2.644237
H	-4.051269	1.724778	-1.067497
H	-1.749037	-1.572808	-0.032853
H	-4.970637	-2.423279	-3.230987
H	-0.629339	0.638314	-0.654273
H	-1.983481	1.507772	0.091701
H	-0.920104	0.506104	1.088587
H	-2.949777	-0.679879	2.000420
H	-4.106537	0.157586	0.961221
H	-4.020692	-1.623196	0.952572
H	-3.282020	3.415536	-2.722414
H	-2.012323	2.228557	-2.374725
H	-2.914836	2.147999	-3.899794
H	-6.234232	1.147884	-2.081603
H	-5.741801	2.791594	-2.520526
H	-5.616452	1.491705	-3.710293
H	-3.781132	-3.497935	-0.596013
H	-4.712970	-4.445687	-1.765876
H	-3.141913	-3.778177	-2.236521
H	-5.973708	-1.900570	-0.356519
H	-6.648469	-1.200354	-1.846019
H	-6.759665	-2.944501	-1.549676
C	-2.707809	-0.898990	-5.045650
C	-2.015584	-1.238666	-6.202325
C	-0.740999	-1.801327	-6.141583
C	-0.215540	-2.015214	-4.866677
C	-0.931933	-1.673336	-3.726333
H	-2.488428	-1.055204	-7.168449
H	0.772463	-2.463130	-4.749588

C	-0.344537	-1.958360	-2.378050
H	-0.234436	-1.041726	-1.784126
H	-0.974057	-2.663255	-1.815371
H	0.648109	-2.410587	-2.482202
C	-4.066785	-0.276956	-5.171928
H	-4.014322	0.803990	-4.983040
H	-4.454716	-0.414614	-6.187756
H	-4.799444	-0.710613	-4.478517
C	0.008705	-2.193305	-7.377193
H	-0.209748	-3.245140	-7.622603
H	-0.287084	-1.582402	-8.240024
H	1.093777	-2.106252	-7.233046

68

TS$_{\text{NTf-col}}$

Sn	-19.753724	-17.085458	-7.285062
C	-20.413357	-17.067320	-9.356018
C	-21.923089	-17.249526	-9.495463
C	-19.620993	-18.036352	-10.233201
H	-20.153721	-16.040416	-9.663715
H	-22.249381	-18.244043	-9.151198
H	-22.231943	-17.151679	-10.550763
H	-22.489018	-16.505786	-8.914044
H	-19.907509	-17.924552	-11.293439
H	-18.538719	-17.857261	-10.160185
H	-19.807606	-19.088018	-9.959550
C	-18.449656	-18.590498	-6.421783
C	-17.674892	-19.399525	-7.459900
C	-19.126925	-19.465441	-5.371435
H	-17.734180	-17.942905	-5.898866
H	-16.937490	-20.052159	-6.962165
H	-17.119813	-18.745456	-8.147515
H	-18.331167	-20.048988	-8.063258
H	-19.834123	-20.182045	-5.818050
H	-19.676476	-18.870227	-4.625460
H	-18.372400	-20.055467	-4.824209
C	-20.292220	-15.377373	-6.071548
C	-20.152004	-15.702408	-4.586233
C	-21.682402	-14.858712	-6.433261
H	-19.538432	-14.619458	-6.330543
H	-20.411234	-14.823372	-3.972335
H	-19.120744	-15.977931	-4.326343
H	-20.826841	-16.521185	-4.281285
H	-21.937022	-13.975372	-5.822784
H	-22.463403	-15.616392	-6.248869
H	-21.753727	-14.556567	-7.490131
C	-22.311588	-21.075028	-6.909116
C	-22.860348	-22.280994	-6.481038
C	-23.597841	-22.334678	-5.295166
C	-23.755200	-21.147673	-4.571141
C	-23.182526	-19.966927	-5.031748
N	-22.491073	-19.965667	-6.180787
H	-22.707389	-23.181191	-7.079578
H	-24.321880	-21.139857	-3.637978
C	-21.527567	-20.947783	-8.181546

H -21.114998 -21.916092 -8.490665
H -20.702054 -20.232296 -8.065093
H -22.173477 -20.576706 -8.992305
C -23.280234 -18.665666 -4.291775
H -22.282505 -18.342473 -3.958035
H -23.674861 -17.873032 -4.943334
H -23.928670 -18.758987 -3.412559
H -21.869320 -18.832210 -6.512448
H -21.440649 -17.976603 -6.694498
S -16.028983 -15.193428 -4.725571
S -16.623204 -15.557885 -7.481723
O -14.740059 -14.657415 -5.111883
O -15.336453 -16.118768 -7.826704
F -14.771758 -16.914509 -3.209565
F -16.306308 -13.804521 -9.391166
N -17.038865 -15.452754 -5.965116
F -15.250949 -17.681647 -5.166852
F -15.753766 -13.080118 -7.436993
F -16.793643 -17.493924 -3.676449
F -17.832603 -13.279699 -7.962895
C -15.686956 -16.935670 -4.162224
C -16.623497 -13.806305 -8.107759
O -16.790849 -14.608600 -3.643353
O -17.805122 -16.119792 -8.195575
C -24.172330 -23.627816 -4.793228
H -23.471682 -24.097062 -4.084253
H -25.120088 -23.465358 -4.262003
H -24.343920 -24.338810 -5.612331

21
[col–H]$^{+}$
C 2.871773 12.834824 8.770305
C 2.937368 11.432990 8.793582
C 2.012799 10.691722 9.507225
N 1.049010 11.367414 10.179668
C 0.923039 12.716890 10.206367
C 1.845550 13.461894 9.493946
C 2.001619 9.200129 9.591758
C -0.200543 13.292945 11.005021
H 1.763287 14.549562 9.505674
H 3.722982 10.907906 8.248591
H 2.825421 8.774646 9.008169
H 2.111601 8.867656 10.635487
H 1.056413 8.794287 9.199520
H -0.195104 14.386850 10.944961
H -1.170759 12.932438 10.629963
H -0.113396 13.006027 12.064313
H 0.370237 10.820115 10.707098
C 3.850944 13.636727 7.973743
H 4.818123 13.124493 7.887787
H 3.456674 13.777102 6.953515
H 4.006844 14.632528 8.408797

36

[col-H]$^+$[NTf$_2$]$^-$

S	1.003271	1.541767	-1.903504
S	-1.207486	1.276521	-3.737779
O	0.544029	0.381113	-1.176748
O	-2.099328	1.021660	-2.630557
F	-0.855039	3.072162	-0.823630
F	-0.222288	-1.169737	-3.637289
N	0.269754	1.797723	-3.325136
F	0.889251	4.135694	-1.505073
F	-0.051392	-0.218468	-5.561802
F	0.983406	2.953917	0.295844
F	-1.965223	-0.946081	-4.885829
C	0.459230	3.019778	-0.913722
C	-0.837650	-0.381311	-4.496299
O	2.421743	1.778189	-2.127226
O	-1.625851	2.088724	-4.870617
C	3.426938	3.380573	-6.677015
C	2.719292	2.655482	-5.727960
N	1.629240	3.221223	-5.175081
C	1.174543	4.451270	-5.482325
C	1.866775	5.190085	-6.432073
C	3.007840	4.663244	-7.047496
C	3.082644	1.280462	-5.273959
C	-0.045251	4.929143	-4.766446
H	1.508735	6.188355	-6.687938
H	4.314558	2.934590	-7.128005
H	4.018372	0.951365	-5.740084
H	3.180990	1.263601	-4.177259
H	2.280999	0.575402	-5.538067
H	-0.360370	5.908143	-5.145158
H	-0.859233	4.197506	-4.888194
H	0.160297	5.008488	-3.688974
H	1.089749	2.656531	-4.440248
C	3.744361	5.440957	-8.098179
H	4.808748	5.172208	-8.125731
H	3.318105	5.218175	-9.089489
H	3.655092	6.523121	-7.933996

17
lut

C	2.937671	11.440658	8.790361
C	1.985441	10.726069	9.526851
N	1.015684	11.339533	10.208862
C	0.938332	12.672128	10.198668
C	1.850795	13.460526	9.487578
C	2.864458	12.829540	8.774164
C	2.000673	9.222695	9.590732
C	-0.184112	13.283568	10.992828
H	1.763274	14.548663	9.496625
H	3.719801	10.912587	8.241560
H	2.824489	8.793191	9.004912
H	2.097619	8.891605	10.635334
H	1.048985	8.820492	9.212933
H	-0.182085	14.380268	10.933000
H	-1.151551	12.909728	10.626099

H -0.103567 12.985568 12.048731
H 3.592475 13.416369 8.208983

48
[**1**·(lut)]·
C -6.102914 -2.069165 -1.444076
C -4.769179 -2.309911 -2.155799
C -4.052252 -3.567921 -1.660657
Sn -3.441294 -0.601889 -1.962938
C -4.064526 1.477423 -2.143520
C -3.008419 2.352215 -2.822908
N -2.158101 -1.103049 -3.825937
C -2.337395 -0.644973 -0.082227
C -1.418922 0.561557 0.111294
C -3.420156 -0.700452 1.004802
C -5.486085 1.729082 -2.642703
H -4.049099 1.726869 -1.067147
H -1.751060 -1.572686 -0.028782
H -4.962770 -2.426147 -3.234192
H -0.626759 0.636455 -0.649673
H -1.980769 1.508687 0.093419
H -0.920588 0.506024 1.092629
H -2.952781 -0.677361 2.002624
H -4.106893 0.162160 0.962441
H -4.024245 -1.619015 0.954109
H -3.278790 3.415811 -2.722521
H -2.010347 2.227374 -2.376060
H -2.914500 2.148394 -3.900544
H -6.233616 1.151239 -2.079496
H -5.739851 2.794450 -2.518412
H -5.616952 1.495030 -3.708719
H -3.779236 -3.498688 -0.595395
H -4.707374 -4.447636 -1.767130
H -3.135874 -3.779528 -2.234337
H -5.975559 -1.904775 -0.362685
H -6.646543 -1.204981 -1.854341
H -6.756302 -2.949258 -1.558662
C -2.711209 -0.897037 -5.049347
C -2.020826 -1.237491 -6.210584
C -0.753875 -1.795502 -6.124788
C -0.209824 -2.018692 -4.867974
C -0.929681 -1.673825 -3.726651
H -2.489824 -1.060319 -7.178667
H 0.776424 -2.469773 -4.757745
C -0.347158 -1.957160 -2.376380
H -0.239073 -1.039692 -1.783352
H -0.978155 -2.661837 -1.815112
H 0.645967 -2.409117 -2.477272
C -4.070553 -0.275690 -5.169536
H -4.016804 0.805575 -4.982618
H -4.462475 -0.414579 -6.183705
H -4.800253 -0.708316 -4.472515
H -0.200304 -2.062584 -7.026903

46

1-NTf_2

Sn	1.102665	1.312307	5.889865
C	0.015848	1.293982	7.757721
C	0.301798	0.018637	8.553374
C	-1.475071	1.516846	7.505710
H	0.422193	2.151174	8.316130
H	-0.226331	0.040921	9.521703
H	1.374705	-0.102492	8.770107
H	-0.039829	-0.886418	8.024178
H	-2.023892	1.591828	8.459608
H	-1.922639	0.684251	6.938673
H	-1.666938	2.442077	6.942008
C	3.205881	0.792125	5.915356
C	4.019178	1.583794	4.892680
C	3.366614	-0.720136	5.738756
H	3.537503	1.078313	6.924931
H	3.949125	2.668331	5.057121
H	3.698057	1.377104	3.859664
H	5.085813	1.311745	4.964702
H	4.428365	-1.005171	5.830571
H	2.810257	-1.297660	6.494663
H	3.029710	-1.056720	4.744778
C	-0.009254	0.332748	4.304707
C	-0.301174	-1.102429	4.758014
C	0.691487	0.379318	2.949170
H	-0.955731	0.887385	4.233287
H	-0.859458	-1.139844	5.706841
H	-0.915248	-1.621268	4.002418
H	0.617711	-1.697832	4.884935
H	1.686805	-0.093406	2.978565
H	0.097606	-0.162120	2.193219
H	0.814388	1.409277	2.590043
O	2.782066	5.421680	5.861777
S	2.009656	4.418867	6.554251
O	2.631450	3.447824	7.437332
N	1.082315	3.514180	5.515401
C	0.777188	5.338902	7.650775
S	0.191908	4.259073	4.338531
F	0.648278	6.580415	7.259483
F	1.263565	5.309478	8.877796
F	-0.395318	4.728909	7.637738
O	-0.195125	5.586686	4.756849
C	1.399207	4.495856	2.923757
O	-0.769064	3.289905	3.858509
F	0.699082	4.548147	1.806298
F	2.233049	3.465616	2.864063
F	2.080899	5.604394	3.073142

65

TS$_{NTf\text{-}lut}$

Sn	-12.922697	-31.997700	-2.643296
C	-13.680587	-31.939979	-4.679959
C	-15.182652	-32.203306	-4.757817
C	-12.878507	-32.829799	-5.629071

H -13.493185 -30.889526 -4.958899
H -15.436301 -33.226964 -4.438290
H -15.546634 -32.085093 -5.793282
H -15.761151 -31.515409 -4.122591
H -13.223155 -32.699755 -6.669762
H -11.806160 -32.588962 -5.601000
H -12.989967 -33.899401 -5.385145
C -11.462099 -33.431143 -1.918341
C -10.691699 -34.138830 -3.030880
C -12.010992 -34.394683 -0.870679
H -10.766628 -32.752531 -1.408243
H -9.881967 -34.754151 -2.602957
H -10.225609 -33.418234 -3.717996
H -11.332697 -34.810619 -3.626305
H -12.689585 -35.144552 -1.307582
H -12.556690 -33.871391 -0.069822
H -11.185351 -34.948074 -0.392269
C -13.513828 -30.379099 -1.335176
C -13.276632 -30.749137 0.127055
C -14.952472 -29.945460 -1.608059
H -12.827670 -29.561019 -1.598703
H -13.564196 -29.914495 0.788487
H -12.216943 -30.960261 0.325421
H -13.877196 -31.624530 0.429770
H -15.236269 -29.107576 -0.948356
H -15.670230 -30.762863 -1.420980
H -15.096705 -29.606631 -2.646156
C -15.192396 -36.162927 -2.286062
C -15.662503 -37.412529 -1.884576
C -16.309388 -37.528268 -0.657926
C -16.470209 -36.405431 0.149090
C -15.974933 -35.179412 -0.291340
N -15.368555 -35.103224 -1.484789
H -15.517009 -38.279632 -2.529960
H -16.968011 -36.473125 1.117120
C -14.500004 -35.933283 -3.595997
H -14.108985 -36.872935 -4.004795
H -13.669173 -35.223064 -3.483146
H -15.201313 -35.506027 -4.329187
C -16.059156 -33.919898 0.517883
H -15.054029 -33.614931 0.847373
H -16.467505 -33.092991 -0.079861
H -16.686599 -34.063738 1.405421
H -14.853731 -33.940625 -1.817874
H -14.497077 -33.039577 -2.018622
S -9.211875 -29.944959 -0.185268
S -9.919056 -30.232919 -2.924206
O -7.984998 -29.300755 -0.606874
O -8.613475 -30.679786 -3.354903
F -7.762015 -31.631495 1.191099
F -9.824181 -28.379328 -4.761375
N -10.262556 -30.224155 -1.385582
F -8.280636 -32.348821 -0.775062
F -9.234178 -27.699769 -2.802107
F -9.757690 -32.338094 0.791632

F -11.315172 -28.034234 -3.243830
C -8.718921 -31.679659 0.281380
C -10.078628 -28.460737 -3.466592
O -9.957179 -29.464162 0.958170
O -11.091415 -30.850589 -3.605816
H -16.685221 -38.498528 -0.326688

65
TS'$_{\text{NTf-lut}}$
Sn -6.748466 -12.933083 -6.141809
C -8.162840 -12.343672 -7.704944
C -9.591079 -12.294503 -7.161338
C -8.068131 -13.206421 -8.962273
H -7.856195 -11.325148 -7.976363
H -9.701523 -11.595103 -6.320695
H -10.287392 -11.969022 -7.953799
H -9.935839 -13.280778 -6.808148
H -8.792922 -12.853889 -9.716825
H -8.300273 -14.263956 -8.762487
H -7.071674 -13.148805 -9.416560
C -5.419780 -14.637430 -6.417998
C -5.286574 -15.035569 -7.886048
C -5.774141 -15.814213 -5.513051
H -4.458881 -14.231783 -6.076917
H -4.501932 -15.801986 -8.008808
H -6.220828 -15.458079 -8.291331
H -5.010152 -14.177465 -8.515913
H -5.010985 -16.607459 -5.594871
H -5.828690 -15.517808 -4.453703
H -6.741006 -16.272749 -5.778167
C -6.737028 -11.732206 -4.324711
C -6.319109 -12.575559 -3.122988
C -8.077411 -11.037133 -4.099018
H -5.966761 -10.967616 -4.502411
H -6.306855 -11.962385 -2.204940
H -5.311665 -12.992060 -3.257687
H -7.024536 -13.403759 -2.949408
H -8.333112 -10.351137 -4.920443
H -8.903385 -11.761639 -3.993769
H -8.049849 -10.440265 -3.170866
C -9.760078 -16.767728 -5.878520
C -10.490888 -17.920015 -5.595345
C -10.821109 -18.204953 -4.273910
C -10.416185 -17.343808 -3.258579
C -9.678330 -16.208033 -3.586820
N -9.383709 -15.962973 -4.872529
H -10.795254 -18.580000 -6.408351
H -10.663133 -17.545290 -2.215613
C -9.379136 -16.361668 -7.268063
H -9.936115 -15.461692 -7.568838
H -8.309514 -16.114030 -7.324623
H -9.596478 -17.161206 -7.985965
C -9.167555 -15.241359 -2.562554
H -8.077507 -15.349546 -2.454275
H -9.360955 -14.203352 -2.866218

H -9.631977 -15.423777 -1.586249
H -8.693613 -14.926060 -5.133415
H -8.145047 -14.069929 -5.303551
S -3.452156 -11.468021 -6.001191
S -4.795029 -10.611459 -8.322010
O -2.987071 -10.127065 -5.726020
O -3.472411 -10.210104 -8.756763
F -1.422989 -13.108695 -6.139050
F -4.848887 -8.331888 -6.976947
N -4.764660 -11.536335 -6.981945
F -1.231388 -11.426306 -7.459876
F -6.746084 -9.341719 -7.079147
F -2.565652 -13.045731 -7.959557
F -5.965139 -8.332113 -8.817713
C -2.069909 -12.310539 -6.975019
C -5.633636 -9.044101 -7.753869
O -3.713189 -12.385166 -4.901790
O -5.734973 -11.194842 -9.259886
H -11.396068 -19.101823 -4.034357

67
TS$_{lut\text{-}lut}$
C 0.954343 -5.076581 0.262910
N 2.115098 -5.017423 -0.424013
C 2.076693 -5.022563 -1.774357
C 0.877601 -5.184832 -2.469217
C -0.310842 -5.325520 -1.766973
C -0.270563 -5.249730 -0.383024
Sn 4.275081 -5.307317 0.949495
C 5.826934 -5.731733 -0.532921
C 6.725225 -6.875586 -0.057718
C 3.623820 -7.176935 1.877450
C 3.302784 -7.072666 3.367357
C 2.576062 -7.961797 1.093016
C 4.214757 -3.223606 1.593556
C 3.901761 -3.066729 3.080805
C 3.376228 -2.303270 0.712654
C 6.638933 -4.470359 -0.828810
H 5.278454 -2.967615 1.443849
H 5.327690 -6.063621 -1.451521
H 4.583664 -7.714402 1.787851
H 6.024178 -3.639294 -1.208765
H 7.155500 -4.106728 0.074564
H 7.416881 -4.673228 -1.583055
H 7.488135 -7.098741 -0.821757
H 7.262790 -6.617322 0.868086
H 6.164469 -7.806428 0.118799
H 3.641966 -2.381349 -0.352406
H 2.300372 -2.514895 0.799138
H 3.526670 -1.252796 1.011955
H 4.080533 -2.026652 3.400835
H 2.849096 -3.291846 3.310366
H 4.527323 -3.718940 3.709819
H 2.332284 -6.590810 3.556675
H 3.246322 -8.079511 3.814376

H	4.068049	-6.505931	3.920259
H	2.485804	-8.983170	1.498483
H	1.578094	-7.503958	1.158173
H	2.829541	-8.053673	0.025577
H	0.888045	-5.190694	-3.559923
H	-1.184204	-5.307951	0.210306
H	5.732326	-5.400651	2.384269
H	6.514382	-5.573347	2.826281
N	7.729203	-5.791478	3.545306
C	8.031899	-7.018036	3.993531
C	9.199275	-7.222035	4.728705
C	10.033151	-6.137703	4.985502
C	9.690127	-4.875853	4.508103
C	8.511619	-4.728053	3.778167
H	9.445497	-8.219698	5.094433
H	10.325771	-4.010204	4.698719
C	3.341536	-4.824342	-2.556168
H	3.119076	-4.343545	-3.517282
H	4.054494	-4.190205	-2.016317
H	3.826386	-5.786352	-2.779250
C	0.944951	-4.873965	1.750804
H	1.927017	-5.012900	2.209920
H	0.618109	-3.846788	1.976964
H	0.237267	-5.557805	2.238627
C	7.075261	-8.127336	3.663978
H	7.372927	-9.064512	4.149205
H	6.056604	-7.872412	3.990213
H	7.043985	-8.295784	2.576916
C	8.059887	-3.408970	3.219767
H	8.730894	-2.598042	3.527016
H	8.042470	-3.443393	2.119851
H	7.041746	-3.169358	3.560222
H	10.951099	-6.275754	5.560412
H	-1.257444	-5.465203	-2.292434

18
[lut-H]·

C	2.941374	11.429318	8.788074
C	2.014322	10.687918	9.506343
N	1.055082	11.371784	10.176836
C	0.920807	12.720276	10.207906
C	1.843712	13.469285	9.492191
C	2.853495	12.820691	8.782720
C	1.997721	9.197123	9.593606
C	-0.204605	13.290622	11.006975
H	1.765835	14.556570	9.494981
H	3.726888	10.912037	8.237039
H	2.819704	8.769112	9.009298
H	2.108116	8.865934	10.637745
H	1.050705	8.793598	9.203203
H	-0.202208	14.384553	10.947147
H	-1.173653	12.927012	10.631739
H	-0.116239	13.003204	12.066075
H	3.581530	13.407228	8.218317
H	0.374910	10.823959	10.703764

33
[lut-H]$^{+\cdot}$[NTf_2]$^-$
S 1.034135 1.567702 -1.902227
S -1.199902 1.293583 -3.708620
O 0.582490 0.411731 -1.163753
O -2.079081 1.056531 -2.587687
F -0.810116 3.106270 -0.809678
F -0.224086 -1.155727 -3.592431
N 0.284760 1.813896 -3.318366
F 0.926424 4.163835 -1.519657
F -0.073649 -0.226994 -5.529617
F 1.041996 2.993568 0.287561
F -1.981925 -0.938006 -4.820941
C 0.502671 3.052345 -0.915356
C -0.846945 -0.374690 -4.452449
O 2.449736 1.802424 -2.145229
O -1.626265 2.095522 -4.845767
C 3.405585 3.350976 -6.712092
C 2.703092 2.636013 -5.747383
N 1.623902 3.216792 -5.187962
C 1.165308 4.446189 -5.493161
C 1.848535 5.179347 -6.458081
C 2.972243 4.625905 -7.065674
C 3.060225 1.261728 -5.287756
C -0.045068 4.928560 -4.765334
H 1.494966 6.175724 -6.722973
H 4.283268 2.902413 -7.177251
H 3.986456 0.921611 -5.764718
H 3.174381 1.252833 -4.192451
H 2.249103 0.561434 -5.535004
H -0.359127 5.908871 -5.141403
H -0.863398 4.200446 -4.879459
H 0.171053 5.007117 -3.689912
H 3.516111 5.194344 -7.823040
H 1.088311 2.656527 -4.441203

33
[lut-H]$^{+\cdot}$[NTf_2]$^-$ I
S -0.748569 2.406362 -2.516976
S -0.769498 0.458962 -4.645944
O -0.795217 1.407996 -1.469804
O -2.201488 0.256735 -4.583376
F -3.356676 1.955440 -2.565887
F -0.812662 -1.242442 -2.617826
N -0.269500 1.831117 -3.950668
F -2.699589 3.454093 -3.971001
F 1.166651 -0.586085 -3.168762
F -2.776692 3.904352 -1.866127
F 0.104152 -1.983712 -4.416212
C -2.524888 2.953722 -2.752647
C -0.032401 -0.930015 -3.626089
O -0.010357 3.647915 -2.333977
O -0.059630 0.389971 -5.915285

C	3.689122	3.470144	-6.266881
C	2.745872	2.727916	-5.563902
N	1.549668	3.293269	-5.314278
C	1.191159	4.533783	-5.695570
C	2.116141	5.297218	-6.400129
C	3.368217	4.758901	-6.684345
C	2.960679	1.336801	-5.070423
C	-0.176813	4.995026	-5.320259
H	1.847531	6.304388	-6.718539
H	4.664096	3.032264	-6.480434
H	3.972878	0.990193	-5.307310
H	2.804913	1.289324	-3.983144
H	2.218152	0.667974	-5.532297
H	-0.365469	6.006277	-5.697878
H	-0.934763	4.308587	-5.724093
H	-0.278787	4.979343	-4.224182
H	4.101537	5.349939	-7.236949
H	0.826777	2.711359	-4.770788

33

[lut-H]$^{+\cdot}$[NTf$_2$]$^-$ II

S	2.931180	1.900898	-1.810169
S	0.262895	1.311754	-2.683423
O	2.616597	1.477105	-0.463380
O	-0.368327	1.881811	-1.512176
F	1.644285	4.199012	-1.530185
F	0.856099	-0.923083	-1.455472
N	1.806463	1.586173	-2.913474
F	3.256236	4.256755	-2.954518
F	0.638830	-1.116567	-3.590071
F	3.687620	4.223423	-0.843202
F	-1.107534	-0.885621	-2.346858
C	2.874621	3.762058	-1.773535
C	0.156398	-0.533218	-2.502661
O	4.219615	1.606521	-2.409624
O	-0.368697	1.557714	-3.999509
C	3.300700	4.017914	-6.222056
C	2.490147	2.980710	-5.767647
N	1.300285	3.306074	-5.231287
C	0.853628	4.564242	-5.036551
C	1.648251	5.612818	-5.475905
C	2.874189	5.332208	-6.077722
C	2.895034	1.546052	-5.785285
C	-0.447466	4.727086	-4.319647
H	1.309395	6.638790	-5.333745
H	4.267776	3.781868	-6.665873
H	3.505069	1.358060	-4.885855
H	2.026587	0.878825	-5.723055
H	3.488044	1.320667	-6.680822
H	-0.773173	5.773281	-4.344651
H	-1.225298	4.086439	-4.756981
H	-0.332348	4.415619	-3.269909
H	3.508746	6.150583	-6.423799
H	0.692985	2.536217	-4.855231

33
[lut-H]$^{+\cdot}$[NTf_2]$^-$ III
S 0.366579 0.286134 0.628725
S 0.644760 -0.446235 -2.140127
O -1.076715 0.227096 0.708816
O 0.327627 0.863651 -2.673037
F -0.030797 2.694058 -0.365517
F -1.981326 -0.660431 -1.873657
N 1.066377 -0.436974 -0.588428
F 2.033305 2.257519 0.076613
F -0.893488 -2.459201 -1.389721
F 0.648704 2.665430 1.676848
F -1.121795 -1.850962 -3.445027
C 0.774601 2.101756 0.485275
C -0.954389 -1.411925 -2.207590
O 1.152170 -0.140342 1.808000
O 1.601665 -1.312222 -2.809849
C 4.590579 -3.127238 -0.186585
C 3.364625 -2.640833 0.263361
N 3.364701 -1.492467 0.964491
C 4.462336 -0.759783 1.248482
C 5.692857 -1.225352 0.808705
C 5.752181 -2.416849 0.086310
C 2.065568 -3.308872 -0.029345
C 4.262448 0.519001 1.994559
H 6.593005 -0.651605 1.028661
H 4.615276 -4.055634 -0.757041
H 2.186280 -4.399749 -0.023955
H 1.285265 -3.011161 0.680846
H 1.739246 -2.988073 -1.031170
H 5.226536 0.941018 2.300733
H 3.742183 1.243165 1.351372
H 3.628546 0.365489 2.878589
H 6.714922 -2.790001 -0.268791
H 2.446181 -1.087191 1.275508

9
EtOH
C -1.553611 -0.223512 0.011780
H -1.210096 0.290587 -0.908032
H -2.661492 -0.222484 -0.019024
O -1.071724 0.415820 1.167472
H -1.390250 1.321608 1.171225
C -1.051291 -1.652109 0.007428
H -1.404893 -2.184675 0.902374
H -1.407069 -2.189439 -0.883828
H 0.048349 -1.670989 0.012551

55
(EtOH)·**1**-NTf_2
Sn 1.315217 2.367738 3.276495
C 1.941132 0.361216 2.733516
C 0.726649 -0.548280 2.538075

C	2.924648	-0.207192	3.758328
H	2.470862	0.460509	1.769991
H	1.042730	-1.562730	2.240598
H	0.042973	-0.174005	1.759484
H	0.150026	-0.642994	3.471224
H	3.840735	0.398947	3.835188
H	3.229215	-1.229849	3.477328
H	2.470366	-0.262374	4.759641
C	2.816971	3.687303	4.115111
C	3.325704	3.205815	5.472414
C	2.374476	5.149877	4.180494
H	3.627397	3.584772	3.372005
H	2.550805	3.324977	6.240676
H	4.193731	3.812386	5.781342
H	3.641264	2.152252	5.466288
H	3.208562	5.776111	4.540243
H	2.066700	5.550369	3.202972
H	1.534117	5.293235	4.875071
C	-0.553646	3.044099	2.404218
C	-0.706757	4.565660	2.437596
C	-1.786246	2.338566	2.969201
H	-0.416054	2.725755	1.355402
H	0.136221	5.088182	1.960514
H	-1.625398	4.865985	1.906085
H	-0.793642	4.948411	3.464267
H	-2.662127	2.564061	2.338005
H	-1.675724	1.245188	3.008288
H	-2.032870	2.692467	3.979306
O	2.334472	2.989526	1.026544
C	2.514743	4.239210	0.367644
O	0.491597	1.420401	5.143681
S	-0.375221	1.985060	6.232462
O	-1.733081	1.494156	6.283940
N	-0.086305	3.525422	6.306956
C	0.466065	1.284560	7.737786
S	-1.181335	4.719887	6.357698
F	1.758113	1.555696	7.736142
F	0.298861	-0.025419	7.732586
F	-0.086275	1.796834	8.820324
O	-0.484157	5.952214	6.052156
C	-1.598216	4.824274	8.164822
O	-2.427144	4.397051	5.690274
F	-2.410031	5.847969	8.358090
F	-0.500051	4.996210	8.880111
F	-2.198046	3.710799	8.552317
H	2.442233	4.999577	1.157118
H	3.537883	4.293135	-0.041643
C	1.481539	4.476411	-0.714414
H	2.359758	2.274317	0.381630
H	1.639063	5.458963	-1.182313
H	1.553644	3.715791	-1.508378
H	0.463656	4.451337	-0.299646

40

[**1**·(EtOH)]$^{+}$

Sn	-0.296850	-0.020673	0.661037
C	-0.044291	-2.156418	0.875121
C	1.413256	-2.545273	1.131185
C	-0.653929	-2.881510	-0.328284
H	-0.640343	-2.406311	1.769908
H	1.499391	-3.638576	1.235097
H	1.810433	-2.096776	2.053043
H	2.075473	-2.246906	0.302470
H	-1.713455	-2.628640	-0.484829
H	-0.596079	-3.971868	-0.182658
H	-0.115561	-2.664059	-1.266468
C	0.737988	1.403338	1.912989
C	2.221049	1.079738	2.090246
C	-0.005530	1.528386	3.248638
H	0.636409	2.359883	1.371548
H	2.370962	0.144134	2.650006
H	2.715495	1.880922	2.662574
H	2.753399	0.984501	1.131737
H	0.469606	2.302896	3.871588
H	-1.060172	1.819913	3.122136
H	0.023412	0.590912	3.827050
C	-2.135279	0.654756	-0.247609
C	-2.095046	2.157613	-0.528403
C	-3.327286	0.247797	0.626371
H	-2.195051	0.106806	-1.203256
H	-1.264470	2.442119	-1.193161
H	-3.026864	2.478093	-1.021376
H	-2.002917	2.746329	0.398370
H	-4.270064	0.543910	0.139210
H	-3.378400	-0.839342	0.794660
H	-3.308489	0.743717	1.610405
O	1.077638	0.138090	-1.112239
C	1.657645	1.332766	-1.695385
H	1.039515	1.631059	-2.555477
H	1.562033	2.103794	-0.919016
C	3.098976	1.105859	-2.080128
H	3.192509	0.324677	-2.850303
H	3.514754	2.031627	-2.502074
H	3.706347	0.821821	-1.209207
H	1.210630	-0.627964	-1.686051

39

1-OEt

Sn	-0.081099	0.076245	0.456806
C	-0.123892	-2.032764	0.935613
C	1.192013	-2.480987	1.574285
C	-0.452805	-2.831128	-0.328179
H	-0.939875	-2.169183	1.666771
H	1.175476	-3.563861	1.788866
H	1.389132	-1.961707	2.525296
H	2.047398	-2.291923	0.906039
H	-1.427042	-2.546446	-0.757263
H	-0.491382	-3.912961	-0.111801
H	0.310407	-2.672983	-1.106406
C	0.705117	1.382771	2.006165

C	2.218122	1.218543	2.152961
C	-0.038290	1.169308	3.326732
H	0.496948	2.407011	1.651283
H	2.483728	0.211222	2.512066
H	2.623744	1.941414	2.882300
H	2.743446	1.370707	1.198142
H	0.337073	1.852413	4.108671
H	-1.121430	1.348966	3.230475
H	0.094108	0.142452	3.707215
C	-1.958874	0.802404	-0.366627
C	-2.007064	2.331075	-0.381288
C	-3.153268	0.197016	0.374531
H	-1.968037	0.437382	-1.407917
H	-1.172259	2.768616	-0.950977
H	-2.943792	2.694409	-0.839071
H	-1.964740	2.748419	0.638797
H	-4.106650	0.530422	-0.071401
H	-3.146185	-0.904069	0.347504
H	-3.173874	0.501169	1.434879
O	1.287603	0.100100	-1.018413
C	1.571433	1.259537	-1.742539
H	0.706628	1.571230	-2.367735
H	1.790637	2.122483	-1.074546
C	2.770513	1.019608	-2.643198
H	2.564770	0.185622	-3.330551
H	3.009083	1.915254	-3.237612
H	3.651158	0.752343	-2.040127

9
CF_3CH_2OH

C	-1.552883	-0.206848	0.022613
H	-1.195431	0.254339	-0.916727
H	-2.656415	-0.262048	-0.021714
O	-1.077030	0.427158	1.165137
H	-1.393456	1.333045	1.172556
C	-1.048037	-1.636076	0.022045
F	-1.496374	-2.263720	-1.072701
F	0.282261	-1.693528	0.008189
F	-1.475927	-2.315177	1.084574

55
(CF_3CH_2OH)-**1**-NTf_2

Sn	1.299776	2.538757	3.487376
C	2.048031	0.630014	2.769494
C	1.073197	0.011293	1.766042
C	2.398097	-0.332981	3.904806
H	2.984448	0.884745	2.240158
H	1.481494	-0.926253	1.351857
H	0.860939	0.681706	0.920020
H	0.112981	-0.239716	2.244466
H	3.139463	0.091022	4.598877
H	2.821033	-1.266264	3.495751
H	1.509582	-0.596875	4.496110
C	2.829834	3.824765	4.328933

C	3.983187	2.985732	4.884068
C	2.353599	4.882330	5.322805
H	3.177821	4.333610	3.413156
H	3.672448	2.409667	5.769180
H	4.814389	3.639093	5.198776
H	4.386218	2.274951	4.144785
H	3.176385	5.586236	5.534757
H	1.493086	5.462309	4.960747
H	2.043585	4.429707	6.273540
C	-0.478216	3.312435	2.529969
C	-0.584118	4.833648	2.651662
C	-1.758783	2.602168	2.968084
H	-0.286534	3.045796	1.477298
H	0.338817	5.353673	2.345550
H	-1.405750	5.212646	2.020715
H	-0.797454	5.151018	3.682056
H	-2.597590	2.918082	2.326014
H	-1.680273	1.507231	2.895938
H	-2.044391	2.856620	3.998025
O	2.401786	3.303552	1.131615
C	1.984041	4.097658	0.056418
O	0.374383	1.527186	5.215956
S	-0.488023	2.062265	6.329923
O	-1.754965	1.396654	6.509961
N	-0.397695	3.620415	6.271677
C	0.574426	1.603500	7.786923
S	-1.591258	4.708891	6.412043
F	1.789405	2.110829	7.644349
F	0.658545	0.288583	7.854714
F	0.035773	2.071081	8.894884
O	-1.048743	5.983454	5.988454
C	-1.802134	4.856479	8.251544
O	-2.864561	4.238062	5.907418
F	-2.666689	5.820451	8.507343
F	-0.644628	5.142830	8.823133
F	-2.258348	3.716280	8.743504
H	1.124049	4.694018	0.386701
H	2.775445	4.784316	-0.286776
C	1.560919	3.246453	-1.127646
F	1.283338	4.013554	-2.175878
F	2.551047	2.408134	-1.466563
F	0.486583	2.503474	-0.858493
H	3.156483	2.765417	0.864231

40

[**1**·(CF_3CH_2OH)]$^+$

Sn	-0.283156	0.012740	0.634460
C	0.190046	-2.095475	0.700382
C	1.683833	-2.368215	0.513865
C	-0.684913	-2.870648	-0.287930
H	-0.095135	-2.382699	1.728022
H	1.881870	-3.444505	0.638359
H	2.308446	-1.832132	1.242425
H	2.032556	-2.093132	-0.493041
H	-1.760888	-2.713295	-0.119730

H	-0.493836	-3.951180	-0.192327
H	-0.464504	-2.603766	-1.335038
C	0.707788	1.465791	1.890846
C	2.091606	1.016429	2.359145
C	-0.229030	1.808475	3.057505
H	0.803301	2.365151	1.257051
H	2.033753	0.114646	2.988574
H	2.555830	1.806213	2.971120
H	2.774594	0.799827	1.525603
H	0.227830	2.592023	3.682588
H	-1.205203	2.190871	2.721574
H	-0.407150	0.942336	3.715105
C	-2.222012	0.583623	-0.122382
C	-2.252028	2.066772	-0.493301
C	-3.307519	0.200264	0.890708
H	-2.362119	-0.023179	-1.033104
H	-1.497964	2.324976	-1.252676
H	-3.236305	2.333947	-0.909989
H	-2.088155	2.714010	0.383103
H	-4.302003	0.443339	0.483794
H	-3.310216	-0.875874	1.124777
H	-3.206356	0.754511	1.837528
O	0.854079	0.459204	-1.328903
C	1.887650	1.395601	-1.607561
H	1.654344	1.965058	-2.518778
H	1.960382	2.085535	-0.758494
C	3.210528	0.667410	-1.796573
H	0.780632	-0.180947	-2.052410
F	3.046594	-0.312149	-2.694798
F	3.623022	0.104862	-0.661304
F	4.136221	1.502243	-2.224388

39

1-OCH_2CF_3

Sn	-0.097398	0.096416	0.350886
C	0.319942	-2.026839	0.514532
C	1.711573	-2.358443	-0.026366
C	-0.773472	-2.835049	-0.187875
H	0.292096	-2.255827	1.594339
H	1.906222	-3.442441	0.045493
H	2.509298	-1.840261	0.525606
H	1.809619	-2.068512	-1.083483
H	-1.774838	-2.640485	0.227702
H	-0.582109	-3.917666	-0.090491
H	-0.810748	-2.609780	-1.266327
C	0.872667	1.361875	1.836345
C	1.788764	0.534031	2.739530
C	-0.134426	2.183617	2.643226
H	1.500073	2.051843	1.247984
H	1.224176	-0.214951	3.319507
H	2.305932	1.182235	3.467879
H	2.561961	0.002292	2.166678
H	0.387247	2.856902	3.345170
H	-0.776577	2.808872	2.004271
H	-0.794552	1.541081	3.249006

C	-2.197191	0.494715	-0.023186
C	-2.400280	1.885562	-0.623519
C	-3.069427	0.250934	1.209486
H	-2.459503	-0.253904	-0.790583
H	-1.778727	2.031137	-1.519647
H	-3.453778	2.039316	-0.915013
H	-2.147264	2.682174	0.095800
H	-4.139016	0.369745	0.964029
H	-2.941907	-0.763863	1.620289
H	-2.844498	0.966816	2.016386
O	0.670111	0.572734	-1.472884
C	1.648514	1.487039	-1.761739
H	1.600257	1.781183	-2.826723
H	1.597134	2.425768	-1.170749
C	3.051940	0.942275	-1.543590
F	3.253790	0.601922	-0.255375
F	3.970546	1.863300	-1.854711
F	3.298877	-0.143239	-2.275748

79

TS$_{\text{red-prot}}$

C	-6.819882	-2.872404	7.183832
O	-7.612128	-3.804343	7.085195
C	-7.320329	-1.593910	7.918376
Sn	-6.943642	-1.538765	3.776177
C	-5.578543	-3.050525	2.986670
C	-6.302871	-4.243872	2.374380
C	-4.538875	-3.453529	4.023438
H	-5.038176	-2.530694	2.188058
H	-6.926154	-3.938692	1.522983
H	-5.574540	-4.982475	1.994226
H	-6.949681	-4.759954	3.102760
H	-3.906341	-2.597262	4.303181
H	-4.996752	-3.853957	4.940460
H	-3.861333	-4.224578	3.613575
C	-6.298045	0.525482	3.863610
C	-4.876106	0.665521	4.398582
C	-7.307154	1.391340	4.616129
H	-6.292265	0.811011	2.801631
H	-4.158518	0.079005	3.804594
H	-4.548206	1.718109	4.354477
H	-4.806507	0.356764	5.455536
H	-8.312949	1.336033	4.170014
H	-7.392579	1.103328	5.675856
H	-6.999648	2.451419	4.592238
C	-9.100989	-1.731152	3.531245
C	-9.839182	-1.605233	4.861174
C	-9.514671	-2.960931	2.725903
H	-9.331033	-0.845133	2.917333
H	-9.635161	-0.642019	5.353003
H	-10.932146	-1.674231	4.714969
H	-9.549701	-2.386085	5.581593
H	-9.075946	-2.934272	1.718679
H	-9.197919	-3.902892	3.202107

H	-10.613506	-3.003846	2.614743
O	-7.348926	-1.079642	1.178463
H	-6.810267	-2.022119	5.582616
C	-8.502059	-6.178754	4.888036
C	-8.482520	-7.061365	3.816313
C	-7.287147	-7.684475	3.465121
C	-6.130370	-7.441269	4.197369
C	-6.173039	-6.556165	5.269064
N	-7.346343	-5.956599	5.552301
H	-9.399779	-7.241519	3.256164
H	-5.186717	-7.922306	3.940254
C	-5.000269	-6.271390	6.150127
H	-4.081415	-6.212941	5.552953
H	-5.125885	-5.331469	6.702970
H	-4.884807	-7.092374	6.875444
C	-9.729494	-5.483728	5.378779
H	-10.104192	-5.991923	6.281260
H	-9.511148	-4.444166	5.653634
H	-10.515054	-5.500359	4.614943
H	-7.361379	-5.189080	6.281990
H	-7.258356	-8.363806	2.611047
S	-6.209832	-1.069994	0.241969
O	-5.910992	-2.307181	-0.455854
N	-5.011401	-0.336091	0.955760
C	-6.752914	0.134772	-1.058484
S	-3.442835	-0.586515	0.712228
F	-7.822629	-0.337029	-1.682211
F	-5.782478	0.313901	-1.936238
F	-7.057297	1.297985	-0.504573
O	-2.832757	-1.151301	1.909901
C	-2.892331	1.187498	0.685002
O	-3.085482	-1.118883	-0.587893
F	-3.492109	1.836711	-0.300466
F	-1.582281	1.221890	0.489044
F	-3.167156	1.797482	1.828665
O	-5.520902	-3.145027	7.266042
C	-4.492441	-2.145590	7.254628
H	-4.621182	-1.473781	8.115130
H	-4.598416	-1.557537	6.330432
C	-3.161565	-2.853400	7.317898
H	-2.353142	-2.109118	7.314540
H	-3.077405	-3.452630	8.236002
H	-3.022576	-3.508679	6.447113
F	-7.024529	-1.748581	9.214877
F	-8.626953	-1.473951	7.798418
F	-6.754482	-0.462437	7.513269

15

$[CF_3COHOEt]^+$

C	3.331499	3.759032	-1.004082
O	2.275528	2.736348	0.973907
C	2.429284	3.781642	0.264181
O	1.875449	4.857366	0.543467
C	0.974819	5.034599	1.737532
H	0.175233	4.292201	1.609450

H 1.593750 4.774061 2.606989
F 4.305937 4.616798 -0.846983
F 2.602818 4.056037 -2.048467
F 3.815403 2.526916 -1.114832
C 0.495655 6.454701 1.733243
H -0.085035 6.681304 0.829536
H -0.161739 6.587213 2.604579
H 1.330465 7.161821 1.824415
H 2.769529 1.962524 0.636761

14
CF_3CO_2Et
C 3.244297 3.738902 -1.016196
O 2.088890 2.656897 0.811984
C 2.320570 3.668679 0.219712
O 1.852993 4.870530 0.494810
C 0.972407 4.980294 1.622983
H 0.112296 4.312680 1.461033
H 1.503985 4.620537 2.517284
F 4.269111 4.555822 -0.781786
F 2.573940 4.199880 -2.069928
F 3.715958 2.539755 -1.305550
C 0.556022 6.425042 1.750930
H 0.030664 6.763115 0.846699
H -0.120888 6.539798 2.609216
H 1.430030 7.072390 1.908992

7
CF_3CHO
C 3.241000 3.714153 -1.004849
O 2.115349 2.590117 0.792574
C 2.324922 3.618254 0.228003
F 4.239263 4.559953 -0.744333
F 2.544005 4.202151 -2.032363
F 3.743876 2.542787 -1.341345
H 1.886874 4.599417 0.530240

61
TS-1 f
C -6.383733 13.576209 10.876852
O -6.790034 14.428650 13.046870
C -6.565728 13.412803 12.414555
O -7.207950 12.255962 12.791342
C -6.779105 10.967676 12.403116
H -5.677336 10.915451 12.446552
H -7.075570 10.755616 11.362124
Sn -3.729749 13.174661 13.851958
C -2.203604 12.069429 12.728095
C -3.706956 15.340108 13.672494
C -4.875215 12.126409 15.375755
C -2.861327 11.034387 11.812816
C -1.112215 11.434684 13.586661
H -1.741061 12.843506 12.090786
C -2.309278 15.864940 13.347805

C -4.313155 16.021053 14.897863
H -4.378722 15.516004 12.817716
C -4.980940 12.859410 16.710323
C -4.369280 10.694401 15.558428
H -5.876286 12.105637 14.913634
H -2.105413 10.545762 11.171765
H -3.625485 11.475233 11.156012
H -3.346241 10.233001 12.396556
H -0.519504 12.179091 14.131942
H -0.410874 10.859769 12.955183
H -1.528333 10.731628 14.324686
H -1.607795 15.664893 14.171536
H -2.336490 16.957917 13.186522
H -1.892831 15.410792 12.434006
H -4.293578 17.119470 14.775508
H -5.363069 15.721976 15.032794
H -3.754791 15.781834 15.816363
H -5.391901 13.872662 16.594222
H -5.650737 12.304212 17.391412
H -4.004061 12.936243 17.204693
H -5.048749 10.126505 16.219671
H -4.304996 10.142359 14.605681
H -3.376735 10.679972 16.033930
H -5.083682 12.933444 12.568565
S -0.651430 11.022436 18.248104
S -1.017225 13.321804 16.627356
O 0.554313 11.614471 18.799701
O 0.380643 13.380671 16.240405
F 0.711543 10.361490 16.077063
F -0.458111 14.438888 18.948288
N -1.537915 12.011507 17.337755
F -1.059075 9.177353 16.397602
F -2.480573 14.761048 18.288365
F 0.683057 8.863303 17.624243
F -0.862311 15.826002 17.347845
C -0.042227 9.785150 16.999674
C -1.218597 14.668879 17.892955
O -1.543974 10.257365 19.093781
O -2.018290 13.710897 15.621335
F -5.843381 12.514396 10.255063
F -7.571823 13.793390 10.302663
F -5.602038 14.617684 10.610434
C -7.398416 9.960235 13.348127
H -7.110398 8.939683 13.054476
H -7.056614 10.134216 14.378299
H -8.495684 10.033908 13.329320

46
TS-2 f
C -3.598820 9.476621 7.653627
O -3.267882 11.455838 8.939149
C -3.161231 10.203450 8.962752
O -3.605999 9.585743 10.112664
C -3.240590 8.257979 10.438471
H -2.195994 8.073537 10.123957

H	-3.875481	7.537275	9.898425
Sn	-0.700339	11.337379	9.105515
C	1.061817	10.046350	8.829982
C	-0.863446	12.703378	7.429479
C	-1.155752	11.781905	11.177975
C	0.885938	8.683002	9.494232
C	2.338600	10.758765	9.285992
H	1.116845	9.898078	7.737370
C	0.521731	13.058217	6.886012
C	-1.711384	13.930750	7.750665
H	-1.400273	12.094252	6.684948
C	-1.844381	13.136831	11.326223
C	0.053499	11.621201	12.098431
H	-1.898261	10.998989	11.405410
H	1.768794	8.043064	9.322343
H	0.010003	8.144773	9.099669
H	0.758861	8.769014	10.586480
H	2.484516	11.726534	8.780523
H	3.228768	10.143449	9.066456
H	2.339112	10.945192	10.371578
H	1.109722	13.650547	7.607241
H	0.425941	13.672616	5.974874
H	1.113945	12.169358	6.618115
H	-1.829948	14.553752	6.847692
H	-2.709812	13.632976	8.096942
H	-1.245419	14.564158	8.522991
H	-2.741517	13.183301	10.694323
H	-2.154789	13.290106	12.373955
H	-1.177723	13.973689	11.060139
H	-0.248431	11.770575	13.149132
H	0.508910	10.621423	12.028622
H	0.839900	12.363585	11.884443
H	-1.873991	9.783326	8.908348
C	-3.383682	8.083892	11.934773
H	-3.141358	7.050619	12.223060
H	-2.708628	8.764484	12.474232
H	-4.413927	8.301178	12.250565
F	-4.911379	9.560133	7.491380
F	-3.260637	8.178301	7.626304
F	-3.002851	10.047746	6.603432

54

TS-3 f

C	-17.693263	11.320535	7.507846
O	-17.648401	8.943484	7.788286
C	-17.323236	9.883294	7.088863
Sn	-14.165691	10.286249	8.246156
C	-12.970708	9.091802	6.861367
C	-13.794989	12.434410	8.143088
C	-15.007906	9.253739	9.960434
C	-13.778040	7.879543	6.390868
C	-11.596959	8.688832	7.389505
H	-12.831256	9.765730	5.996907
C	-12.393669	12.728396	7.606500
C	-14.061721	13.155796	9.462684

H -14.538651 12.774444 7.402723
C -15.162181 10.158116 11.182043
C -14.212725 7.990460 10.293563
H -16.010744 8.968050 9.598969
H -13.237467 7.332307 5.597440
H -14.765603 8.159444 5.991747
H -13.948975 7.164786 7.211993
H -10.966894 9.557385 7.624642
H -11.055492 8.080380 6.642896
H -11.674459 8.082883 8.305482
H -11.614567 12.376417 8.298340
H -12.250637 13.815883 7.470573
H -12.210704 12.249847 6.630775
H -13.892890 14.242535 9.350936
H -15.097658 13.016201 9.806345
H -13.387252 12.797852 10.254065
H -15.799837 11.030660 10.975482
H -15.630274 9.598818 12.012270
H -14.185280 10.518755 11.535978
H -14.699679 7.441125 11.119355
H -14.150372 7.298706 9.439045
H -13.185825 8.225402 10.613636
S -9.209859 8.192367 11.313166
S -10.790855 10.359255 10.406481
O -8.084143 9.098429 11.459339
O -9.729569 10.879436 9.559493
F -8.714904 8.105955 8.714650
F -9.657960 11.372562 12.564452
N -10.620197 8.904032 10.997216
F -9.858385 6.433988 9.446974
F -11.792773 11.152613 12.714733
F -7.751952 6.568481 9.875685
F -10.956703 12.727865 11.505672
C -8.870874 7.272774 9.732344
C -10.795436 11.467724 11.899368
O -9.432361 7.144276 12.287734
O -12.172227 10.496379 9.928292
F -19.021952 11.475430 7.408599
F -17.135845 12.238278 6.709873
F -17.353536 11.600738 8.764768
H -17.174150 9.808071 5.985006
H -15.687954 10.251690 7.198121

39
TS-4 f
C -22.239431 7.321653 2.205072
O -22.309529 9.121711 3.819381
C -22.010090 7.905621 3.615126
Sn -19.652621 9.196924 4.088949
C -17.786017 8.103956 3.716732
C -20.023264 10.726890 2.604187
C -20.128388 9.341119 6.202859
C -17.794440 6.743043 4.410807
C -16.556463 8.941801 4.078486
H -17.788450 7.941247 2.624988

C	-18.734493	11.135487	1.891390
C	-20.788444	11.910168	3.191344
H	-20.687339	10.200069	1.903389
C	-21.204549	10.382701	6.500928
C	-18.855493	9.550425	7.027643
H	-20.533528	8.340279	6.430846
H	-16.881708	6.171896	4.168380
H	-18.655759	6.128706	4.104304
H	-17.829608	6.841315	5.508555
H	-16.527527	9.899947	3.536792
H	-15.628956	8.399128	3.825314
H	-16.511017	9.164788	5.156536
H	-18.035253	11.658002	2.565427
H	-18.963758	11.833212	1.068451
H	-18.202028	10.277571	1.452116
H	-21.020118	12.639422	2.396483
H	-21.736940	11.575670	3.632485
H	-20.205984	12.445484	3.959798
H	-22.102209	10.193736	5.896696
H	-21.476945	10.348591	7.569622
H	-20.850887	11.404048	6.286709
H	-19.100506	9.567427	8.103046
H	-18.113498	8.751899	6.874811
H	-18.367464	10.512364	6.798257
H	-20.717221	7.627690	3.641063
H	-22.302200	7.115402	4.356643
F	-23.535122	7.296353	1.912854
F	-21.772635	6.067881	2.122071
F	-21.617761	8.039113	1.259475

14
EtOAc

C	2.605777	4.724830	-0.619301
O	2.413384	3.238664	1.270750
C	2.563596	4.350307	0.838055
O	2.715952	5.427722	1.619448
C	2.693061	5.205741	3.028452
H	1.736610	4.733727	3.303983
H	3.489119	4.492264	3.294410
H	3.559051	5.220932	-0.850001
H	2.490369	3.825050	-1.232937
H	1.801495	5.439949	-0.843076
C	2.880382	6.538304	3.715634
H	2.075503	7.236233	3.443907
H	2.867630	6.403101	4.806559
H	3.841083	6.992979	3.434392

7
MeCHO

C	2.906969	3.408484	-1.038213
O	2.838122	2.664134	1.242532
C	3.424165	3.232090	0.361798
H	2.848521	4.482070	-1.278502
H	3.615162	2.960504	-1.753391

H 1.918381 2.943577 -1.144303
H 4.434106 3.683348 0.549239

61
TS-5
C -16.537396 13.407268 5.193478
O -16.362240 15.573928 6.191666
C -16.244505 14.334714 6.385999
O -16.911018 13.874085 7.576841
C -16.670819 12.569881 8.004044
H -15.664509 12.232434 7.679618
H -17.397027 11.860159 7.556417
Sn -13.726803 15.495588 7.163640
C -12.204597 13.967791 7.613863
C -13.551988 16.170382 5.114040
C -14.880590 16.215807 8.843086
C -12.705517 12.935836 8.623313
C -10.863154 14.560314 8.037588
H -12.075648 13.460461 6.640498
C -12.096906 16.123705 4.649088
C -14.193954 17.538491 4.906439
H -14.143222 15.422827 4.561081
C -15.509017 17.572150 8.535462
C -14.046547 16.231593 10.123119
H -15.686918 15.469268 8.912882
H -11.976713 12.113478 8.741835
H -13.664160 12.486139 8.322499
H -12.847240 13.381527 9.620944
H -10.448299 15.248137 7.286875
H -10.115211 13.763951 8.204058
H -10.951985 15.120097 8.981345
H -11.467351 16.834322 5.205782
H -12.027406 16.392331 3.579696
H -11.648706 15.123391 4.764732
H -14.104082 17.847995 3.849034
H -15.260332 17.496368 5.166758
H -13.699793 18.310990 5.515389
H -16.164729 17.488156 7.658048
H -16.117390 17.908172 9.394726
H -14.743881 18.343192 8.355207
H -14.667847 16.568439 10.972140
H -13.653515 15.236634 10.384456
H -13.189249 16.918409 10.050374
H -15.034472 13.972935 6.672572
S -9.302338 18.246881 10.200107
S -11.019051 18.070334 7.959464
O -8.447875 19.139401 9.437245
O -9.925886 17.909058 7.017361
F -8.227408 16.197826 8.917909
F -10.601157 20.664279 8.130493
N -10.712136 17.896796 9.495843
F -9.117269 15.681371 10.810668
F -12.629049 20.073176 8.537437
F -7.243364 16.740986 10.755534
F -11.891152 20.066456 6.511909

C -8.424833 16.607479 10.161326
C -11.569296 19.837516 7.779428
O -9.540984 18.487406 11.607440
O -12.274332 17.353347 7.668454
C -16.752403 12.513463 9.518695
H -16.619081 11.483209 9.884276
H -15.971859 13.147295 9.966238
H -17.729128 12.884891 9.862799
H -17.598698 13.533684 4.927882
H -16.336550 12.343121 5.390951
H -15.924555 13.732291 4.341407

46
TS-6
C -17.447322 17.362447 11.011397
O -16.654558 19.529135 11.670041
C -16.833517 18.319439 12.026173
O -17.312962 18.178580 13.319407
C -17.397621 16.893368 13.886267
H -16.502885 16.301303 13.607887
H -18.281729 16.354403 13.499753
Sn -14.318035 19.195756 12.176578
C -12.729240 17.711214 12.606955
C -14.035794 19.938119 10.152997
C -14.779829 20.387566 13.931817
C -13.139875 16.749799 13.719271
C -11.383097 18.381379 12.894085
H -12.640551 17.138682 11.666308
C -12.564163 19.933271 9.738463
C -14.708147 21.291811 9.938328
H -14.575104 19.185864 9.552002
C -15.359107 21.746976 13.546963
C -13.616036 20.497129 14.915551
H -15.588660 19.788789 14.382647
H -12.372981 15.971448 13.879397
H -14.086117 16.234827 13.489585
H -13.274103 17.270206 14.682490
H -11.062577 19.050555 12.080791
H -10.587058 17.626279 13.023493
H -11.411197 18.975608 13.820942
H -11.969018 20.651505 10.327031
H -12.461544 20.228249 8.679959
H -12.096997 18.942221 9.848294
H -14.638221 21.591461 8.878169
H -15.769981 21.247656 10.215748
H -14.226392 22.086370 10.531305
H -16.215435 21.623165 12.870254
H -15.705901 22.282379 14.447779
H -14.610754 22.391167 13.056081
H -13.931121 21.048727 15.818163
H -13.247821 19.514152 15.246316
H -12.761469 21.047670 14.488290
H -15.584546 17.697510 12.170445
C -17.479948 17.036198 15.391091
H -17.583063 16.050133 15.866998

H -16.573246 17.519965 15.783091
H -18.346281 17.652089 15.671754
H -18.499405 17.661174 10.879685
H -17.404082 16.306664 11.310828
H -16.926912 17.490449 10.054293

54
TS-7
C -17.523339 8.810559 6.330365
O -17.541989 10.743037 7.779620
C -17.192060 9.520526 7.651101
Sn -14.735142 10.879244 8.185775
C -12.972346 9.569235 8.033319
C -15.118524 11.977809 6.361475
C -15.547945 11.071130 10.183100
C -13.223026 8.247556 8.760530
C -11.669376 10.228032 8.477421
H -12.908427 9.355792 6.951092
C -13.811691 12.264307 5.622394
C -15.947035 13.234947 6.606804
H -15.730922 11.271557 5.778268
C -16.411374 12.323221 10.313628
C -14.445119 11.005891 11.239796
H -16.200342 10.186526 10.271254
H -12.392806 7.537979 8.590299
H -14.152459 7.758443 8.426725
H -13.299496 8.392822 9.850673
H -11.427839 11.119558 7.881691
H -10.819325 9.528366 8.379443
H -11.709089 10.540565 9.532673
H -13.157206 12.937660 6.196271
H -14.019008 12.754741 4.654329
H -13.237385 11.348198 5.408446
H -16.127887 13.765557 5.653861
H -16.916274 12.958260 7.043108
H -15.428149 13.937083 7.277150
H -17.237255 12.278415 9.590261
H -16.834031 12.389978 11.332798
H -15.819553 13.236307 10.144607
H -14.886888 11.051374 12.251317
H -13.857926 10.075779 11.182764
H -13.741012 11.846961 11.150573
H -15.900759 9.330931 7.662865
S -10.209125 13.763310 10.986024
S -12.242801 13.674798 9.019615
O -9.578751 14.842913 10.247330
O -11.307534 13.795168 7.915099
F -9.141733 12.049728 9.276676
F -12.098882 16.248640 9.556205
N -11.670157 13.338774 10.449405
F -9.686916 11.177935 11.169829
F -13.966718 15.338877 10.114607
F -7.953733 12.448360 11.028498
F -13.535933 15.725592 8.038422
C -9.191948 12.259442 10.583110

C -13.008736 15.359337 9.200620
O -10.242393 13.789515 12.433227
O -13.438517 12.840174 8.807445
H -18.619976 8.759426 6.231905
H -17.110429 7.788606 6.287833
H -17.140240 9.394943 5.479699
H -17.396160 8.815675 8.511249

39
TS-8
C -23.253732 10.313607 -5.754564
O -22.893672 12.200145 -4.287420
C -22.682933 10.952434 -4.497597
Sn -20.413641 12.350315 -4.379867
C -18.481854 11.343813 -4.773107
C -20.896731 13.651864 -6.048813
C -20.640696 12.807286 -2.265803
C -18.350405 10.055323 -3.963395
C -17.281638 12.273962 -4.581075
H -18.546081 11.076025 -5.842938
C -19.642953 14.107978 -6.795727
C -21.798177 14.812580 -5.636073
H -21.478481 12.980613 -6.703093
C -21.630152 13.946224 -2.030699
C -19.294479 13.045863 -1.580470
H -21.082043 11.877389 -1.867815
H -17.427473 9.509810 -4.228253
H -19.196155 9.370563 -4.135617
H -18.303593 10.254699 -2.879763
H -17.350890 13.182768 -5.198601
H -16.341627 11.764789 -4.859627
H -17.171941 12.592268 -3.532379
H -19.017693 14.775031 -6.179023
H -19.921507 14.678822 -7.698021
H -19.012627 13.266307 -7.122527
H -22.093223 15.401228 -6.521992
H -22.707479 14.434947 -5.149966
H -21.288220 15.503374 -4.944459
H -22.589004 13.725541 -2.518171
H -21.805074 14.081871 -0.949415
H -21.249505 14.904793 -2.420038
H -19.441923 13.216645 -0.500317
H -18.607443 12.192828 -1.685617
H -18.782692 13.938706 -1.976575
H -21.342642 10.691420 -4.716208
H -24.350569 10.315428 -5.651832
H -22.909505 9.277602 -5.892451
H -23.000268 10.914126 -6.639806
H -22.738337 10.249685 -3.626199

45
[**1**·(CF_3CO_2Et)]$^+$
Sn -5.206580 11.104986 15.259888
C -4.656314 9.222991 14.353201

C	-5.890689	8.410226	13.960228
C	-3.714675	8.454301	15.287545
H	-4.098157	9.504147	13.444317
H	-5.588187	7.473062	13.465816
H	-6.546717	8.953525	13.263323
H	-6.493509	8.131106	14.839443
H	-2.801678	9.021556	15.525125
H	-3.396425	7.513319	14.810764
H	-4.202733	8.180861	16.237233
C	-3.633128	12.448781	15.865565
C	-2.512447	12.468172	14.825061
C	-3.138384	12.085542	17.270018
H	-4.111995	13.441400	15.901755
H	-2.023742	11.485307	14.728586
H	-1.733084	13.186991	15.125173
H	-2.870881	12.771296	13.829912
H	-2.358343	12.796306	17.586810
H	-3.938239	12.126442	18.025556
H	-2.687048	11.080921	17.305094
C	-7.131049	11.194774	16.240744
C	-7.650058	12.627876	16.354061
C	-7.036394	10.492171	17.600149
H	-7.801271	10.614015	15.586258
H	-8.638349	12.637630	16.842236
H	-6.985120	13.260065	16.963635
H	-7.768214	13.116443	15.374171
H	-8.025784	10.472433	18.085099
H	-6.699267	9.446965	17.514791
H	-6.354280	11.014257	18.290168
C	-6.785256	13.247065	11.495316
O	-5.698798	12.252338	13.372782
C	-6.705100	12.239277	12.676722
O	-7.674966	11.433575	12.922154
C	-8.938475	11.324489	12.180473
H	-8.705752	10.830333	11.228657
H	-9.310600	12.338213	11.986893
F	-5.647359	13.879078	11.368760
F	-7.755846	14.118587	11.746991
F	-7.062944	12.595874	10.374061
C	-9.882910	10.524461	13.036005
H	-9.481799	9.522391	13.240721
H	-10.086261	11.035608	13.987113
H	-10.834593	10.408897	12.499033

47

([NTf_2]$^-$)·**1**-H

Sn	1.067145	3.612870	4.241808
C	2.032613	2.779418	2.465784
C	2.461334	1.322202	2.621168
C	3.190268	3.672299	2.020758
H	1.237556	2.818491	1.704755
H	2.949885	0.955193	1.698688
H	1.596788	0.673863	2.818747
H	3.184062	1.185856	3.444088
H	2.871443	4.713902	1.849374

H 3.637873 3.306205 1.077593
H 3.995428 3.701354 2.774705
C 0.315851 2.323650 5.828057
C 0.601645 2.940183 7.196788
C 0.784395 0.873918 5.738609
H -0.771625 2.317030 5.666038
H 1.683642 2.991766 7.408773
H 0.134810 2.340561 7.999137
H 0.204553 3.965325 7.283540
H 0.332783 0.275679 6.549771
H 0.464698 0.416416 4.792957
H 1.881446 0.779554 5.821722
C -0.455368 5.077154 3.653338
C -1.773674 4.836127 4.388084
C -0.667368 5.101471 2.138860
H -0.046329 6.052762 3.970606
H -1.655353 4.820517 5.483008
H -2.515980 5.618198 4.144959
H -2.219447 3.875734 4.093491
H -1.399604 5.879523 1.853733
H 0.264921 5.308255 1.587652
H -1.059745 4.134438 1.787944
O -0.853023 1.832768 2.826376
S -2.157537 1.190215 2.982722
O -3.297256 1.779020 2.301176
N -2.345686 0.804599 4.508805
C -1.896337 -0.456061 2.160475
S -3.727269 0.450474 5.238641
F -1.754590 -0.280689 0.850682
F -2.922880 -1.264184 2.371343
F -0.796791 -1.042675 2.623338
O -4.814512 0.047309 4.363063
C -4.253004 2.106167 5.905737
O -3.435537 -0.321992 6.430856
F -4.504336 2.964167 4.927356
F -3.316594 2.625996 6.692054
F -5.361965 1.954205 6.625466
H 2.352569 4.548775 4.996293

46
1-acF
Sn 1.337573 3.142372 2.735107
C 1.306410 1.025346 3.207734
C 0.377763 0.221646 2.300492
C 0.957726 0.856555 4.689850
H 2.342223 0.686301 3.045585
H 0.395056 -0.847336 2.575060
H 0.672472 0.310394 1.246531
H -0.668348 0.561770 2.385763
H 1.652467 1.399128 5.350714
H 0.993644 -0.207442 4.980910
H -0.062266 1.212516 4.914780
C 2.524651 4.254301 4.164747
C 2.604410 5.731415 3.774059
C 3.911061 3.617416 4.285314

H	2.005373	4.168746	5.135688
H	1.612713	6.210747	3.754723
H	3.227379	6.295672	4.489945
H	3.054485	5.854182	2.776165
H	4.534259	4.161846	5.016055
H	4.440438	3.636105	3.319364
H	3.859852	2.567356	4.615282
C	-0.604558	4.030828	2.352712
C	-0.515555	5.173130	1.342402
C	-1.255644	4.466886	3.667495
H	-1.205168	3.216765	1.914274
H	-0.064724	4.845079	0.394584
H	-1.517761	5.578230	1.117477
H	0.095601	6.007270	1.723039
H	-2.260853	4.887266	3.490191
H	-1.373834	3.629958	4.374526
H	-0.665735	5.247514	4.175878
C	3.342406	1.873057	-0.355053
O	2.546135	3.546732	1.126298
C	2.305885	2.977332	-0.071542
O	1.024296	2.398396	-0.089298
C	0.276636	2.476871	-1.286855
H	0.246074	3.527544	-1.634652
H	0.761947	1.880301	-2.077276
H	2.394710	3.713431	-0.901509
F	3.320072	0.922080	0.581420
F	4.573448	2.376356	-0.400147
F	3.103556	1.281194	-1.535298
C	-1.120579	1.966892	-1.016107
H	-1.720015	1.995259	-1.937274
H	-1.090694	0.929693	-0.652794
H	-1.620994	2.585984	-0.257438

46

TS$_{\text{ald-F}}$

Sn	-0.417635	5.643255	9.341310
C	0.349251	3.685120	9.873385
C	1.870764	3.729503	10.016152
C	-0.102098	2.584956	8.915043
H	-0.092490	3.501128	10.869494
H	2.255674	2.753820	10.359309
H	2.204087	4.488043	10.741685
H	2.343920	3.949154	9.047033
H	-1.198326	2.491037	8.873905
H	0.298071	1.607222	9.235128
H	0.262969	2.785447	7.897291
C	-0.796837	6.689240	11.225350
C	0.304682	6.440457	12.256811
C	-2.165698	6.257006	11.761417
H	-0.841628	7.768024	10.997186
H	0.396205	5.368657	12.499308
H	0.088551	6.965460	13.203906
H	1.293126	6.782133	11.913168
H	-2.388952	6.751999	12.722733
H	-2.984267	6.507138	11.068745

H	-2.209500	5.169931	11.948153
C	-2.058241	5.965783	7.969825
C	-2.502887	7.427156	8.022899
C	-3.214006	4.992963	8.207985
H	-1.607056	5.760651	6.988469
H	-1.672847	8.114820	7.803134
H	-3.292875	7.618341	7.276432
H	-2.918024	7.698387	9.007979
H	-4.021749	5.170247	7.477030
H	-2.902446	3.943036	8.098918
H	-3.659198	5.109390	9.209989
C	1.472166	7.110883	6.092926
O	0.896958	5.020352	7.100061
C	1.673009	5.977304	7.111786
O	1.153284	6.879440	8.634105
C	1.804243	7.949867	9.287727
H	1.842156	8.812329	8.603546
H	1.191304	8.260195	10.149965
H	2.746849	5.868836	7.383579
F	1.800590	6.658132	4.880303
F	2.268286	8.156233	6.353018
F	0.218158	7.545555	6.042374
C	3.202483	7.578431	9.748085
H	3.851084	7.342943	8.891712
H	3.660881	8.414817	10.296725
H	3.177790	6.700486	10.411569

38

[**1**·(CF_3CHO)]$^+$

Sn	-5.162882	11.087680	15.317360
C	-4.590254	9.222413	14.395310
C	-5.805145	8.483655	13.833913
C	-3.790783	8.381011	15.397692
H	-3.923146	9.516640	13.567979
H	-5.485513	7.551355	13.341590
H	-6.348424	9.072600	13.078276
H	-6.519065	8.202130	14.624318
H	-2.891555	8.900289	15.763844
H	-3.451383	7.450612	14.915218
H	-4.395498	8.085308	16.270125
C	-3.644727	12.533555	15.822587
C	-2.511004	12.508182	14.796875
C	-3.163234	12.294856	17.258685
H	-4.160114	13.507585	15.778090
H	-1.987646	11.538864	14.786702
H	-1.762214	13.276149	15.048438
H	-2.862600	12.717468	13.775358
H	-2.419625	13.060318	17.532036
H	-3.977618	12.358723	17.997220
H	-2.669908	11.316506	17.375196
C	-7.104989	11.196969	16.260175
C	-7.477375	12.635732	16.621447
C	-7.134113	10.255199	17.471022
H	-7.812308	10.808772	15.506054
H	-8.484656	12.668215	17.066694

H -6.783664 13.063624 17.362098
H -7.486359 13.309729 15.750025
H -8.135608 10.265530 17.929904
H -6.913422 9.210800 17.201015
H -6.422400 10.564381 18.253348
C -6.783997 13.078627 11.376686
O -5.774113 12.119109 13.322146
C -6.805023 12.388890 12.751488
F -5.554347 13.319690 10.988393
F -7.461936 14.210606 11.480505
F -7.387554 12.275429 10.514375
H -7.807877 12.162471 13.168786

45
[**1**·(EtOAc)]+
Sn -5.237764 11.162137 15.194945
C -4.695603 9.270025 14.303072
C -5.926714 8.471690 13.872508
C -3.798490 8.489061 15.270730
H -4.103325 9.536843 13.411764
H -5.621832 7.522815 13.402044
H -6.545847 9.017628 13.145083
H -6.568046 8.214617 14.731158
H -2.886256 9.043433 15.539898
H -3.477268 7.541502 14.808859
H -4.323582 8.226412 16.203665
C -3.635312 12.450796 15.845157
C -2.459797 12.388047 14.868784
C -3.229873 12.118819 17.285187
H -4.068582 13.464722 15.822833
H -2.009022 11.383218 14.832566
H -1.666775 13.085021 15.184788
H -2.751871 12.666642 13.845094
H -2.431724 12.801619 17.618496
H -4.064726 12.226781 17.994704
H -2.833308 11.095006 17.380372
C -7.122778 11.233495 16.251032
C -7.622492 12.666440 16.429593
C -6.985382 10.485931 17.582095
H -7.822795 10.681837 15.603410
H -8.590926 12.671833 16.956406
H -6.926798 13.273455 17.030741
H -7.771519 13.182684 15.468417
H -7.955342 10.461095 18.104958
H -6.664557 9.440566 17.449258
H -6.269960 10.975920 18.261763
C -6.822640 13.172780 11.444040
O -5.678922 12.330321 13.351281
C -6.694166 12.301122 12.647119
O -7.648505 11.487824 12.995874
C -8.895248 11.352311 12.270587
H -8.667398 10.958287 11.268878
H -9.350051 12.348453 12.167954
C -9.778545 10.415508 13.054192
H -9.306006 9.430040 13.167016

H	-9.998837	10.824074	14.050141
H	-10.729091	10.281977	12.519906
H	-5.892612	13.731101	11.299790
H	-7.657025	13.877289	11.579869
H	-7.040494	12.568117	10.551913

46

1-ac

Sn	1.351550	3.154425	2.701337
C	1.308198	1.040544	3.207902
C	0.396693	0.218050	2.299941
C	0.941836	0.880099	4.686432
H	2.349534	0.703096	3.066256
H	0.424338	-0.850414	2.577077
H	0.688344	0.310358	1.244672
H	-0.653610	0.546419	2.380069
H	1.622359	1.435545	5.351148
H	0.980005	-0.180568	4.990212
H	-0.083271	1.232687	4.892409
C	2.489720	4.257308	4.183363
C	2.609683	5.729411	3.783592
C	3.860671	3.607664	4.382074
H	1.921777	4.189748	5.128361
H	1.626643	6.221247	3.709145
H	3.203846	6.294701	4.523280
H	3.109227	5.835028	2.807341
H	4.453047	4.152193	5.138497
H	4.438144	3.611199	3.443844
H	3.781526	2.561328	4.718818
C	-0.584954	4.057860	2.319903
C	-0.487261	5.187279	1.295904
C	-1.229703	4.514349	3.630386
H	-1.192606	3.244689	1.889740
H	-0.047108	4.837532	0.350631
H	-1.485496	5.603630	1.072123
H	0.136879	6.018256	1.662744
H	-2.231808	4.941748	3.450915
H	-1.353148	3.686595	4.347382
H	-0.631939	5.295245	4.129208
C	3.321921	1.906635	-0.506583
O	2.631431	3.480267	1.151560
C	2.331832	2.982362	-0.082017
O	1.009143	2.452588	-0.019771
C	0.313345	2.304196	-1.229759
H	0.384364	3.239447	-1.820494
H	0.764449	1.500958	-1.843644
H	2.321573	3.803137	-0.836615
C	-1.135457	1.981057	-0.931014
H	-1.694213	1.826765	-1.865448
H	-1.211760	1.066098	-0.325924
H	-1.609415	2.803181	-0.375222
H	4.337941	2.324557	-0.510274
H	3.101729	1.518617	-1.512931
H	3.285615	1.075926	0.214429

46
TS$_{ald}$
Sn -3.579549 6.048781 10.259429
C -2.605113 4.269754 11.026953
C -1.088345 4.419433 10.903106
C -3.104972 2.994858 10.351286
H -2.875224 4.247413 12.098007
H -0.573276 3.544064 11.335724
H -0.709502 5.314639 11.421091
H -0.795828 4.488053 9.843991
H -4.184185 2.836553 10.503366
H -2.583683 2.109463 10.755855
H -2.915406 3.035718 9.268319
C -3.737677 7.418798 11.972366
C -2.458022 7.441484 12.808829
C -4.947421 7.028301 12.826127
H -3.917227 8.429176 11.565271
H -2.228037 6.444681 13.221167
H -2.551890 8.129048 13.668484
H -1.579705 7.763233 12.228590
H -5.035711 7.678126 13.715046
H -5.894292 7.109034 12.270011
H -4.870712 5.992047 13.199343
C -5.487512 6.042878 9.226628
C -5.998779 7.473867 9.062215
C -6.519801 5.127718 9.886406
H -5.224873 5.634802 8.239358
H -5.267315 8.116675 8.546972
H -6.930369 7.493886 8.470016
H -6.224586 7.944743 10.033604
H -7.460636 5.123790 9.308458
H -6.170759 4.085389 9.945774
H -6.774187 5.452959 10.908326
C -2.445800 7.101910 6.601416
O -2.682034 5.247146 8.110148
C -1.987122 6.225483 7.741194
O -2.248595 7.311240 9.171590
C -1.643853 8.549438 9.432954
H -1.806878 9.218038 8.566505
H -2.153549 9.025883 10.287950
H -0.878805 6.162298 7.838213
C -0.156897 8.414716 9.718445
H 0.376591 7.996933 8.851746
H 0.285767 9.395169 9.950848
H 0.014979 7.744508 10.574372
H -2.292469 6.545936 5.663204
H -3.517913 7.320200 6.703352
H -1.873947 8.039097 6.540058

38
[**1**·(MeCHO)]$^{\cdot}$
Sn -5.150820 11.130486 15.220101
C -4.572902 9.237480 14.361875

C	-5.782731	8.493104	13.796577
C	-3.801333	8.414714	15.400357
H	-3.888041	9.501196	13.538806
H	-5.464048	7.544995	13.334419
H	-6.306592	9.068701	13.017223
H	-6.513950	8.239129	14.580728
H	-2.904873	8.936033	15.770434
H	-3.461647	7.467402	14.951890
H	-4.425441	8.150391	16.269323
C	-3.617428	12.524760	15.813535
C	-2.407928	12.434752	14.882329
C	-3.256703	12.299087	17.286423
H	-4.085264	13.518169	15.710597
H	-1.926142	11.445075	14.929692
H	-1.648995	13.177024	15.177499
H	-2.670604	12.635141	13.832662
H	-2.502729	13.037002	17.604060
H	-4.122269	12.412521	17.957680
H	-2.818882	11.302648	17.459214
C	-7.076643	11.229829	16.198404
C	-7.443854	12.665281	16.578202
C	-7.078387	10.282011	17.404775
H	-7.803601	10.846093	15.460941
H	-8.439666	12.694410	17.049155
H	-6.731936	13.090135	17.303368
H	-7.474489	13.343966	15.710931
H	-8.067662	10.289776	17.889832
H	-6.864369	9.239268	17.123211
H	-6.345983	10.585288	18.170280
C	-6.931330	13.042812	11.449197
O	-5.715153	12.141911	13.281860
C	-6.798541	12.373577	12.756056
H	-7.731143	12.071763	13.278594
H	-5.954207	13.297209	11.022720
H	-7.495916	12.383160	10.769480
H	-7.550906	13.946180	11.575667

70

[**1**·(**1**-OEt)]·

Sn	1.045910	2.912907	2.910786
C	0.753312	5.040579	2.616553
C	0.069670	5.615524	3.863323
C	-0.016288	5.366264	1.335844
H	1.764061	5.476362	2.548560
H	0.643654	5.429700	4.784532
H	-0.942325	5.203133	4.006957
H	-0.042400	6.707688	3.767569
H	0.462612	4.956361	0.432571
H	-0.091490	6.457441	1.200115
H	-1.045765	4.976555	1.371066
C	-0.647202	1.719196	2.274355
C	-0.861670	1.769611	0.760763
C	-1.885669	2.192080	3.045406
H	-0.429871	0.682856	2.576007
H	-1.099910	2.786247	0.413695

H	-1.707282	1.123075	0.473972
H	0.016269	1.428424	0.191826
H	-2.142232	3.238121	2.812801
H	-1.762795	2.107541	4.136284
H	-2.760526	1.580361	2.771246
C	2.013823	2.434730	4.798082
C	3.333762	1.675309	4.664293
C	1.022137	1.732920	5.731392
H	2.234741	3.431702	5.216374
H	3.775154	1.514255	5.661317
H	4.072283	2.224601	4.065589
H	3.201920	0.682450	4.209833
H	1.480826	1.565541	6.719417
H	0.108538	2.324927	5.897305
H	0.715925	0.746394	5.347681
O	2.520608	2.438619	1.420081
Sn	2.997246	0.514651	0.567691
C	1.642533	-0.969317	1.392132
C	2.452397	0.782661	-1.521133
C	5.071590	0.336705	1.182081
C	1.712254	-1.217356	2.895028
C	1.898577	-2.252098	0.586345
H	0.635693	-0.605762	1.132756
C	3.453084	0.067096	-2.433988
C	2.193814	2.222431	-1.961503
H	1.493558	0.236211	-1.562565
C	6.053003	1.047470	0.248581
C	5.437372	-1.139059	1.372453
H	5.088349	0.829646	2.168974
H	2.716808	-1.529639	3.220801
H	1.016190	-2.022811	3.181766
H	1.435190	-0.328518	3.479549
H	1.800463	-2.099647	-0.500364
H	1.165569	-3.025987	0.866361
H	2.897415	-2.673324	0.781941
H	4.429764	0.575110	-2.442874
H	3.084014	0.058481	-3.472480
H	3.622572	-0.982172	-2.143921
H	1.752527	2.232306	-2.971331
H	1.497323	2.751668	-1.293511
H	3.124792	2.807501	-2.016662
H	7.076946	0.973499	0.649919
H	6.067006	0.589137	-0.751923
H	5.832674	2.118086	0.123311
H	6.470823	-1.226990	1.745095
H	5.391104	-1.701583	0.425880
H	4.785763	-1.645999	2.099859
C	3.336699	3.524052	0.945730
H	3.859187	3.188818	0.036729
H	2.675364	4.345970	0.628872
C	4.344845	4.003978	1.967788
H	3.858762	4.359531	2.889571
H	5.053691	3.207753	2.235709
H	4.919626	4.844596	1.552667

70

[**1**·(**1**-OCH_2CF_3)]$^+$

Sn	1.186748	2.950310	2.941978
C	0.827256	4.918500	2.110680
C	-0.324134	5.578673	2.879296
C	0.553768	4.878761	0.605370
H	1.748020	5.493410	2.300759
H	-0.121043	5.665469	3.957478
H	-1.270519	5.027415	2.755292
H	-0.497293	6.598784	2.499987
H	1.354702	4.387831	0.030991
H	0.451031	5.902608	0.210761
H	-0.382661	4.349148	0.375175
C	-0.443890	1.547822	2.667622
C	-1.158467	1.683072	1.324476
C	-1.407687	1.724220	3.849085
H	0.001032	0.545610	2.746851
H	-1.671887	2.653046	1.235292
H	-1.930162	0.902410	1.221592
H	-0.477552	1.589035	0.466076
H	-1.840251	2.737129	3.892362
H	-0.928351	1.518468	4.817909
H	-2.252211	1.022720	3.751563
C	2.122469	2.745441	4.886851
C	2.354411	1.276810	5.236416
C	1.291003	3.484430	5.941352
H	3.095395	3.246876	4.804779
H	2.817514	1.191982	6.232976
H	3.035775	0.788045	4.523143
H	1.416253	0.698831	5.268842
H	1.777915	3.399212	6.926452
H	1.196946	4.559047	5.722374
H	0.276493	3.069950	6.050721
O	2.781487	2.316965	1.555474
Sn	3.127888	0.440109	0.467117
C	1.607326	-0.961412	1.102641
C	2.749506	1.080752	-1.572240
C	5.151178	-0.072012	1.067065
C	1.780578	-1.467455	2.533472
C	1.598605	-2.107028	0.080609
H	0.651519	-0.422614	1.015341
C	3.632375	2.210535	-2.104590
C	1.262710	1.378803	-1.775207
H	3.000386	0.159529	-2.129664
C	6.247485	0.705714	0.337206
C	5.328203	-1.585131	0.885032
H	5.194507	0.165598	2.141793
H	2.720978	-2.025095	2.661445
H	0.961001	-2.155843	2.797312
H	1.779623	-0.656319	3.275007
H	1.416713	-1.758295	-0.948041
H	0.795811	-2.821426	0.324933
H	2.541947	-2.676028	0.083946
H	3.373550	3.178154	-1.646788
H	3.479177	2.328087	-3.189384

H	4.706027	2.031723	-1.945240
H	1.052106	1.575613	-2.838814
H	0.614438	0.544792	-1.464942
H	0.952570	2.276171	-1.215432
H	7.236783	0.362506	0.680537
H	6.213181	0.542827	-0.751566
H	6.212326	1.788436	0.522439
H	6.330303	-1.888065	1.228888
H	5.251168	-1.888834	-0.172023
H	4.598531	-2.173128	1.461031
C	3.747563	3.280640	1.198877
H	4.375583	2.913790	0.374491
H	3.284231	4.217790	0.851853
C	4.703542	3.640316	2.331231
F	5.068345	2.566826	3.031302
F	4.145361	4.508865	3.186770
F	5.791596	4.211400	1.829918

13. References

1 Scott, D. J.; Phillips, N. A.; Sapsford, J. S.; Deacy, A. C.; Fuchter, M. J.; Ashley, A. E., Versatile Catalytic Hydrogenation Using A Simple Tin(IV) Lewis Acid, *Angew. Chem. Int. Ed.*, **2016**, *55*, 14738–14742.

2 Dolomanov, O. V; Bourhis, L. J.; Gildea, R. J.; Howard, J. A. K.; Puschmann, H., OLEX2: A Complete Structure Solution, Refinement and Analysis Program, *J. Appl. Crystallogr.*, **2009**, *42*, 339–341.

3 Palatinus, L.; Chapuis, G., SUPERFLIP – A Computer Program for the Solution of Crystal Structures by Charge Flipping in Arbitrary Dimensions, *J. Appl. Crystallogr.*, **2007**, *40*, 786–790.

4 Sheldrick, G. M., Crystal structure refinement with SHELXL, *Acta Crystallogr. Sect. C Struct. Chem.*, **2015**, *71*, 3–8.

5 Mao, C.; Wang, Z.; Ji, P.; Cheng, J.-P., Is Amine a Stronger Base in Ionic Liquid Than in Common Molecular Solvent? An Accurate Basicity Scale of Amines, *J. Org. Chem.*, **2015**, *80*, 8384–8389.

6 Nava, M.; Reed, C. A., Triethylsilyl Perfluoro-Tetraphenylborate, $[Et_3Si^+][F_{20}\text{-}BPh_4^-]$, a Widely Used Nonexistent Compound, *Organometallics*, **2011**, *30*, 4798-4800.

7 Huang, P.-Q.; Lang, Q.-W.; Wang, Y.-R., Mild Metal-Free Hydrosilylation of Secondary Amides to Amines, *J. Org. Chem.*, **2016**, *81*, 4235–4243.

8 Bartoszewicz, A.; Marcos, R.; Sahoo, S.; Inge, A. K.; Zou, X.; Martín-Matute, B., A Highly Active Bifunctional Iridium Complex with an Alcohol/Alkoxide-Tethered N-Heterocyclic Carbene for Alkylation of Amines with Alcohols, *Chem. Eur. J.*, **2012**, *18*, 14510–14519.

9 Fulmer, G. R.; Miller, A. J. M.; Sherden, N. H.; Gottlieb, H. E.; Nudelman, A.; Stoltz, B. M.; Bercaw, J. E.; Goldberg, K. I., NMR Chemical Shifts of Trace Impurities: Common Laboratory Solvents, Organics, and Gases in Deuterated Solvents Relevant to the Organometallic Chemist, *Organometallics*, **2010**, *29*, 2176–2179.

10 Scott, D. J.; Fuchter, M. J.; Ashley, A. E., Nonmetal Catalyzed Hydrogenation of Carbonyl Compounds, *J. Am. Chem. Soc.*, **2014**, *136*, 15813–15816.

11 Mahdi, T.; Stephan, D. W., Enabling Catalytic Ketone Hydrogenation by Frustrated Lewis Pairs, *J. Am. Chem. Soc.*, **2014**, *136*, 15809–15812.

12 Głaszczka, R.; Jaźwiński, J., Complexation of Oxygen Ligands with Dimeric Rhodium(II) tetrakistrifluoroacetate in Chloroform: ^{1}H, ^{13}C NMR and DFT studies, *J. Mol. Struct.*, **2013**, *1036*, 78–89.

13 Leszczyńska, K.; Mix, A.; Berger, R. J. F.; Rummel, B.; Neumann, B.; Stammler, H. G.; Jutzi, P., The Pentamethylcyclopentadienylsilicon(II) cation as a Catalyst for the Specific Degradation of Oligo(ethyleneglycol) Diethers, *Angew. Chem. Int. Ed.*, **2011**, *50*, 6843–6846.

14 Gaussian 16, Revision A.03, M. J. Frisch, G. W. Trucks, H. B. Schlegel, G. E. Scuseria, M. A. Robb, J. R. Cheeseman, G. Scalmani, V. Barone, G. A. Petersson, H. Nakatsuji, X. Li, M. Caricato, A. V. Marenich, J. Bloino, B. G. Janesko, R. Gomperts, B. Mennucci, H. P. Hratchian, J. V. Ortiz, A. F. Izmaylov, J. L. Sonnenberg, D. Williams-Young, F. Ding, F. Lipparini, F. Egidi, J. Goings, B. Peng, A. Petrone, T. Henderson, D. Ranasinghe, V. G. Zakrzewski, J. Gao, N. Rega, G. Zheng, W. Liang, M. Hada, M. Ehara, K. Toyota, R. Fukuda, J. Hasegawa, M. Ishida, T. Nakajima, Y. Honda, O. Kitao, H. Nakai, T. Vreven, K. Throssell, J. A. Montgomery, Jr., J. E. Peralta, F. Ogliaro, M. J. Bearpark, J. J. Heyd, E. N. Brothers, K. N. Kudin, V. N.

Staroverov, T. A. Keith, R. Kobayashi, J. Normand, K. Raghavachari, A. P. Rendell, J. C. Burant, S. S. Iyengar, J. Tomasi, M. Cossi, J. M. Millam, M. Klene, C. Adamo, R. Cammi, J. W. Ochterski, R. L. Martin, K. Morokuma, O. Farkas, J. B. Foresman, D. J. Fox, Gaussian, Inc., Wallingford CT, 2016.

15 MacroModel; Schrödinger, LLC: New York, NY, 2017.

16 Legault, C. Y., CYLview, 1.0b; Universite de Sherbrooke, 2009 (http://www.cylview.org).

17 Sapsford, J. S.; Csókás, D.; Scott, D. J.; Turnell-Ritson, R. C.; Piascik, A. D.; Pápai, I.; Ashley, A. E., Establishing the Role of Triflate Anions in H_2 Activation by a Cationic Triorganotin(IV) Lewis Acid, *ACS Catal*. **2020**, *10*, 7573–7583.

18 (a) Chai, J.-D.; Head-Gordon, M., Long-range corrected hybrid density functionals with damped atom–atom dispersion corrections, *Phys. Chem. Chem. Phys.* **2008**, *10*, 6615-6620. (b) Chai, J.-D.; Head-Gordon, M., Systematic Optimization of Long-range Corrected Hybrid Density Functionals, *J. Chem. Phys.*, **2008**, *128*, 084106.

19 Marenich, A. V.; Cramer, C. J.; Truhlar, D. G., Universal Solvation Model Based on Solute Electron Density and on a Continuum Model of the Solvent Defined by the Bulk Dielectric Constant and Atomic Surface Tensions, *J. Phys. Chem. B*, **2009**, *113*, 6378-6396.

20 Bootsma, A. N.; Wheeler, S., Popular Integration Grids Can Result in Large Errors in DFT-Computed Free Energies, *ChemRxiv*. Preprint. https://doi.org/10.26434/chemrxiv.8864204.v5, **2019**.

21 Weigend, F.; Ahlrichs, R., Balanced Basis Sets of Split Valence, Triple Zeta Valence and Quadruple Zeta Valence Quality for H to Rn: Design and Assessment of Accuracy, *Phys. Chem. Chem. Phys.*, **2005**, *7*, 3297-3305.

22 Das, S.; Pati, S. K., Unravelling the Mechanism of Tin-based Frustrated Lewis Pair Catalysed Hydrogenation of Carbonyl Compounds, *Catal. Sci. Technol*. **2018**, *8*, 5178−5189. An alternative association between lut and **1**-H was also investigated, however, calculations for **1**-H/lut and found no datively bound structures; the two Me groups of lut hinder the coordination to the Sn center, and they clash with the *i*Pr groups of **1**-H.